

Investigation of flow characteristics of coal and oil slurry

A Dissertation submitted
in partial fulfilment of the requirements
for the degree of

Master of Engineering
in
Thermal Engineering

by

Puneet Juneja
Registration No.: 801483029

Under the Supervision of

Dr.S.K. Mohapatra

Senior Prof. and H.O.D

Dr. Satish Kumar

Assistant Prof.

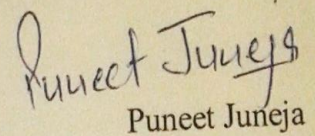


MECHANICAL ENGINEERING DEPARTMENT
THAPAR UNIVERSITY, PATIALA

Month, Year

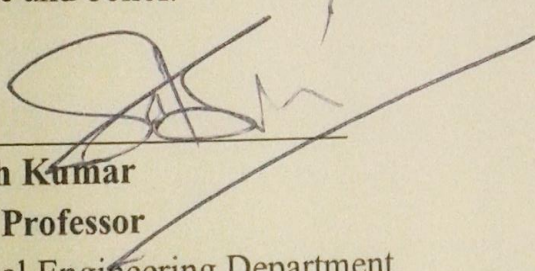
CERTIFICATE

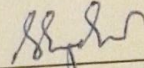
I hereby declare that the thesis entitled “Investigation of flow characteristics of coal and oil slurry” is an authentic record of my work carried out as requirements for the award of the degree of **Master of Engineering in Thermal Engineering** at **Thapar University, Patiala** under the supervision of **Dr. S.K. Mohapatra (Senior Professor and Head of Department)** and **Dr. Satish Kumar (Assistant Professor)**, Mechanical Engineering Department, Thapar University, Patiala. No part of the matter embodied in this report has been submitted to any other university or institute for the award of any degree.


Puneet Juneja

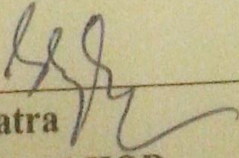
Date: 5-July-2016

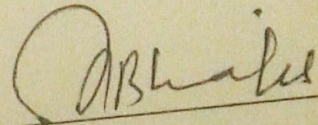
It is certified that the above statement made by the student is correct to the best of my/our knowledge and belief.


Dr. Satish Kumar
Assistant Professor
Mechanical Engineering Department
Thapar University, Patiala – 147004


Dr. S.K. Mohapatra
Senior Professor and HOD
Mechanical Engineering Department
Thapar University, Patiala - 147004

Countersigned by


Dr. S.K. Mohapatra
Senior Professor and HOD,
Mechanical Engineering Department
Thapar University, Patiala – 147004


Dr. S.S. Bhatia
Dean of Academic Affairs
Thapar University, Patiala - 147004

Dedicated to
Family

Acknowledgements

It gives me immense pleasure to record my deep sense of gratitude to work under the esteemed guidance of my research supervisor, Dr. S.K. Mohapatra, Senior Professor & Head of Department, Mechanical Engineering Department, Thapar University, Patiala. Words are inadequate to describe the great care and interest shown by him at all times during the course of the present work.

I would like to express my deepest respect towards my co-supervisor, Dr. Satish Kumar, Assistant Professor, Mechanical Engineering Department, Thapar University, Patiala for guiding and inspiring me in the course of the research work. The fruitful discussions with him throughout the research work were a great help for the successful completion of the present work.

I acknowledge my sincere thanks to all my friends and classmates for providing the companionship and making my stay at Thapar University, Patiala pleasant and joyful. My heartfelt thanks are due to all the Faculty and staff members of the Mechanical Engineering Department, Thapar University, Patiala for providing the necessary instrumentation facility for carrying out the research work.

Last but not the least; I would like to express my love and affection towards my parents for their constant moral support and encouragement throughout my life.

PUNEET JUNEJA

Abstract

The present study on the coal-oil slurry rheology and its transportation performance was conducted at the Mechanical Engineering Department, Thapar University, Patiala. The rheological behaviour of three different ranked Indian coal samples were investigated by using Anton Paar RheolabQC rheometer to generate extensive rheological data with a perspective to study the effect of solids concentration, particle size distribution, blended coal-oil, temperature effect and ash content on the slurry rheology. The lower ranked coal was washed with chemical to produce ultra-clean coal. The coal oilslurry was prepared with chemically treated coal and without treated coal to study the effect of ash content present in coal. The rheological results revealed that the coal oil slurry exhibited non-Newtonian behaviour. The coal oil slurry flow behaviour was described by the Power-Law and Herschel-Bulkley models. The apparent viscosities of coal oil slurry increased with solids loading. The Particle Size Distribution affected the slurry rheology due to increase in frictional forces within particle to particle. The apparent viscosity of coal oil slurry decreases when high ranked coal is blended with lower ranked coal at all concentration. Also the apparent viscosity of slurry decreases with increase in temperature due to breakdown of oil particles. The rheological data best fitted for Herschel-Bulkley model which exhibits shear thinning behaviour. The rheological data so obtained were utilized to numerically evaluate the pressure drop characteristics of coal oil slurry flowing in 90 degree pipe bend using ANSYS FLUENT 14.0 computational fluid dynamics code. The pressure drop predictions were obtained by utilizing the rheological data and the results revealed that in 90° pipe bend, with increase in solids loading and mean flow velocities, the pressure drop increased.

Key words: Ash content; CFD; Coal; Coal blending; COSL; EDS; HF; HNO₃; Leaching; Rheology; SEM; Ultra-clean coal.

Content

| | TITLE | Pg. no. |
|------------------|---|----------------|
| | List of figures | viii |
| | List of tables | xiii |
| | Nomenclature | xiv |
| Chapter 1 | INTRODUCTION | |
| 1.1 | Energy scenario of India | 1 |
| 1.2 | Coal and its types | 2 |
| 1.3 | Rheometry | 4 |
| 1.4 | Types of fluid | 5 |
| 1.5 | Slurry | 7 |
| 1.6 | Utilization areas of coal oil slurry | 8 |
| 1.7 | Slurry parameters | 8 |
| 1.8 | Viscosity measurement | 10 |
| 1.9 | Rheology measurement | 12 |
| 1.10 | Rheometer and viscometer | 13 |
| 1.11 | Rheological properties of fluid | 14 |
| 1.12 | Coal-oil mixture technology | 15 |
| 1.13 | Requirement and uses of coal-oil mixtures | 16 |
| 1.14 | Role of rheology in design of coal slurry | 16 |
| 1.15 | Leaching | 19 |
| 1.16 | Computational fluid dynamics | 19 |
| Chapter 2 | LITERATURE SURVEY | |
| 2.1 | Literature review | 21 |
| 2.2 | Gaps in literature | 32 |
| Chapter 3 | CHARACTERIZATION OF COAL | |
| 3.1 | Introduction | 33 |
| 3.2 | Collection of samples | 34 |
| 3.3 | Material and method | 34 |
| 3.4 | Coal sample preparation | 36 |

| | | |
|------------------|---|----|
| 3.5 | Particle size distribution | 37 |
| 3.6 | Proximate analysis and EDS | 37 |
| 3.7 | Morphological characteristics of coal samples | 38 |
| 3.8 | Bomb calorimeter | 39 |
| 3.9 | Ash content determination | 39 |
| 3.10 | Results and discussion | 39 |
| Chapter 4 | RHEOLOGY OF CHEMICAL LEACHED COAL OIL SLURRY | |
| 4.1 | Introduction | 45 |
| 4.2 | Description of equipment | 45 |
| 4.3 | Materials and methods | 46 |
| 4.4 | Results and discussion | 48 |
| Chapter 5 | RHEOLOGY OF BLENDED COAL AND OIL SLURRY | |
| 5.1 | Materials and methods | 55 |
| 5.2 | Proximate analysis and EDS | 56 |
| 5.3 | Particle size distribution | 57 |
| 5.4 | Results and discussion | 58 |
| 5.5 | Rheological model fitting | 77 |
| Chapter 6 | SIMULATION OF PIPE FLOW CHARACTERISTICS | |
| 6.1 | Introduction | 78 |
| 6.2 | Modelling of 90° pipe bend | 78 |
| 6.3 | Meshing of 90° pipe bend | 79 |
| 6.4 | Problem formulation | 81 |
| 6.5 | Boundary conditions | 81 |
| 6.6 | Results | 82 |
| Chapter 7 | CONCLUSION AND FUTURE SCOPE | |
| 7.1 | Summary and conclusion | 89 |
| 7.2 | Future scope in COSL technology | 90 |
| | References | 92 |
| | Appendix | 96 |

List of Figures

| Fig. no. | Description | Page no. |
|-----------------|--|-----------------|
| 1.1 | India's domestic coal production, consumption and production targets | 1 |
| 1.2 | India energy scenario 2015 | 2 |
| 1.3 | Types of coal | 3 |
| 1.4 | Moving plates in identical direction | 4 |
| 1.5 | (a) variation of shear stress with increase in shear rate and (b) viscosity trend with shear rate for Newtonian fluids | 5 |
| 1.6 | Different types of fluids | 6 |
| 1.7 | Different continuum fluid models | 7 |
| 1.8 | Homogeneous mixture | 9 |
| 1.9 | Pseudo homogeneous mixture | 9 |
| 1.10 | Heterogeneous partially stratified | 10 |
| 1.11 | Heterogeneous fully stratified | 10 |
| 1.12 | U-Tube Viscometer | 10 |
| 1.13 | Falling sphere viscosity | 11 |
| 1.14 | Piston Viscometer | 11 |
| 1.15 | Rotational rheometer having plate/cone measuring system and cylindrical measuring system | 12 |
| 1.16 | Newtonian flow behaviour | 14 |
| 1.17 | Flow and Viscosity curves | 14 |
| 1.18 | Typical example of coal-oil mixture technology | 15 |
| 1.19 | Schematic layout of a long distance slurry pipeline | 18 |
| 2.1 | Viscosity variation with coal concentration for several coal-oil slurries | 21 |
| 2.2 | Viscosity variation for different oil with shear rate at 40 and 100 °C | 23 |
| 2.3 | Effect of shear rate on apparent viscosity of UCSFCOS at 307 K | 24 |
| 2.4 | Effect of shear rate with variation in temperature on rheological behaviour | 25 |
| 2.5 | Variation of apparent viscosity of PCOS containing 30 wt.% daqing with different grinding time | 25 |

| | | |
|------|--|----|
| 2.6 | Effect of loading on viscosity and sedimentation velocity of PCOS | 26 |
| 2.7 | Variation of apparent viscosity of lignite char slurries with different solid concentrations with 1.0 dwb% D102 and zeta potential is 70 mV at pH 9.5 | 26 |
| 2.8 | Viscosity variations COSL for temperature of 450°C and with the preliminary hydrogen pressure of 5 Mpa | 27 |
| 2.9 | Relationship between η_c and solid concentration for PCSS with different SMP | 29 |
| 2.10 | Comparison of calculated with experimental pressure drop using CFD | 29 |
| 2.11 | The influence of solids loading on the apparent viscosities of different slurries. Error bars indicate repeatability error | 30 |
| 2.12 | Variation of k_p with α | 31 |
| 3.1 | Process diagram for the materials and methodology | 35 |
| 3.2 | Particle size distribution (PSD) of two coal samples | 36 |
| 3.3 | SEM micrograph of Coal A | 38 |
| 3.4 | SEM image of Coal B | 38 |
| 3.5 | Percentage of ash reduction with increased concentration of aqueous solution | 40 |
| 3.6 | (a) represents the EDS image of untreated Coal A whereas (b) with 40% treated with HF and HNO ₃ and Figure 3.6(c) represent the EDS image of untreated Coal B whereas (d) with 40% treated with HF and HNO ₃ | 43 |
| 3.7 | (a) shows the SEM image of ash for untreated Coal A (b) shows the SEM image after washing (c) represents the SEM image of ash for untreated Coal B (d) | 43 |
| 4.1 | Rheometer (anton parr) | 46 |
| 4.2 | Cylindrical cup and bob | 46 |
| 4.3 | Detailed procedure of methodology adopted | 47 |
| 4.4 | Shear stress variation with increased shear rate for untreated and chemically treated coal oil slurry for 20% solid concentration at 293K | 50 |
| 4.5 | Shear stress variation with increased shear rate for untreated and chemically treated coal oil slurry for 30% solid concentration at 293K | 50 |
| 4.6 | Shear stress variation with increased shear rate for untreated and chemically treated coal oil slurry for 40% solid concentration at 293K | 51 |
| 4.7 | Influence of shear rate on apparent viscosity of untreated and chemically treated coal oil slurry for 20% solid concentration at | 52 |

| | | |
|------|---|----|
| | 293K | |
| 4.8 | Influence of shear rate on apparent viscosity of untreated and chemically treated coal oil slurry for 30% solid concentration at 293K | 52 |
| 4.9 | Influence of shear rate on apparent viscosity of untreated and chemically treated coal oil slurry for 40% solid concentration at 293K | 53 |
| 5.1 | Methodology adopted for rheology | 56 |
| 5.2 | Particle size distribution for all samples of coal | 58 |
| 5.3 | Shear stress and shear strain at 30% solid loading of coal | 59 |
| 5.4 | Apparent viscosity with shear strain at 30% solid concentration | 59 |
| 5.5 | Apparent viscosity with shear strain at 40% solid concentration | 60 |
| 5.6 | Shear stress and shear strain at 40% solid loading of coal | 60 |
| 5.7 | Apparent viscosity with shear strain at 50% solid concentration | 61 |
| 5.8 | Shear stress and shear strain at 50% solid loading of coal | 61 |
| 5.9 | Influence on apparent viscosity with increase in shear rate at 20°C for 50% solid concentration | 62 |
| 5.10 | Influence on shear stress with increase in shear rate at 20°C for 50% solid concentration | 62 |
| 5.11 | Influence on apparent viscosity with increase in shear rate at 45°C for 50% solid concentration | 63 |
| 5.12 | Influence on shear stress with increase in shear rate at 20°C for 50% solid concentration | 63 |
| 5.13 | Influence on apparent viscosity with increase in shear rate at 70°C for 50% solid concentration | 64 |
| 5.14 | Influence on shear stress with increase in shear rate at 70°C for 50% solid concentration | 64 |
| 5.15 | Influence on apparent viscosity with increase in shear rate at 20°C for 30% solid concentration | 65 |
| 5.16 | Influence on shear stress with increase in shear rate at 20°C for 30% solid concentration | 65 |
| 5.17 | Influence on apparent viscosity with increase in shear rate at 20°C for 40% solid concentration | 66 |
| 5.18 | Influence on shear stress with increase in shear rate at 20°C for 40% solid concentration | 66 |
| 5.19 | Influence on apparent viscosity with increase in shear rate at 20°C for 50% solid concentration | 67 |
| 5.20 | Influence on shear stress with increase in shear rate at 20°C for 50% | 67 |

| | | |
|------|---|----|
| | solid concentration | |
| 5.21 | Influence on apparent viscosity with increase in shear rate at 20°C for 30% solid concentration | 68 |
| 5.22 | Influence on shear stress with increase in shear rate at 20°C for 30% solid concentration | 68 |
| 5.23 | Influence on apparent viscosity with increase in shear rate at 20°C for 40% solid concentration | 69 |
| 5.24 | Influence on shear stress with increase in shear rate at 20°C for 40% solid concentration | 69 |
| 5.25 | Influence on apparent viscosity with increase in shear rate at 20°C for 50% solid concentration | 70 |
| 5.26 | Influence on shear stress with increase in shear rate at 20°C for 50% solid concentration | 70 |
| 5.27 | Influence on apparent viscosity with increase in shear rate at 20°C for 40% solid concentration | 71 |
| 5.28 | Influence on shear stress with increase in shear rate at 20°C for 40% solid concentration | 71 |
| 5.29 | Influence on apparent viscosity with increase in shear rate at 45°C for 40% solid concentration | 72 |
| 5.30 | Influence on shear stress with increase in shear rate at 45°C for 40% solid concentration | 72 |
| 5.31 | Influence on apparent viscosity with increase in shear rate at 70°C for 40% solid concentration | 73 |
| 5.32 | Influence on shear stress with increase in shear rate at 70°C for 40% solid concentration | 73 |
| 5.33 | Influence on apparent viscosity with increase in shear rate at 20°C for 30% solid concentration | 74 |
| 5.34 | Influence on shear stress with increase in shear rate at 20°C for 50% solid concentration | 74 |
| 5.35 | Influence on apparent viscosity with increase in shear rate at 20°C for 40% solid concentration | 75 |
| 5.36 | Influence on shear stress with increase in shear rate at 20°C for 40% solid concentration | 75 |
| 5.37 | Influence on apparent viscosity with increase in shear rate at 20°C for 50% solid concentration | 76 |
| 5.38 | Influence on shear stress with increase in shear rate at 20°C for 50% solid concentration | 76 |
| 6.1 | Modelling of pipe bend having curvature ratio 1 | 78 |
| 6.2 | Modelling of pipe bend having curvature ratio 2 | 79 |

| | | |
|------|--|----|
| 6.3 | Modelling of pipe bend having curvature ratio 3 | 79 |
| 6.4 | Meshing of pipe bend having curvature ratio 1 | 80 |
| 6.5 | Meshing of pipe bend having curvature ratio 2 | 80 |
| 6.6 | Meshing of pipe bend having curvature ratio 3 | 80 |
| 6.7 | Pressure drop variation with velocity for pipe bend having curvature ratio 1 | 82 |
| 6.8 | Pressure drop variation with velocity for pipe bend having curvature ratio 2 | 83 |
| 6.9 | Pressure drop variation with velocity for pipe bend having curvature ratio 3 | 83 |
| 6.10 | Pressure drop for 30% volume fraction of coal | 84 |
| 6.11 | Pressure drop for 40% volume fraction of coal | 84 |
| 6.12 | Pressure drop for 50% volume fraction of coal | 84 |
| 6.13 | Contour of static pressure of COSL at $C_s=30\%$ for 3.5 m/sec curvature ratio 1 | 85 |
| 6.14 | Contour of static pressure of COSL at $C_s=40\%$ for 3.5 m/sec curvature ratio 1 | 85 |
| 6.15 | Contour of static pressure of COSL at $C_s=50\%$ for 3.5 m/sec curvature ratio 1 | 86 |
| 6.16 | Contour of static pressure of COSL at $C_s=30\%$ for 3.5 m/sec curvature ratio 2 | 86 |
| 6.17 | Contour of static pressure of COSL at $C_s=40\%$ for 3.5 m/sec curvature ratio 2 | 86 |
| 6.18 | Contour of static pressure of COSL at $C_s=50\%$ for 3.5 m/sec curvature ratio 2 | 87 |
| 6.19 | Contour of static pressure of COSL at $C_s=30\%$ for 3.5 m/sec curvature ratio 3 | 87 |
| 6.20 | Contour of static pressure of COSL at $C_s=40\%$ for 3.5 m/sec curvature ratio 3 | 87 |
| 6.21 | Contour of static pressure of COSL at $C_s=50\%$ for 3.5 m/sec curvature ratio 3 | 88 |
| 6.22 | Contour of dynamic pressure of 3.5 m/s for curvature ratio 1, 2 and 3 | 88 |

List of Tables

| Table no. | Title of the table | Page no. |
|------------------|--|-----------------|
| 1.1 | Constitutive equations of non-Newtonian fluids | 5 |
| 1.2 | Utilization areas of coal-oil slurry | 8 |
| 3.1 | Proximate and EDS analysis on air dried basis | 37 |
| 3.2 | EDS analysis of ultra-clean coal samples | 40 |
| 3.3 | Ash composition retained from untreated and ultra-clean coal | 41 |
| 3.4 | Calorific value of coal samples with varying concentration of leaching | 44 |
| 4.1 | Herschel-Bulkley model parameters for nonlinear equation for treated and untreated coal and oil slurry | 49 |
| 5.1 | Proximate and EDS analysis on moisture free basis | 57 |

Nomenclature

τ = Shear stress, Pa

γ = Shear rate

τ_H = Yield stress, Pa

η = Apparent viscosity, mPa-s

μ = Dynamic viscosity

C_s = Weight concentration of solid

n = Flow behaviour index

K = Flow consistency index

g = Acceleration due to gravity, m²/sec

d_{50} = Mass median particle diameter, μm

D = Diameter of pipe, mm

R_c = Radius of curvature, mm

Acronyms

HF \equiv Hydrofluoric acid

HNO₃ \equiv Nitric acid

COSL \equiv Coal oil slurry

UCC \equiv Ultra-clean coal

CV \equiv Calorific value

Chapter 1

Introduction

1.1 Energy scenario of India

In India, the coal consumption is overtaking India's domestic production basically in electric power sector. From 2005 to 2014, the growth rate for India's coal production occurred only by 4.7% per year (about 600 million metric tons), while the coal-fired electric ability developed by plentiful greater rate of about 9.4% per year, attained up to 150 GW. India has established mark for coal production (1.50 billion metric ton by 2020) so as to support prolonged coal fired generation and to avoid the shortage measures in coal stock.

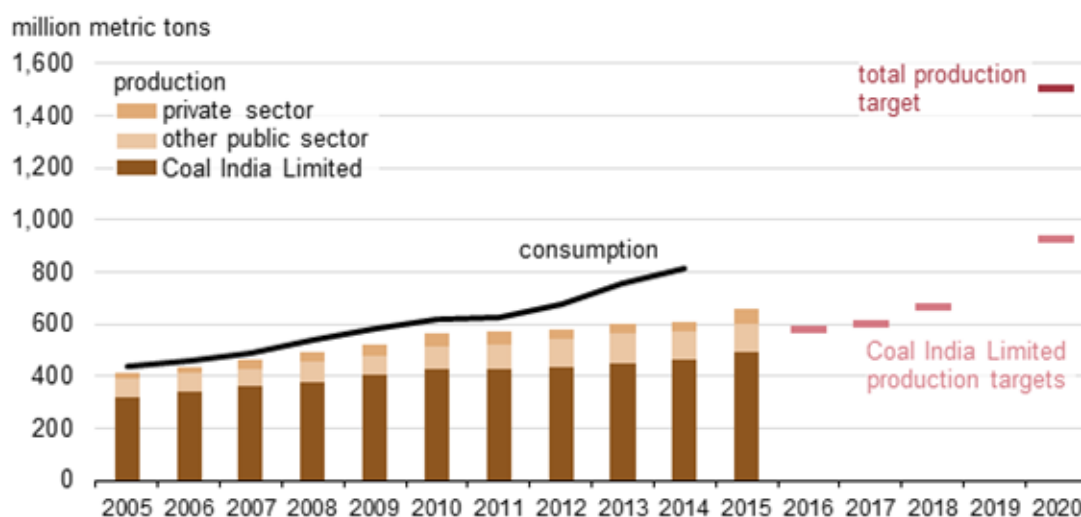


Fig.1.1: India's domestic coal production, consumption and production targets (Source: Energy statistics 2015)

Figure 1.2 shows the India energy scenario for 2015, in which the total energy produced in India was produced from 60.44% coal. Coal is considered as primary energy source in India, for power generation. Over next 10-12 years, the energy demand is predictable to rise in India. Although new gas and oil plants are scheduled, coal is likely to endure prevailing fuel for energy generation. Regardless of significant rise in total installed capacity, the gap among demand and energy supply remains to increase. As a result, the shortage criterion for production has negative impact on economic growth as well as on

output from industry. Also Indian coal is normally of poor quality with large ash content and required to beneficiate to increase the value of coal.

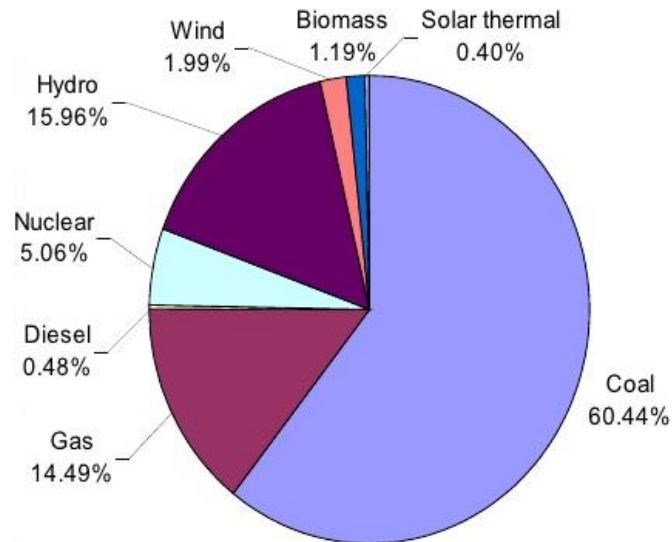


Fig. 1.2: India energy scenario 2015 (Source: Energy statistics 2015)

1.2 Coal and its types

Coal is a combustible brownish-black or black sedimentary rock frequently happening in rock strata in veins otherwise in layers is termed as **coal seams** or **coal beds**. The hardest form of coal (anthracite coal) may be observed as metamorphic rock due to later exposure to eminent temperature as well as pressure. Coal consists of carbon (as primary constituent) along with mutable amounts of other elements, mostly sulphur, oxygen, hydrogen as well as nitrogen. The basic function of coal is for the production of electricity and/or heat. This heat can be utilized for industrialized purposes like refining metals. Coal is formed from dead plant matter, which is converted into peat (lowest rank of coal). The further processing formed lignite, sub-bituminous, bituminous lastly anthracite i.e. conversion from lower rank to higher rank.

- **Peat (lowest ranked coal):** It has industrial significance as fuel in certain areas, e.g. Finland and Ireland. When peat available in dehydrated form, it is enormously effective absorbent for oil spills and fuel on water and land. Peat coal can also be utilized for soil (as conditioner) to make it enough reliable and gently release water.

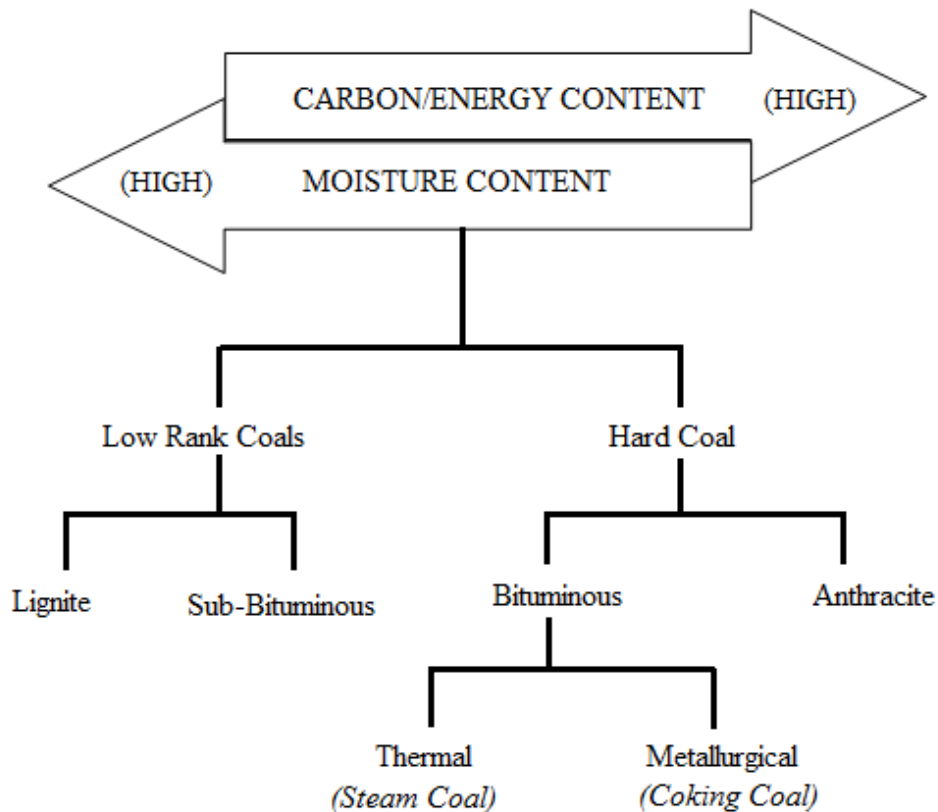


Fig. 1.3: Types of coal

- **Lignite (brown) coal:** It is considered amongst the lower rank in coal and utilized entirely as fuel for power generation. The compact form is jet lignite coal that is occasionally refined and is used as a decorative stone.
- **Sub-bituminous coal:** Their property lies between bituminous and lignite coal and is primarily used for steam electric power generation, as fuel and is a significant source of light aromatic hydrocarbons for chemical synthesis industry.
- **Bituminous coal:** It is a kind of thick sedimentary rock, generally black in colour but at times dark brown habitually with definite bands of dull and bright material, consumed in steam electric power generation and for producing coke.
- **Steam coal:** It is ranked between anthracite and bituminous, earlier utilized for steam locomotives. For its particular use, sometimes steam coal is referred to as sea coal in the United States. Dry small steam nuts/DSSN (small steam coal) was utilized for water heating purposes at the domestic level.
- **Anthracite coal:** It is considered as the highest grade amongst coal and is a solid variety of coal. Lustrous black coal used predominantly for commercial and residential space

heating purpose. They may be distributed further into meta-morphically improved petrified oil and bituminous coal.

- **Graphite**, considered amongst the highest rank of coal, but is not commonly used as fuel because of its ignition difficulty. It is frequently used in pencils and graphite in powdered form is used as a lubricant.

1.3 Rheometry

The usual standard approaches that can be used for experimentation to determine the rheological parameters of fluid or the solid can refer to be rheometry. The idea undertaking rheometry, where shear rate and stress are already known, is to realize the flow which makes it possible to conclude the rheological behaviour from the flow parameters. Basically rheometer is kind of an apparatus, which can apply a force/torque on fluid or solid and precisely measure its response time.

1.3.1 Shear: Viscosity is defined as measurement of fluid's internal friction. When a layer of fluid moves relative to another layer, this friction becomes apparent. Superior the friction, superior will be the intensity of force required for this movement, which is to be referred as shear. The term shearing occur at whatever the requirement of more force for liquid to move liquids that are less viscous. The two parallel planes are moving in an identical direction having unlike velocities (V_1 and V_2) and are equated by distance dx , the requirement of force to keep this difference in velocities is proportional to velocity gradient (dv/dx).

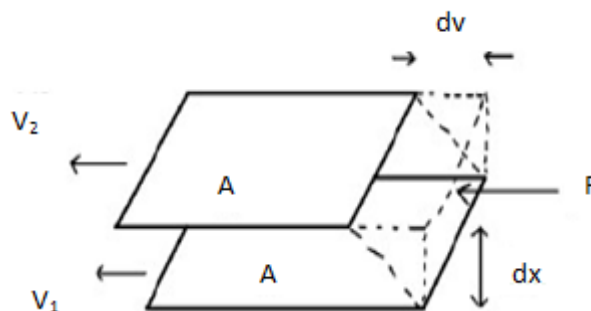


Fig. 1.4: Moving plates in identical direction

1.3.2 Shear rate (R): Velocity gradient (dv/dx) is degree of speed at which in-between layers slides over each other in identical direction. It designates the shearing liquid experience and is referred as shear rate (R). Its unit of degree is the reciprocal of second (sec^{-1}).

1.3.3 Shear stress (S): In fig. 1.4 F/A specifies the required force per unit area for shearing action which is called as shear stress. Its unit is N/m^2 . Viscosity can be described ratio of shear stress to shear rate. The fundamental units of viscosity are poise.

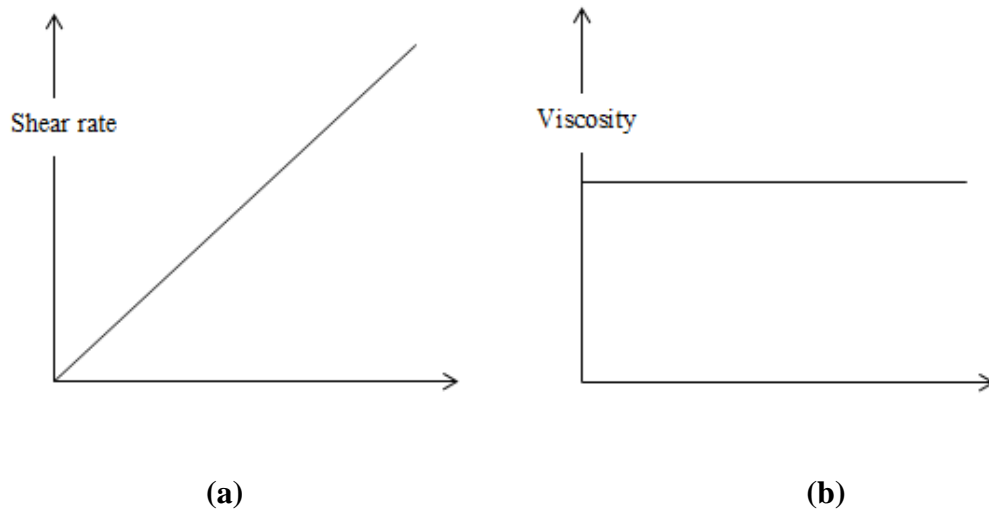


Fig.1.5: Strategy of (a) variation of shear stress with increase in shear rate and (b) viscosity trend with shear rate for Newtonian fluids. Subsequently, at particular temperature the variation in viscosity for Newtonian fluid behaves constant irrespective of type of rheometer spindle, model or speed to be used for measurement.

The performance of Newtonian fluids has the following structures in experiment conducted at constant pressure:

1. The only stress generated is the shear stress (S) in simple shear flow, and difference between two stresses (normal) is zero.
2. The apparent viscosity doesn't fluctuate with shear rate.
3. The apparent viscosity of fluid remains constant with time and stresses falls to zero when there is no shearing. A fluid showing above features will fall into the category of Newtonian fluid.

1.4 Types of fluid

1.4.1 Non-Newtonian fluids: Any fluid showing deviation from above statements falls in category of non-Newtonian fluid. These can be termed as those fluids for which ratio of S/R are not constant. Also the apparent viscosity does not vary for non-Newtonian fluid when shear rate changes. Therefore, the parameter of rheometer like rheometer spindle as well as rotational speed has great impact on viscosity. The measured viscosity is termed as apparent viscosity. For non-Newtonian fluid, the viscosity varies with respect to variation in shear rate.

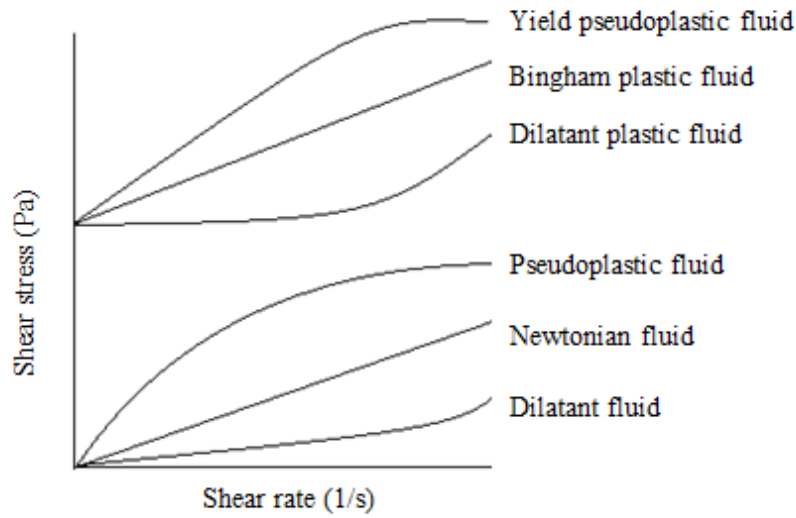


Fig. 1.6: Different types of fluids [1].

In comparison with Newtonian fluid, more than single parameter is required to relate the shear stress to the applied shear strain for non-Newtonian fluids. The different non-Newtonian fluids are Herschel-Bulkley Power-Law, Casson, Bingham, etc. depending on the complications tangled in their constitutive model equations. The constitutive equations for non-Newtonian fluids are shown in Table 1.1:

Table 1.1: Constitutive equations of non-Newtonian fluids

| Types of non-Newtonian fluid | Constitutive equation | Unknown parameters |
|------------------------------|---|--------------------|
| Power-law | $\tau = K\gamma^n$ | Two |
| Bingham | $\tau = \tau_y + \mu_p\gamma$ | Two |
| Herschel-Bulkley | $\tau = \tau_y + K\gamma^n$ | Three |
| Casson | $\tau^{1/2} = \tau_c^{1/2} + (\mu_c\gamma)^{1/2}$ | Two |

Figure 1.7 shows a graphical demonstration of the shear stress with shear strain behaviour plotted as a Rheogram for given number of different continuum fluid models.

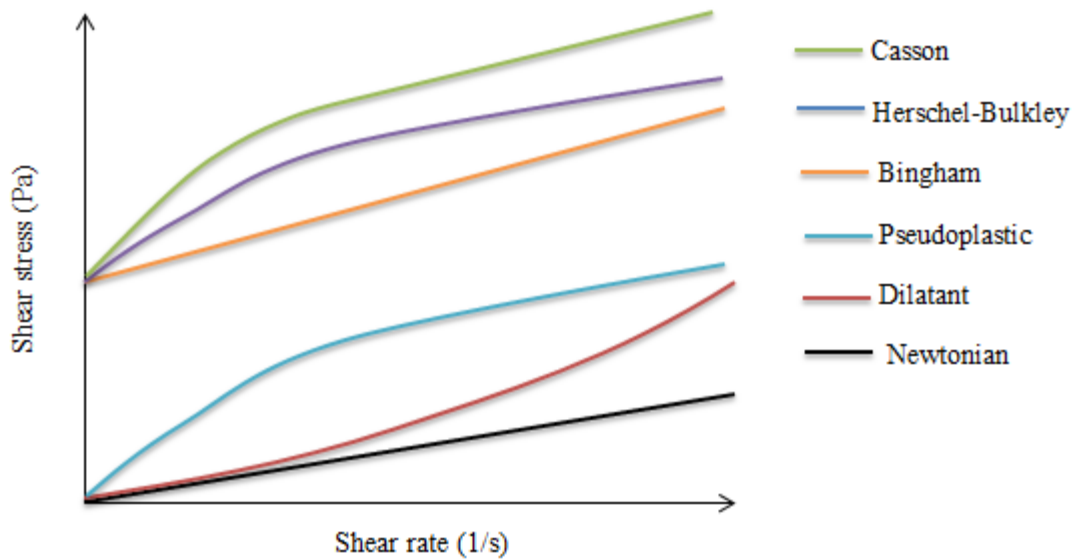


Fig. 1.7: Different continuum fluid models

Power-Law fluids do not contain the yield stress and can be shear-thinning (pseudoplastic) or shear thickening (dilatants) depending on the flow behaviour index, n . The Casson, Herschel-Bulkley and Bingham fluids show the presence of a yield stress. In order for the fluid to flow, the applied shear stress must exceed this yield stress. Once applied shear stress exceeds the yield stress, the rate of deformation of the fluid is determined by the difference between the yield stress and applied stress. In the present work, slurries that exhibit yield stress were represented with the Herschel-Bulkley rheological model.

1.5 Slurry

The knowledge regarding the preparation of slurry for rheological properties is of great importance. The study of slurry preparation is important for severely technical applications e.g. casting of ceramics, storage, process control in chemical engineering, transportation of solids in pipelines and atomization. The mixture of liquid and solid is known as slurry. The physical characteristics of the slurry depends on many factors like temperature, viscosity of carrier, particle size and distribution, solid concentration in liquid phase, conduct size and turbulence level. Slurry is a combination of fluid as well as solid particle held in suspension. However, slurry which is made from two-phase must overcome a viscous transition critical velocity or a deposition critical velocity. The speed of slurry flow is sufficient enough to keep

the solid particles in suspension. The slurry resists flow in highly viscous mixtures due to excessively low shear rate in a pipeline.

1.6 Utilization areas of Coal-oil slurry

For the present global scenario, as the cost of oil is increasing day by day, there is a surge amongst the researchers to progress alternative fuel that can entirely replace the conventional fuel without conceding the thermal efficiency as well as others parameters that affect the efficiency. Therefore, utilizing the conventional fuel in economic manner that can provide reduction in cost having better combustion properties has caused the development of coal oil slurry. The different utilization areas of coal-oil slurries are described in Table

Table 1.2: Utilization areas of coal-oil slurry

| Utilization areas | Required properties |
|----------------------|----------------------------|
| Thermal power plants | Efficient combustion |
| Coal gasification | High loading of coal |
| Diesel engine fuel | Good combustion properties |
| Industrial heating | Stability during storage |

1.7 Slurry parameters

1.7.1 Particle size and distribution (PSD): Particle size is a measure of percentage of particles in mixture with smaller or certain size. The values are measured by separating the solids through screens with varying mesh and there are being weighed for each fraction. PSD curve can be then drawn and percentage of particles of different size can be determined e.g. $d_{85}=300\mu\text{m}$ means that 85% of particles have diameter equal to or less than $300\mu\text{m}$.

1.7.2 Mass fraction of small particles: The fraction of particles less than $75\mu\text{m}$ lies in small particles. It is important criteria to determine the amount of small particles in slurry. Particles size less than $75\mu\text{m}$ helps to facilitate transportation of larger particles to some extent. However, if the amount of smaller particles exceeds 50%, slurry behaves like non-settling slurry.

1.7.3 Concentration of solids: The solid concentration in slurry can be defined as a volume of percentage C_v (i.e. volume of solids in volume of fluid) and weight percentage C_m (i.e. mass of solids in mass of fluid).

1.7.4 Slurry characteristics: Slurries can be distributed into **non-settling** as well as **settling** forms, depending upon the parameters.



Fig. 1.8: Homogeneous mixture

1.7.4.1 Non-settling slurry: Mixture in which solids don't settle down to bottom, but remains in suspension for longer period. Non-settling slurry behaves in viscous as well as homogeneous but its appearances may be non-Newtonian. The range of particles size that falls in this category lies between 60-100 μm . A homogeneous mixture can be termed as non-settling slurry

1.7.4.2 Settling slurry: This type of slurry settles faster during time relevant to process but can be kept in suspension by turbulence. The particle having size greater than 100 μm falls into this category. Settling slurry can be termed as heterogeneous mixture or homogeneous mixture and can be partly or fully stratified.

1.7.5 Pseudo-homogeneous mixture: A kind of slurry in which all the particles remains in suspension but bottom area has maximum solid concentration.

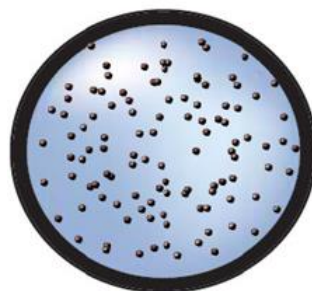


Fig. 1.9: Pseudo homogeneous mixture

1.7.6 Heterogeneous mixture: Slurry in which solids particles are not in uniform trend but tend to remain in more concentrated amount at bottom of pipe as compared to settling slurry.



Fig. 1.10: Heterogeneous partially stratified Fig. 1.11: Heterogeneous fully stratified

1.8 Viscosity measurement

Viscometer is a device used to measure viscosity of fluid and up to some extends for paste fluid applications.

1.8.1 Standard viscometer for liquid (U-tube viscometer): Basically U-tube viscometer are also known as Ostwald viscometer (discovered by Wilhelm Ostwald) or capillary viscometers. Another type of this viscometer comprises of U-shaped glass, held perpendicularly in controlled temperature bath. The arm consists of U-shaped segment of precise thin bore called as capillary. Such viscometers are categorized as reverse flow or as direct flow. The difference in both is due to positioning of reservoir. Direct flow have reservoir below marking whereas reverse flow has reservoir above the marking.

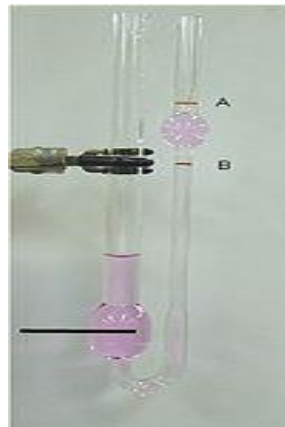


Fig. 1.12: U-Tube Viscometer

1.8.2 Falling sphere viscometer: Falling sphere viscometer works on stokes law in which the fluid remains static in vertical glass tube. In this, sphere of identified density and size is permitted to descend. Two marks on tube help to measure the density when it reaches to its terminal velocity. With the help of electronic sensing for opaque fluid to measure size,

density of sphere, terminal velocity and density of liquid can be measured. Stokes law can be adapted to measure viscosity of fluid.

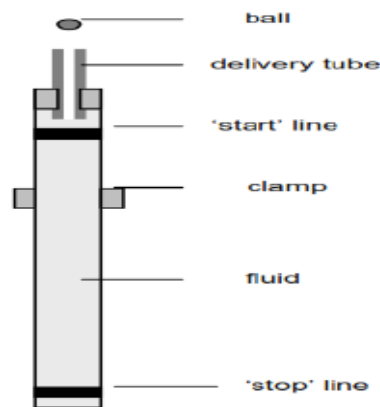


Fig. 1.13: Falling sphere viscosity

1.8.3 Oscillating piston viscometer: This viscometer is adapted to measure micro sample or small sample viscosity for laboratory uses. It can also be amended to measure high temperature and high pressure viscosity in process environment.

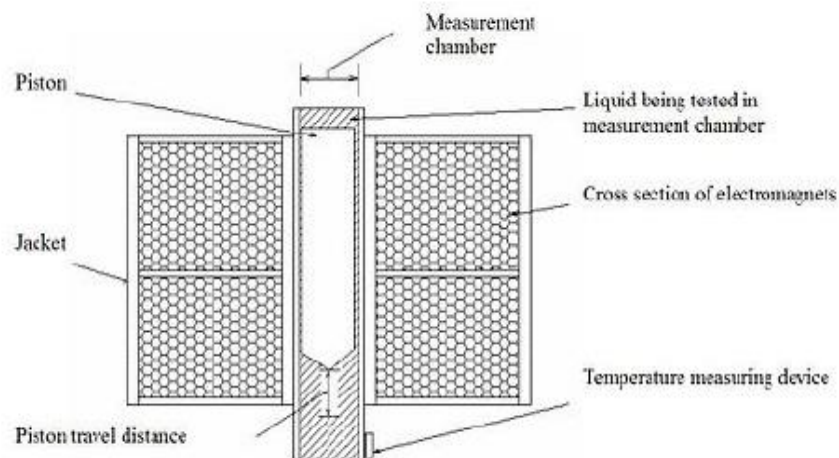


Fig. 1.14: Piston Viscometer

1.9 Rheology measurements

1.9.1 Rheometer: It is a device which is used to determine the behaviour in which suspended particles or slurry or liquid flows in responses to applied forces. Rheometer can be utilized for various fluids that can't be distinct by single value for viscosity, hence more parameters are required. Rheometer measures the rheology of fluid. Rheometer is categorized into two

types, rheometer that apply extensional strain or extensional stresses are extensional rheometer, whereas rheometer that can control applied shear strain or shear stress is rotational type rheometer. Rotational type rheometer are basically considerable as either native stress controlled device (i.e. apply and control a user defined shear stress and measuring resulting shear strain or native strain controlled appliance apply as well as control a user defined shear rate, that can measure subsequent shear stress.

1.9.2 Capillary or pipe rheometer: In this, fluid is being forced down through pipe containing constant cross-section diameter under circumstances of laminar flow. Either pressure drop or the flow rates are fixed and other parameters can be measured. Knowing the parameters, pressure drop can be convertible into value for shear stress whereas flow rate into value of shear rate. Variation of flow and pressure drop helps to determine the flow curve. The pressure drop, for Newtonian fluids, shows linear relation with flow rate, whereas the apparent viscosity is not reliant on applied deforming stress or rate. Rheometer can show shear thickening or shear thinning for non-Newtonian fluid. The flow rate versus pressure drop must be analyzed with the help of Wiesenberger-Rabin witch-Mooney equation.

1.9.3 Rotational rheometer: The fluid is kept within the clearance of one cylinder inside another. In rotational rheometer, one of cylinder is provided to rotate at systematic speed. Hence determines the apparent viscosity as well as shear stress inside the clearance. The fluid tends to drag other container round, and torque is being measured which therefore can be convertible into shear stress. The rotational rheometer Fann V-G rheometer runs at two different speeds (i.e. 300 and 600 rpm) hence provides only two general points for flow curve.



Fig. 1.15: Rotational rheometer having plate/cone measuring system (right) and cylindrical measuring system (left)

1.9.4 Extensional rheometer: The development for this type of rheometer has been occurring more slowly as compared to rotational has been occurring more slowly as compared to rotational rheometer, due to the challenges facing to generate standardized extensional flow. Primarily, interaction of fluid with solid faces troubles in shear flow which will compromise for results. Secondly, there must be knowledge regarding the strain history of material element. Thirdly, strain levels and strain rates must such that so as to stretch chains outside their standard radius of gyration. These types of rheometer are preferred for materials that are subjected to tensile deformation.

1.10 Rheometer and viscometer (a comparison)

Viscometers are relatively simple devices as compared to rheometer. Their simplicity in operation and design offer advantage for easy use of operation, particularly within a busy quality control environment. The movement of spindle in particular direction allows to determine the viscosity whereas rheometer can apply rapid step change in strain and stress and thereby measured viscoelastic properties as well as flow properties. Rheometer employ low friction air bearing whereas viscometer uses mechanical bearing that limits the torque and speed capabilities. Rheometer is more costly, more versatile and wider dynamic range for measurement parameters. Typical, in rotational rheometer stress and strain are controlled by temperature controlled unit (TCU). Rheological measurements are significant for process, formulation and material control across industries and applications. Viscometer is highly suitable for on-line process control and quality control testing whereas rheometer shows great investment, but it is essential for complete material characterization and time simulation of real processes. The performance and versatility make it an excellent tool for product process and development and for quality control testing.

1.11 Rheological properties of fluid

The properties (rheological) of mixture must be as accurate as possible under specific conditions that closely resembles actual size condition for rheological behaviour that are calculated by rheometer. The rheological parameters are mainly dependent on solid concentration in slurry. The slurry exhibits Newtonian behaviour but as solid loading increases the rheological behaviour changes to shear thickening for shear thinning.

The nature of the non-Newtonian behaviour of slurry depends upon solid loading, particle size, PSD, particle shape and suspended rheological properties. At higher solid

loading, the suspension may develop a yield stress or become time dependent as structures develop within the slurry.

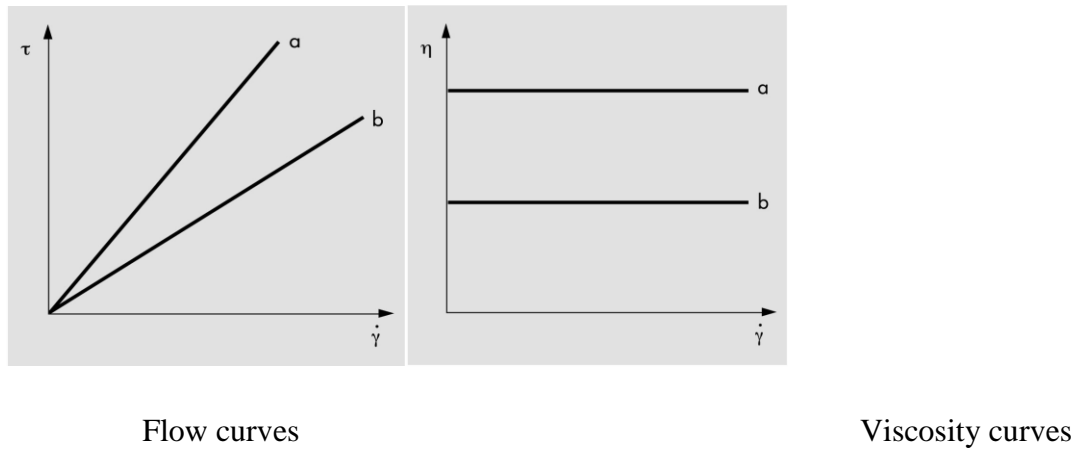


Fig. 1.16: Newtonian flow behaviour

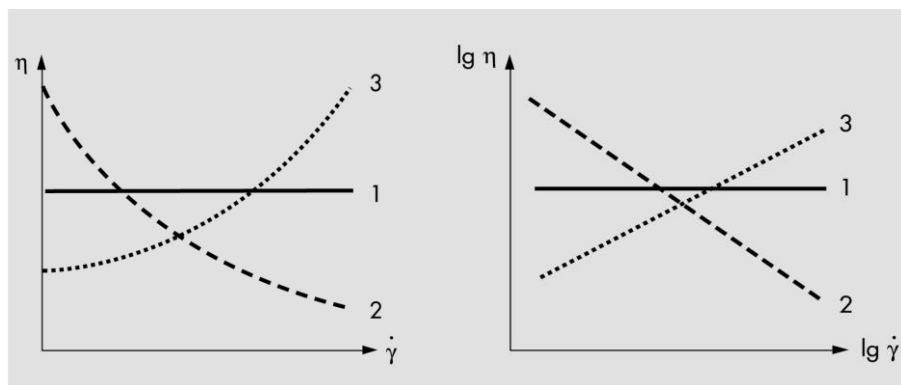


Fig. 1.17: Flow and Viscosity curves

Above graph showing flow and viscosity curves 1 is ideal viscous (Newtonian); 2 is shear thinning (pseudoplastic); 3 is shear thickening (dilatant). Two types of time dependent behaviour of slurry are possible firstly Rheopexy where the slurry thickens with time and shear, secondly Thixotropy where slurry becomes thin with time and shear. This study is basically focused on measurement of various rheological properties of settling slurries where it is essential to continuously shear or circulate slurry for settling.

Slurry pipelines helps to transport solid material with the help of water or other liquid as a carrier medium for large distance or short distance transportation of bulk materials. These kinds of pipelines are used in many industries applications involving transportation of materials such as mineral ores to processing plants, disposal of waste materials like fly as to disposal sites and coal to thermal power plants. Slurry pipelines have

been adapted as reliable, safe and attractive mode of solid material transportation by most of industries due to advantage of low maintenance and being eco-friendly. To have wider applications, there slurry pipelines can be laid over different terrain such as mountains, under deep sea and across bodies which are difficult to exploit for conventional modes of transportation. Other features of these pipelines help to reduce traffic congestion, noise and air pollution.

1.12 Coal-oil mixture technology

In general the "coal-oil" means any solid hydro carbon in pulverized form like coal in liquids at atmospheric temperatures such as heavy residues, high speed and light diesel oil, fuel oil etc. coal oil mixtures are prepared by homogeneously mixing pulverized coal in oil with or without the use of additives.

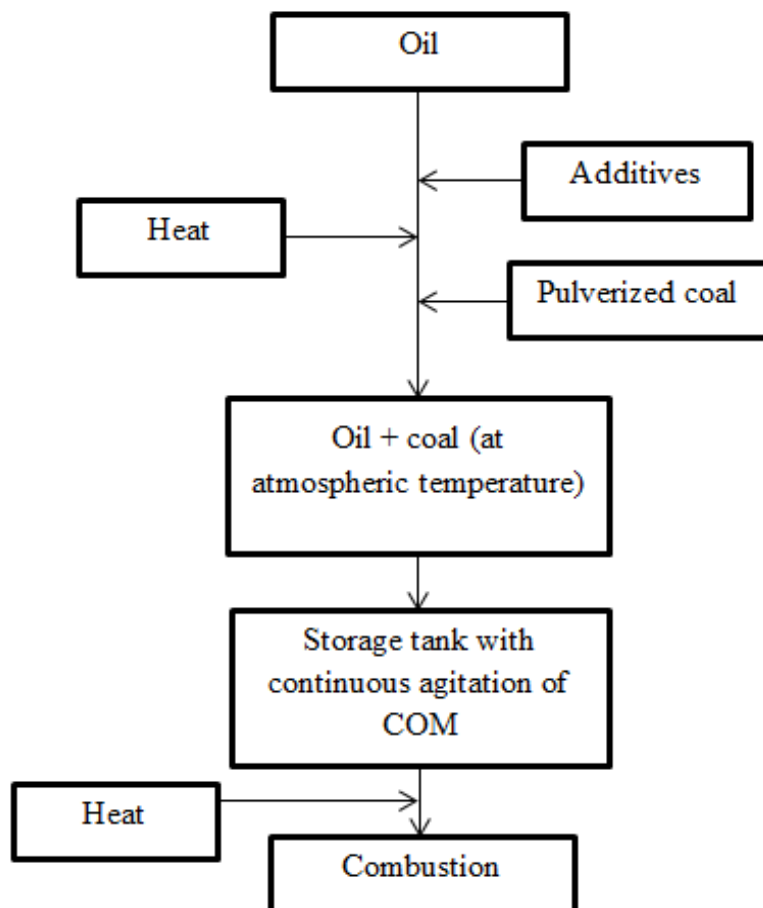


Fig. 1.18 Typical example of coal-oil mixture technology

Initially the oil mixed with pulverized coal so that it can be brought to a flow able condition. Then the required amount of additive mixed to oil along with the required weight of coal in agitation tank. The coal-oil mixture (COM) so organized is then finally kept in a storage tank equipped with an agitator to avoid settling of solid particles. Coal-oil mixture (COM) is heated during atomization and pumping before processing for combustion.

1.13 Requirement and uses of coal-oil mixtures

Requirements for coal-oil mixtures:

- Viscosity must be such that so as to reduce pumping costs.
- The slurry must burn as pollution free as possible.
- The coal oil slurry must be stable for long duration.
- The solid particle must not settle with time.
- Slurry must be non-corroding and non-abrasive.

Uses of coal-oil mixtures:

- Can be utilized as an alternative fuel for oil fired boilers.
- Can be used as fuel for industrial boilers.
- Can be consumed as supplementary fuel during peak load hours in a coal fired boiler.
- Can be used as an alternative fuel in blast and utility furnaces.

1.14 Role of rheology in the design of coal-slurry

The transportation of solid material in particle form by using hydraulic conveying is well known method in mining and chemical industries. Fluids are used as transportation medium in various industries. Complete knowledge regarding the principle of slurry transportation, the phenomena concerning solid transportation leads to well-organized as well as secure system for haulage. Slurry transportation through pipeline can be economical way and environment friendly as compared to road and rail transportation **Wilson et al. (2005)**. Conventionally the slurry transportation using pipelines were based upon moderate concentration (25% by volume). These days higher concentration transportation is in common use. But the high concentration multi-sized particulate slurry is kind of very complex **Kaushal et al. (2013)**. The designer should have precise knowledge regarding pressure drop, critical velocity, flow regimes and hold up etc. for designing pipelines. Though in many industries, such as oil, gas industry, petroleum and chemical industry, two phase or

multiphase is habitually used. The simultaneous flow of several phases can be called as multiphase flow. The two phase flow is made from two distinct phase such as gas-liquid, gas-solid or solid-liquid that coexists in arbitrary space. For two phase flow, basically in solid-liquid, the solid phase exists as discrete particles where liquid phase is continuous. The study of two phase flow is vital from viewpoint for practical applications such as hydro-transport of particles in pipe and pneumatic transport and natural phenomena (biomedical flow and sediments transport in water bodies). Flow which consists of granular materials can be found in mining, petrochemical and chemical and food industry. The flow phenomena for two phase flow are more complex as compared to single phase flow due to presence of dispersed phase. The problem arises when dispersed phase undergo fluctuating or continuous collision with other solid particles or when there is turbulence in flow. In this case, the solid particles mainly modified the fluid phase features due to not following the flow. Some of the advantages associated with pipeline transportation of solids are enumerated below:

- Simplicity in installation as compared to construction of rail road and new highway.
- Less requirement of man power for operation, construction and maintenance.
- Eliminating the traffic problem related with trucking.
- Possibility of complete automation.

However, some limitations are also there for pipeline transportation, some of these are:

- Initial capital cost is comparatively high.
- The pipeline transportation system is especially devoted to transportation of solids whereas highway and rail road has multipurpose utility.
- There is requirement for liquid as carrier fluid in large amount for pipeline transportation which may not be easily available for some places.

1.14.1 Basic Slurry Transportation System: The transportation of mixture can be done either on hydraulic basis or on pneumatic basis. As the only difference in both systems is in their nature of fluid, that has to be transported. Slurry transportation may be different depending upon material that has to be transported and the end requirement. Typically, a general schematic outline of mixture transportation is described in figure. A mixture transportation system can be generally distributed into three sub systems namely-

- i) Main pipeline and pumps ii) Slurry preparation facility iii) Terminal facility

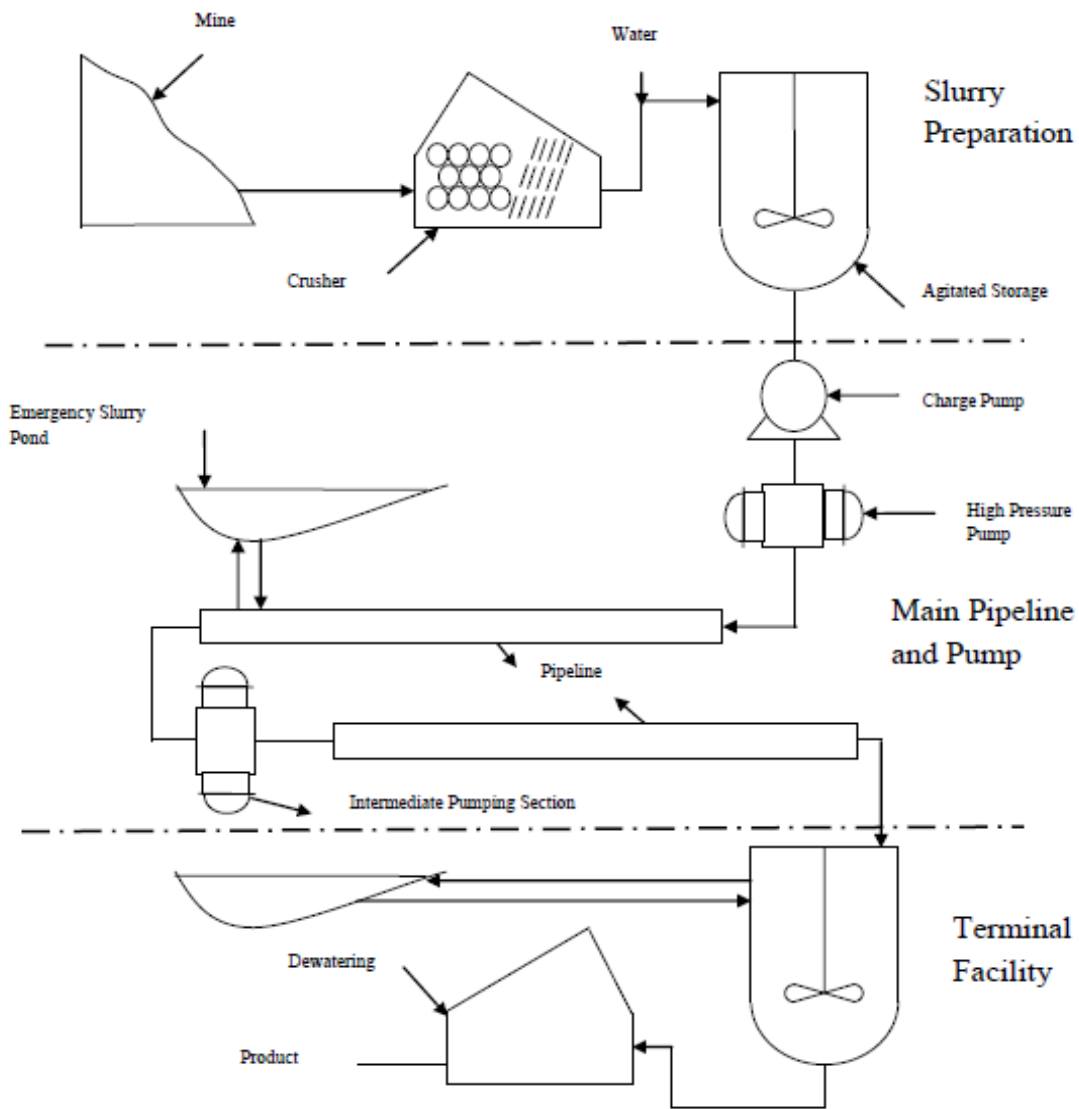


Fig. 1.19: Schematic layout of a long distance slurry pipeline [4].

Firstly, the main step is to crush the solid to convenient size so as to provide technically and economically way to fulfil the necessary requirement for power plant for their slurry transportation with the help of carrier fluid. Further, the optimum mixing of solid and liquid is done in the second stage. Finally the slurry is kept in an agitated or non-agitated storage tank as per the requirement. Depending upon the slurry transportation distance, the overall pumping requirement may be provided from either single point or more than one points throughout the length of pipe. The mixture is received at the terminal end in storage tank. For hydraulic conveying when water is used as a carrier fluid, the slurry needs to be processed for dewatering, filtered and for drying for the end utilization of solids.

1.15 Leaching

Thermal power plants produce ash in large quantity from burning of coal. In India, the major source of fly ash is produced from 125 thermal plants. In 2012, 150 million tons of fly ash is produced annually in India which is to be expected to rise to 200 million tons by 2020. This has caused problem a serious threat to the environment and requirement of large land for ash disposal. Fly ash can be used in domains like building industry, concrete, soil stabilization etc. but only a small amount of total fly ash is being utilized. One of the objectives of present study is to reduce the ash content of coal by chemical leaching so as to provide reliable information about the adverse impact on environment and its utilization as a supplemental material for future use in various industries.

Leaching can be defined as extraction of minerals from solids by dissolving them in a liquid, either in artificial form or through natural process. During leaching, components of solid are released into contacting liquid phase. While some of the species may be more of ecological concern than others, leaching is indiscriminant such that all constituents (organic and inorganic contaminants) are released under a common set of chemical processes which include desorption, desorption, complexion and mass transport processes and mineral dissolution. These phenomena are greatly influenced by certain factors that can affect the extent or rate of leaching.



1.16 Computational fluid dynamics (CFD)

CFD is considered as powerful tool which adopt algorithms and numerical method formodeling actual behaviour of fluids. It helps to optimize the design parameter with neglecting the use of costly multiple prototypes. CFD is considered as powerful graphical tool that helps to visualize flow designs that gives vision to flow physics that else would be costly and difficult to perform experimentally. Governing equation helps to model fluid behaviour but it becomes difficult to apply to complex flow pattern with too many unknown parameters. Yet, CFD creates computational mesh to split the real design continuous fluid into number of discrete sections. Then governing equation to flow can be functional individually for each section nonetheless the properties of each and every segment are allied to the neighbouring section. For this all section must be solved simultaneously to have full clarification for complete flow field. The accuracy and validation depend upon many factors

such as interpretation of result, flow model, level of convergence of solution, accuracy of boundary conditions and the quality and appropriateness of mesh.

1.16.1 Pressure Drop: The main purpose of slurry pipeline designs involves the estimation of head loss and to find the power requirement under operating condition. Several correlations for predicting the pressure drop can be found in literature that are mostly of empirical nature. These relations have been developed on basis of experimental data or rheological parameters on different multi-sized homogeneous slurries. Some of the correlations have been based on narrow data comprising of limited or uniform size-range particles with low to high concentration. Basically, these equations are prone to great hesitation as one leaves from narrow database that support them.

Chapter 2

Literature survey

2.1 Literature review

A lot of research work has been done in the past to investigate the rheological behaviour of coal oil mixtures from different perspectives. Various factors that affect coal-oil mixture rheology have been investigated by researchers. Some of the literature scenario has been given below

Adigaet al. (1983) studied rheological behaviour of coal mixtures in no.2 fuel oil and ethanol with varying concentrations of water at ambient temperature. Rheological measurements were made using Brookfield cone plate viscometer. For calculation of viscosity the shear rate was varied from 1.15-230 s⁻¹. It was found that in the presence of water the mixtures had a tendency for incursion of yield stress and it was also observed that the presence of water, decreases the viscosity of the mixtures. For low coal concentration mixtures, it was observed that when the concentration of water increased, both viscosity and yield stress of mixture increased. The rheological parameters were calculated using the power law and Bingham plastic models. The mixtures behaved as dilatant, Newtonian or pseudoplastic, depending upon the concentration of water, at lower shear rates. At higher shear rates the mixtures depicted pseudoplastic behaviour. It was also observed that mixtures having higher coal concentrations behaved as pseudoplastic fluid for all concentration with water. At 10% of water concentration, both viscosity and yield stress depicted a maximum value.

Adigaet al. (1988) studied rheological behaviour of coal mixtures in no.2 fuel oil and ethanol with varying concentrations of water at ambient temperature in the presence of surfactant. The surfactant used was TRS10-80 (petroleum sulfonate). Rheological measurements were made using Brookfield cone plate viscometer. For calculation of viscosity the shear rate was varied from 1.15-230 s⁻¹. It was found that in the presence of water the mixtures had a tendency for incursion of yield stress and maximum value of yield stress was found at 10% water concentration. It was also observed that when surfactant was added to mixture there was a significant reduction in yield stress. The

rheological parameters were calculated using the power law and Bingham plastic models. It was also observed that when concentration of surfactant was 0.25%, the flow behaviour of mixtures changed from yield pseudo plastic to Newtonian.

Steel et al. (2001) attempted on Australian black coal for production of ultra-clean coal. In study, author utilized hydrochloric acid for dissolution of most of mineral matter present in coal sample. HCL can be dissolved in compounds such as phosphate and carbonates but does not dissolve compounds such as clays and reaction products have to be water soluble which was reported by them. It was found that extent of dissolution of a coal sample was found as a function of HCL concentration at 20°C, 70°C and 100°C. Their experiments were recorded that approximately, 10% wt of the coal sample was notified to be dissolved by HCl at 20°C and extent of dissolution was found to be more when the temperature is raised to a value of 70°C and 100°C. It was also revealed from their experiments that approximately 23% of wt of sample dissolution in HCL concentration of 5.6 M at temperature of 100°C. It was observed that HF was reacted with alumina silicates in mineral matter and form largely AlF_2^+ , AlF_3 and SiF_4 and free fluoride (F^-) and AlF_4^- . From their experiments, it was evident that when the mineral matter in coal treated with HF concentration was greater than that required to dissolve all alumina silicates, AlF_3 , AlF_4^- , SiF_2^- form, the concentration of F^- is high enough to complex Ca^{2+} , Mg^{2+} and form insoluble CaF_2 and MgF_2 .

Steel et al. (2003) produced ultra clean coal by sequential leaching with HF followed by HNO_3 . In this study, the bituminous coal containing sulphur 2.4% by weight, ash content of 5.0% by weight and with particle size less than $62\mu\text{m}$ was used. The sample was treated with sequential leaching of aqueous solution of HF and HNO_3 with different molar ranging from 0 to 1.58 M. the results reveals that after the treatment, the S and ash content reduced to 1.3% by weight and 0.2% by weight respectively. Also there is loss in CV to 29.5 from 31.5 MJ/kg with increase in nitrogen content from 2 to 2.8% by weight which occurs due to attack on carbonaceous matrix. Also during the HF washing, the fluoride content of coal increased to 3240 ppm from 80 ppm yet drops to 130 ppm for the HNO_3 washing. It was found that HNO_3 reacts simultaneously with carbonaceous matrix and pyrite.

Niket al. (2005) examined the rheological properties of different bio-edible oils which included palm, coconut, canola, corn and sunflower oils. The rheological properties were

measured with the help of a Brookfield rotational type viscometer. The temperature was varied from 40°C-100°C and shear rate was varied from 3-100 sec⁻¹. Numerous rheological models such as Arrhenius, Carreau, Ostwald de-Waele and Herschel–Bulkley were used to regulate the flow behaviour of oils. It was found that both shear rate and temperature had a considerable effect on the deviation of apparent viscosity and it was also observed that temperature had more significant impact as compared to shear rate. Results from rheological model fit indicated that the bio-edible oils belonged to pseudo plastic (shear thinning) category. Also the palm oil and sunflower oils were extremely steady in terms of shear rate and temperature, respectively.

Cui et al. (2007) investigated a novel process for the preparation of ultra-clean superfine coal–oil slurry (UCSFCOS). The study involved pumping slurry jet mill and high-pressure water-jet mill. The mean diameter (d_{50}) of coal sample in the suspension was 2.71 μm whereas 1.05% by weight of ash content. The parameters involved that were investigated are stability, rheological behaviour, and heating value of suspension. The result reveals that UCSFCOS contains great heat value, a great stability level, and low apparent viscosity. UCSFCOS can be considered for high speed diesel engine as an application. The requirement of total energy consumption by coal particles to reduce d_{50} from 3 mm to nearly 2.71 μm is 124 kW h per ton whereas the traditional ball milling required 50-70% more energy.

Zhiheng et al. (2007) have utilized the UK bituminous, Harworth (HW) coal for experimental works. The coal was air dried then followed for grinding to a particle size <52 μm coal samples. In the first stage they have used HF at 65°C and ash content has been enumerated by them to be reduced from 5.30 wt% to 1.37 wt% by largely eliminating Al as well as Si containing minerals. Subsequently, these hydrofluoric acid treated coal have leaching with ferric ions as $\text{Fe}(\text{NO}_3)_3$ and it was reported by them to be decreased the ash content further to 990 rpm by removing pyrite and fluoride bearing compounds during HF leaching. CV of coal have revealed from their experimental results that almost no change in calorific value. The dissolved coal samples by suitable chemicals have separated by using filtration by them. They have flashed off the solvent used to be reused and recover a solid mineral free coal product reused. The experimental results investigated by them shows that the hydrochloric acid (HF) has reacting to most of the mineral matter present in

coal sample. Although, they have also envisaged that HF has not reacted with pyrite and formed significant levels of insoluble fluoride compounds. Ferric ions (Fe_{3+}) have employed by them able to oxidized pyrite and also dissolve formed insoluble fluorides because of great stability of iron-fluoride complex.

Yong-gang et al. (2009) investigated the rheological properties of Shengli lignite coal solvent slurries. Three different types of solvent hydrogenated recycle solvent (REC), heavy oil (HAR) and tetralin (THN) were used in the study. The effect of various parameters like temperature, shear rate, particle diameter, coal to solvent ratio and type of solvent were studied. Rheological properties were measured with the help of a rotary viscometer (NXS-11A). Shear rate was varied from 0-1000 s^{-1} and temperature was varied from 30°C-70°C. It was found that with the increase in temperature the behaviour of coal-solvent slurries altered from pseudo plastic fluid to Newtonian fluid. It was also observed that when coal to solvent ratio was increased the behaviour of coal-solvent slurries altered from Newtonian fluid to pseudo plastic fluid. These transformations occurred at 40°C, when REC was used as solvent and at 60°C, when HAR was used as solvent.

He et al. (2011) studied the impact of PSD of petroleum coke on the various properties like static stability, apparent viscosity and rheology of petroleum coke-oil slurry. The rheological measurements were made by using a rotary viscometer (NXS-11A). Shear rate was varied from 0-100 s^{-1} . Temperature was kept constant at 100°C. Scanning electron microscopy and zeta potential techniques were applied for studying the size and morphological characteristics of coal particles with variation in grinding time. It was observed that coal concentration of 30-35% by weight and grinding time of about 1 hour were suitable for the petroleum coke oil slurry. Rheological models were used for investigating the flow behaviour of the slurry and it was observed that the slurry exhibited pseudo plastic behaviour having decrease in viscosity with increase in shear rate.

Chen et al. (2011) investigated the rheological behaviour of lignite char, bio-char and coal slurry fuels. Different solids like biomass char, sub-bituminous coals and a low rank coal were used for the preparation of slurries. These solids in pulverized form were mixed with water along with different additives which included polyacrylic acid, sucrose and co-polymers D-101 and D-102. The rheological properties of the slurries were measured by using Brookfield viscometer. HAAKE VT 550 cone and plate viscometer was also employed for measuring the rheological properties of the slurries at constant shear rates.

The effect of various properties like particle size distribution, solids concentration, additives concentration and type of solid on rheological behaviour of slurries was determined in terms of yield stress and apparent viscosity. It was observed that high concentration slurries with relatively lower values of yield stress and apparent viscosity could be prepared when additives D-101 and D-102 were used. Rheological models were used for investigating the flow behaviour of the slurries and it was observed that the slurries made from low ash lignite, in the presence of these additives exhibited Newtonian and mild dilatant behaviour at higher solids concentrations. It was also observed that the maximum solids concentration that can be used without having a considerable increase in apparent viscosity was found to be 40% for biomass char, 55-62% for sub-bituminous coals and 65% for lignite coal.

Ren et al. (2011) studied the viscosity variations of coal-oil slurry (COSL) under high temperature and high pressure during heating process. The material use for the study was Yanzhou coal (caking and middle rank), Shengli coal (brown coal) and Shenhua coal (non-caking and low rank) and anthracene oil for preparation of COSL. The rheological properties were measured with the help of a rotary viscometer. The COSL from three samples with same environmental conditions showed different viscosity variations for high hydrogen pressure during the process of heating. Yanzhou COSL had a sophisticated viscosity peak, while Shenhua COSL contains two insignificant viscosity peaks and in the case of brown COSL, no such viscosity peak was formed with high hydrogen pressure during heating. It was found that the coal nature was an important factor for viscosity variations of COSL. It was observed that higher was the coal grade, the supplementary caking coal was present, and supplementary was the viscosity variation of the COSL.

Jorjani et al. (2011) produced UCC by microwave irradiation pre-treatment and sequential leaching with HF followed by HNO₃. The coal samples were collected from Iran's Zirab and Tabas coal preparation plants having ash content 8.31 and 10.36 wt% respectively. The proximate analysis, ultimate analysis and XRD were performed on samples to determine ash content, elementary composition and mineralogical composition respectively. The effect of ash removal, including irradiation time for microwave pre-treatment, leaching agent concentration, leaching temperature, PSD for HF acid leaching and washing time for nitric acid washing were examined. The result indicates that reduction in ash ranged from 22 to 76% and from 22 to 82% by weight for Zirab and Tabas coal respectively for HF treatment. Coarse size fraction of coal can be pre-treated

for microwave irradiation. Coal particles having fine size particles were suitable to reduced leached time. When treated with HNO₃, the ash content for Zirab coal reduced to 0.69% from 2.57% and for Tabas to 0.39% from 2.44% by weight for leaching time of 3 hour. The result can be considered as pre-treatment process in chemical washing to produce UCC.

Wang et al. (2012) investigated the rheological behaviour of petroleum coke–sludge slurry (PCSS). The various properties of PCSS like slurry ability, rheology and fluidity were analysed. The rheological properties were measured with the help of a rotational concentric cylinder viscometer (NXS-4C). Measurements were done at temperature of 20±1°C. The results showed that the fixed-viscosity of PCSS solid decreased with increase in sludge mixing proportion (SMP). The flow behaviour of slurry was changed to shear thinning behaviour from shear-thickening behaviour after the addition of petrochemical sludge. The pseudoplastic behaviour was enhanced with increase in either SMP or solid content. Furthermore, the sludge had significant effect to improve slurry stability. The rheological data perfectly fit for Herschel–Bulkley model (R²>0.998).

Mazumder et al. (2012) analysed the effect of elbow radius on pressure drop in multiphase flow using CFD. The CFD was performed in four different 90° elbow radius having air water two phase flows. The internal diameter of elbows was 6.35 mm and 12.7 mm with curvature ratio (R/D) varies from 1.5 to 3. The pressure drop was investigated at two different downstream and upstream locations using experimental, empirical and computational methods. The velocity employed for experiment ranges from 15.24 to 45.72 m/sec with step size of 15.24m/sec for air whereas in case of water, the velocity ranges from 0.1 to 10m/sec. The mixture model was employed with commercial code FLUENT. The linear line represents in Fig. 2.10 depicts a perfect line. The points above linear line are over predicted, while below linear line, it is under predicted for pressure drop. However for elbow 1 and 2, the result was under predicted and the result for elbow 3 and 4 elbow was closer to the linear agreement line.

Mazumder et al. (2012) studied the CFD analysis of single as well as two-phase flow. The analysis was performed for 90° horizontal to vertical elbow with 12.7mm inside diameter. In this, flow behaviour (characteristics) was investigated for downstream as well as upstream at six different locations. Using three different velocities for air and water, the

effect of different phases was evaluated. CFD FLUENT was utilized for analysing single as well as multiphase flow but at commercial level. The result for Pressure and velocity profiles for mentioned location showed rise in pressure for elbow geometry with reducing pressure as fluid leaves from the elbow. It was observed that similar kinds of results were obtained for pressure drop for both the cases. The comparison of simulated result with empirical models was found to have good agreement.

Xuet al. (2014) investigated the rheological behaviour of coal–oily-sludge slurry (COSS). Sodium sulfonate formaldehyde condensate (NSF) was used as a dispersant at a fixed ratio of 0.8 g/100 g dry fuel (oil and coal) in the preparation of COSS. The rheological properties were measured with the help of Malvern Bohlin CVO rheometer. Measurements were done at temperature of $25\pm 0.1^\circ\text{C}$. Shear rate was varied from 0-100 s^{-1} . The results showed that apparent viscosity of COSS decreases with increasing the ratio of oily sludge when oily sludge was firstly mixed with coal. As more oily sludge was added, the yield stress of COSS gradually decreased. The maximum solids loading of COSS increased from 62.2 wt% to 64.0 wt% when oily sludge was added in a ratio of 10.0 wt%.

Dutta et al. (2015) studied the pressure drop characteristics of single phase turbulent flow in 90° pipe bend for high Reynolds number. The pressure drop was studied numerically in computational fluid dynamics (CFD) by opting the k- ϵ RNG turbulence model with the help of standard wall function. For this, after the validation of model with existing experiment results, the complete analysis was executed to study the pressure drop for low and high Reynolds number and the pressure distribution to have pressure loss coefficient at different location in pipe, in terms of curvature ratio (R_c/D) and Reynolds number so as to have cost effective solutions to design 90° bend. The result on the inner core shows normalised pressure that increases with curvature ratio and pressure difference comparatively between outer and inner core of 90° bend decreases with increases curvature ratio and remain constant for high curvature ratio. The pressure loss coefficient is maximum at 30° , due to secondary flow and magnified swirl intensity for high Reynolds number and pressure varies along central symmetry plane for different location for different Reynolds number.

Sui et al. (2015) investigated the rheological behaviour and steam gasification of bio-slurry. A new approach was developed for the use of bi-products of bio char and bio-oil,

which can be imitative from biomass gas station. The bio-slurry was made from blended bio-oil with bio char at different concentration. Hydrogen produced from steam gasification was also investigated. The result shows that the bio-slurry fuels have improved properties comprising stability and calorific value as compared to the fast pyrolysis products. Also the apparent viscosity of slurry changes by introducing bio-char in bio-oil. The apparent viscosity was too affected by the temperature. The result indicates that bio-slurry exhibits good stability. The steam gasification can create enrich hydrogen gas and high gas yields (CO and H₂) was obtainable at 900°C.

Singh et al. (2015) examined the influence of particle size distribution (PSD) and temperature on rheological behaviour of coal water slurry. The effect of solid concentration, temperature and particle size on rheology was investigated. The Anton Parr rotary type rheometer with bath tub was used for the investigation. For particle size less than 75µm in slurry, the increase in apparent viscosity was observed with increase in solid loading of coal. Also the apparent viscosity of mixture decreases with decrease in temperature. With increase in solid concentration the slurry behaviour changes from shear thinning behaviour to shear thickening. Also the rheology of blended coal samples of coarse and fine particles by making bimodal PSD were investigated with different particle sizes. The blended of bimodal was done by mixing fine (53-75µm) and coarse particles (106-150µm). The result shows that at 30% of bimodal slurry sample the apparent viscosity of mixture is found to least as compared to other proportions. The rheology data was best fitted for power law for 30% solid concentration and higher concentration fitted best for Herschel-Bulkley model.

Ganeshan et al. (2016) studied the influence of oil viscosity on rheology of Indian coal and furnace oil slurry. The concentration of slurry was taken up to 50% by weight and temperature was varied from 30°C to 70°C. The rotational type viscometer (Haake RV 100) with MV II sensor system was employed for measuring the viscosity. The result indicates that high viscous and low viscous slurries exhibit Newtonian behaviour at given temperature with 50% solid concentration. Also for high viscous oil slurry, the ratio of suspension viscosity to oil viscosity remains same throughout at specific concentration of coal. A correlation has been developed for relative viscosity of suspension which helps to calculate the apparent viscosity when viscosity of oil is already known.

2.2 Gaps in literature:

A lot of research work has been done in the past to investigate the rheological behavior of coal oil mixtures from different perspectives. Various factors that affect coal-oil mixture rheology have been investigated by researchers. However, a gap in study reveals that so far very limited work has been done on investigating rheological properties of coal-oil mixtures with variation in temperature and coal properties such as ash content and coal blending of different ranked coal. In the present study, prior to the research work, an extensive review of the published works in the field of coal-oil mixture technology with an emphasis on the effects of different factors like solids concentration, temperature, chemical leaching and coal blending of different ranked coal that affects the rheological behaviour of coal-oil mixtures.

Chapter 3

Characterisation of coal

Objectives

- Characteristics of collected coal for conversion of high ash coal to low ash coal with chemical leaching.
- Investigation of rheological characteristics of coal oil suspension by making comparison with chemical leached coal and different ranked coal by making blends, particle size and at different temperature.
- Simulations of pressure drop in pipe bend for two phase fluid using Computational Fluid Dynamics (CFD).

3.1 Introduction

In India, fossil fuel satisfies about 67% consumption of total energy, out of which 57% of chief commercial energy is produced by coal [25]. As India is the third major fabricator of coals, having coal assets of 293.5 billion tons thus contributing distinctive fuel source for Indian domestic energy market [26].

However coal is obtainable in abundance in India, nearly 87% of accessible coals are of inferior quality containing inorganic non-combustible content i.e. ash about 40% to 45% by weight [25]. During the combustion process of the coal, the inorganic constituents that are present in coal undergo various physical as well as chemical transformations that results into fly ash and bottom ash. The fly ash particles that gets carried away by the flue gases deposited on various heat-transfer surfaces causes fouling and slagging that results in reduction of heat transfer, reduces the flow area, obstruct the aerodynamic flow of flue gas and results in corrosion as well as erosion of boiler tubes, as a result affecting the efficiency of a boiler [27-31]. The ash content can be reduced by the chemical leaching of coal before combustion so as to reduce these effects. Also the environmental concerns that are initiated by the fossil fuels and the land requirement for high ash disposal can be reduced by adopting the coal beneficiation process.

Ultra clean coal (UCC) can be defined as the process of conventional method

washing of ground into fine particles of coal with chemical treatment so as to ash content in coal will be less than 1% by wt. UCC has wide number of applications outside of a fuel because of its high purity carbon material. The potential use of UCC can be considered for silicon smelting industry [32]; for the production of coal slurry fuel for replacement of oil in diesel engine [33, 34]; producing activated carbon utilized in filters for air and water purification [35]; replacing petroleum coke by using fabricated carbon anodes [36] and helping as fuel for new power generation technologies for example direct firing in gas turbine [37].

Normally the washing of coal only with water possessing physical technique cannot reduce the mineral matter present in coal according to the requirement for producing Ultra clean coal. Therefore chemical leaching process has been opted using physical technique for production of UCC.

But currently there doesn't exist technical and viable process for producing UCC. The chemical leaching process to reduce mineral matters includes leaching with help of caustic soda [38]; HNO_3 [37, 43]; HCl [37]; HF [37, 43]; H_2SO_4 [39]; oxidizing agents, such as H_2O_2 [40]; FeCl_3 [39]; mixtures of HF and HCl [41]; and sequential leaching by $\text{NaOH-H}_2\text{SO}_4$ [42].

Two stage chemical washing of coal with aqueous HF followed by HNO_3 washing was considered as an effective washing method for coal demineralization. As treatment of coal with HF removes insoluble fluoride compounds whereas HNO_3 removes the pyrite sulphur when its concentration exceeds a particular level [43]. The objective of this work was to study the effect of leaching concentration so as to produce the UCC from low rank Indian coal thereby reducing the high ash disposal problem, for gas turbine to reduce erosion and corrosion of blades that is caused by mineral matter present in gas and for reducing the fouling of the economizer.

3.2 Collection of samples

Three different Indian coals in briquetted form, each varying in ash and moisture contents, were collected from different thermal power plants of origin of India i.e. L & T thermal power plant, Rajpura (labelled as Coal B), Glaxo Smith Kline Pvt Ltd. Nabha (labelled as coal A) and from Yamunagar. The various characterization studies that were done on the three coal samples included Chemical leaching, simulation of pressure drop and proximate

analysis. Also particlesize distribution curves were generated for three coal samples in order to find the mass mediandiameter of coal samples.

3.3 Material and method

Initially, the coal samples have been consisting of large sized lumps. From the large lump size coal sample experiments used coal samples were prepared by employing the following sequential operations like crushing, grinding and finally particle size distribution. The detailed procedure of the investigation is represented by Figure 3.1. The sample was further processed for dry sieving method using mechanical sieve shaker to obtain particle size $<106\mu\text{m}$ having sieves of BS-410 (British Standard). The sieve analysis was used to study the particle size distribution of pulverized coal. For the leaching of coal, 15 gram of pulverized coal was treated with 100ml aqueous solution of HF (hydrofluoric). The concentration of HF in aqueous solution varies from 10 to 40% for 8 hours duration at atmospheric pressure condition. After filtering the coal sample using filter paper, the demineralized coal was again treated with HNO_3 (Nitric acid) for 3 hours duration. After filtration of treated coal, percentage of ash in the coal sample was determined using muffle furnace. The calorific value of coal was calculated with the help of bomb calorimeter. Energy dispersion x-ray spectrograph (EDS-JEOL, 6510LV) was used to measure the morphology and elementary composition of untreated and ultra clean coal sample.

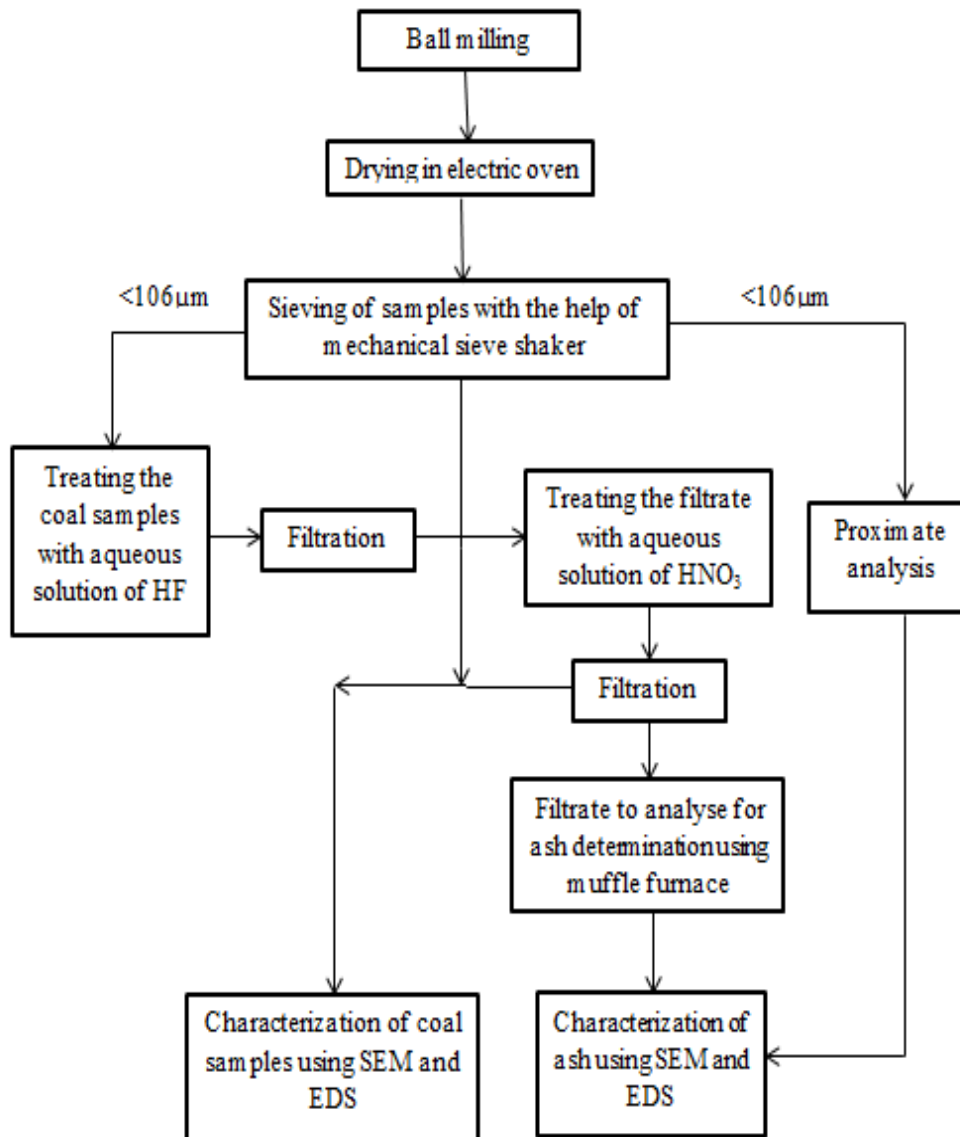


Figure 3.1 Process diagram for the materials and methodology

3.4 Coal sample preparation

Originally, coal samples were comprised of large sized lumps. From the large lump size coal sample experiments used coal samples were prepared by employing the following sequential operations like crushing, grinding and finally particle size distribution. Coal was crushed with the help of jaw crusher and roll mill to obtain the particle size of coal less than 5 cm. The crushed coal was again processed for pulverization in stainless steel ball milling at 120 rpm, with the ball to coal sample ratio of 7:1. The pulverized coal sample was dried in electric oven for 3 hours at $115\pm 2^{\circ}\text{C}$ to remove moisture from the coal.

3.5 Particle size distribution (PSD)

To understand the chemical as well as physical properties of coal samples, PSD has been performed using mechanical sieve shaker having BS-410 (British Standard) sieve on the basis of dry sieving method. The sample retained on each sieve was collected and each of the size fractions so obtained was separately analysed for particle size distribution and the amount retained on each sieve was considered by using standard technique to acquire the sieve curve. Meanwhile each coal sample was sieved for 30 min in a sieve shaker available in sand testing laboratory (Mechanical Engineering Department, Thapar University, Patiala) using sieves no.8, 10, 16, 22,30,44,60,100,150,200 and 300. In this experiment particle size varies from 2000 μ m to 53 μ m. The figure 3.5 shows the particle distribution of two samples of coal. The graph is plotted between the percentage finer coal and the particle size measured in microns.

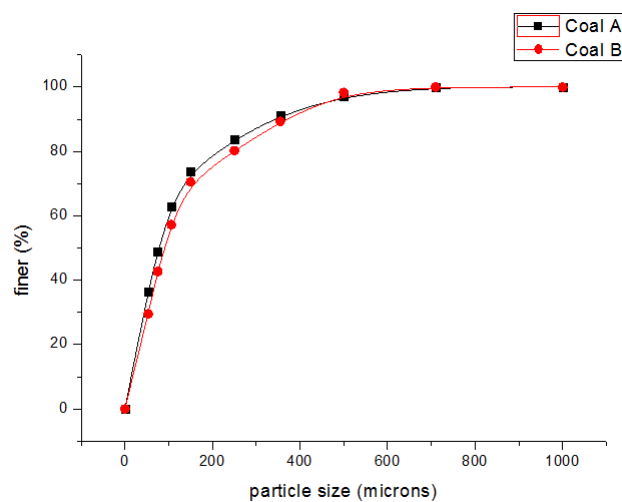


Figure 3.2: Particle size distribution (PSD) of two coal samples

3.6 Proximate analysis and EDS

The proximate analysis of coal was achieved to determine the percentages of ash, inherent moisture, fixed carbon and volatile matter present in a particular sample. The proximate analysis based upon air dried of the three coal samples was conducted according to given testing method of IS: 1350 and the result of the proximate analysis on air dried basis is shown in Table 3.1. Energy dispersion x-ray spectrograph (EDS-JEOL, 6510LV) was used to measure the morphology and elementary composition of untreated and ultra clean coal sample.

Table 3.1: Proximate and EDS analysis on air dried basis

| | Element | Coal A | | Coal B | |
|--------------------|-----------------|----------|----------|----------|----------|
| Proximate analysis | | Weight % | | Weight % | |
| | Volatile matter | 30 | | 27.42 | |
| | Fixed carbon | 58.28 | | 32.46 | |
| | Ash content | 11.72 | | 40.3 | |
| | Total | 100 | | 100 | |
| EDS | | Weight % | Atomic % | Weight % | Atomic % |
| | C | 67.94 | 74.57 | 59.34 | 67.62 |
| | O | 29.17 | 24.04 | 34.75 | 29.73 |
| | F | 0.39 | 0.27 | 0.04 | 0.03 |
| | Al | 0.77 | 0.38 | 1.97 | 1.00 |
| | Si | 1.27 | 0.60 | 2.52 | 1.23 |
| | S | 0.26 | 0.11 | 0.35 | 0.15 |
| | Ti | - | - | 0.46 | 0.13 |
| | Zn | 0.19 | 0.04 | 0.57 | 0.12 |
| | Total | 100 | 100 | 100 | 100 |

3.7 Morphological characteristics of coal samples

The morphological studies on coal samples were done by scanning electron microscopy (SEM) technique. SEM enables the investigation of specimens with resolution down to the nanometre scale. The SEM technique produces images of coal/sample by scanning it with a focussed beam of electrons. The electrons interrelate with the atoms in coal/sample, to produce various signals that can be detected and that contain information about the sample's surface topography as well as its composition. The sample preparation was done before placing the sample for the visualization of the optical images obtained as an output on a visual display unit. The SEM micrographs that were obtained for both coal samples are shown in Fig. 3.3-3.4

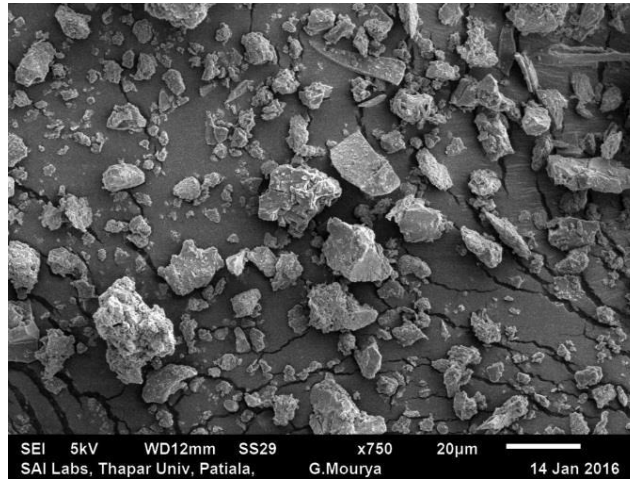


Figure 3.3: SEM micrograph of Coal A

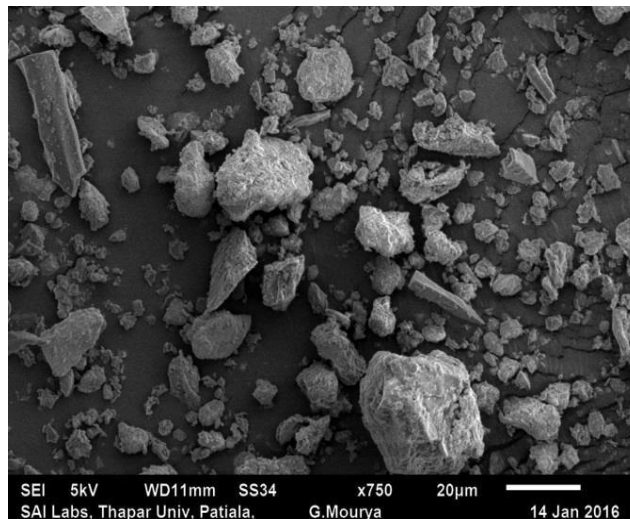


Figure 3.4: SEM image of Coal B

3.8 Bomb calorimeter

Bomb calorimeter was utilized to calculate the calorific value of coal. The CV of coal/sample is defined by number of heat units liberated with unit mass when sample is burned in an addition of constant volume with oxygen. The CV was measured by igniting the specific sample in high pressure oxygen environment enclosed in metal pressure container known as bomb. The energy was released during the combustion and that energy was being absorbed by the calorimeter resulting increase in temperature. The CV was then measured the standard formula that is proportional to rise in temperature.

3.9 Ash content determination

Ash content was decided by weighing the inorganic residue remaining after burning the coal or coke in air under severely organised environments of sample time, weight, temperature, and atmosphere and equipment specification. The ash generally consists of inorganic oxides of the mineral matter initially existent in the coal. Approximately 2 gram weighted of a coal sample was packed in an empty silica crucible. The coal sample was sited in a muffle furnace and ignited to 450°C in 30 minutes without lid. After that the temperature of the furnace was raised to 925±25°C and the sample was heated for about 1 hour at that temperature. After heating the sample, the crucible with the residue was placed in a desiccator and weighed after cooling the crucible. It was desirable to cover the crucible with a lid before it is placed into the desiccator since the rush of air into the desiccator, when it was opened, sometimes causes light ash to be blown away. If incomplete combustion was suspected, the incineration should be repeated until the weight was constant. The residue remained after heating was calculated to a percentage of the coal taken to report the ash content.

3.10 Results and discussion

3.10.1 Influence of leaching concentration on ash content: The washing of coal with chemicals has great impact on ash content of the coal. The ash content was determined by proximate analysis on air dried basis with the help of muffle furnace (IS-1350). The reduction of ash was calculated by using equation 1.

$$RA = \frac{z_1 - z_2}{z_1} \times 100 \quad (3.1)$$

Where z_1 represents reduced ash content in original sample and z_2 is ash content percentage in leached product. The ash content present in the coal sample with variation of concentration of leaching is shown in Figure 3.5. It is observed that concentration of chemical agent HF and HNO₃ greatly influence to ash content present in the coal. In the coal sample, initially ash content was found as 38.5% (by weight). After two stage leaching with 10% concentration of HF and HNO₃, the ash content in the coal sample was reduced to 28.14% (by weight). For given coal sample, 10% concentration of HF and HNO₃ was not sufficient to produce ultra clean coal [25]. With 20% concentration of HF and HNO₃, the ash content in the coal sample was reduced to 14.25% (by weight). Similar, the ash content get reduced to 3.5 and 0.9% (by weight) with the leaching concentration of 30 and 40% (by volume) respectively. Result data shows that ultra clean coal was

produced with the dual acid leaching of HF and HNO₃ at concentration of 40% (by volume). Table 3.2 represents the results for EDS for ultra clean coal.

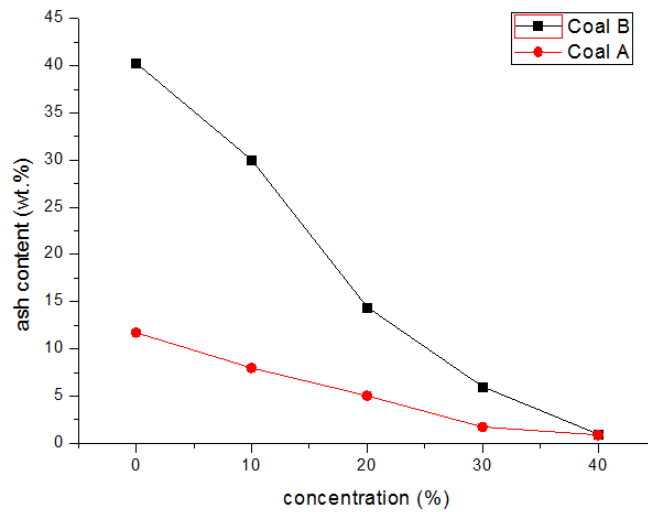


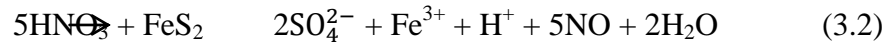
Figure 3.5: Percentage of ash reduction with increased concentration of aqueous solution

Table 3.2: EDS analysis of ultra-clean coal samples

| | Coal A | | Coal B | |
|-------|------------|------------|------------|------------|
| | Weight (%) | Atomic (%) | Weight (%) | Atomic (%) |
| EDS C | 56.04 | 62.73 | 52.58 | 60.99 |
| N | 3.10 | 2.97 | - | - |
| O | 40.77 | 34.26 | 43.83 | 38.16 |
| Al | 0.04 | 0.02 | 0.19 | 0.10 |
| Ti | 0.05 | 0.01 | 0.34 | 0.10 |
| Zn | - | - | 3.06 | 0.65 |
| Total | 100 | 100 | 100 | 100 |

3.10.2 Influence of leaching concentration on chemical composition of ash: When the coal was treated with HF alone, the mineral matters are largely flouride and pyrite that bears compounds like MgF₂, CaF₂ and NaAlF₄ but with the employment of HF and HNO₃ these flouride compounds as well as pyrite Sulphur was removed as represented in Table 3.3. Also there is little effect on C,O, Al and Zn, as the value for C and Al was reduced for both the samples whereas there is dramatically increase in the value of O and Zn for both

samples. From the discussion point of view, Fe in pyrite gets oxidized when reacted with HNO₃, from Fe²⁺ to Fe³⁺, and helps to oxidize the S in the form of sulphate SO₄²⁻ as represented by equation (3.2).

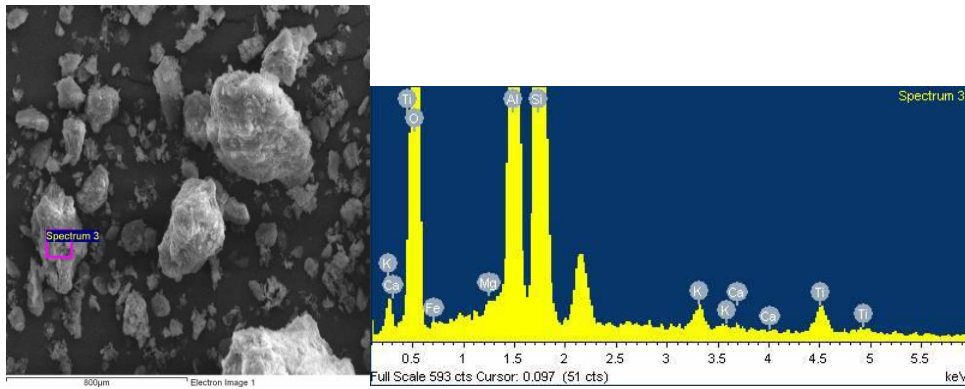


The reaction 3.2 represents that 5 mol of HNO₃ are required for every mol of pyrite. With the increased concentration of nitric acid, it can be seen that there is dramatic effect on carbonaceous matrix which leads to the loss of carbon as well as to calorific value but with increased nitrogen and oxygen content. The result shows that nitric acid, carbonaceous matrix all undergo reaction during the same period. Typically Al and Si are present in coal in the form of quartz such as (SiO₂) and the compounds of aluminosilicate like kaolinite (Al₂Si₂O₅(OH)₄) which reacts with the HF for the formation of fluoride complexed Si and Al species. During the HF leaching, the Al is not much extracted which is to be believed that NaAlF₄, AlF₃ and KAlF₄ precipitate. The Table 3.3 represents the slight decrease in Al₂O₃ and Na₂O when leached with both the chemicals. It is to be believed that the fluoride compounds have been dissolved. The level for CaO and MgO also reduces, the reason being that when HNO₃ is employed, H⁺ ions gets combined with F⁻ ions that are present in solution.

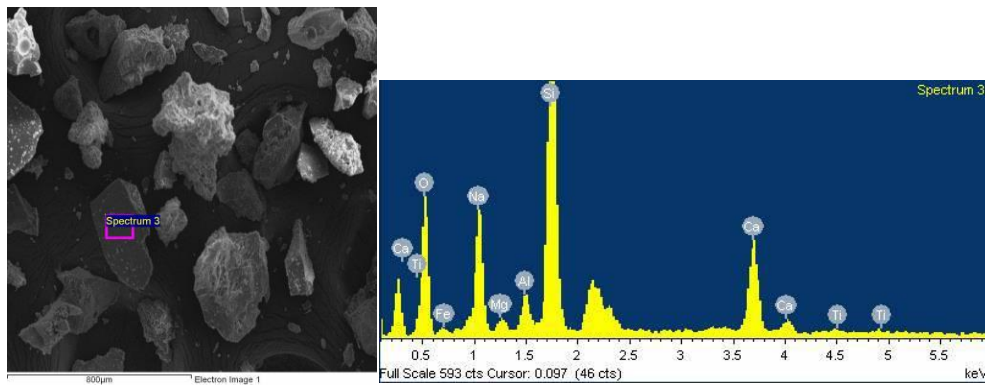
Table 3.3 Ash composition retained from untreated and ultra-clean coal

| Parameters | Constituents in ash (% by weight) | | | | | | | | |
|------------------|-----------------------------------|------------------|--------------------------------|------------------|------------------|-------|-------|--------------------------------|-----------|
| | Ash | SiO ₂ | Al ₂ O ₃ | K ₂ O | TiO ₂ | CaO | MgO | Fe ₂ O ₃ | Unburnt C |
| Untreated Coal A | 40.3 | 9.6 | 13.85 | 3.725 | 7.3 | 3.574 | 3.571 | 10.80 | 20.35 |
| Treated Coal A | 0.96 | 0.162 | 0.181 | - | 0.117 | 0.082 | 0.06 | 0.195 | 3.68 |
| Untreated Coal B | 11.2 | 2.385 | 3.606 | - | 2.051 | 1.014 | 1.013 | 3.105 | 6.22 |
| Treated Coal B | 0.87 | 0.25 | 0.29 | - | 0.117 | 0.082 | 0.06 | 0.195 | 26.56 |

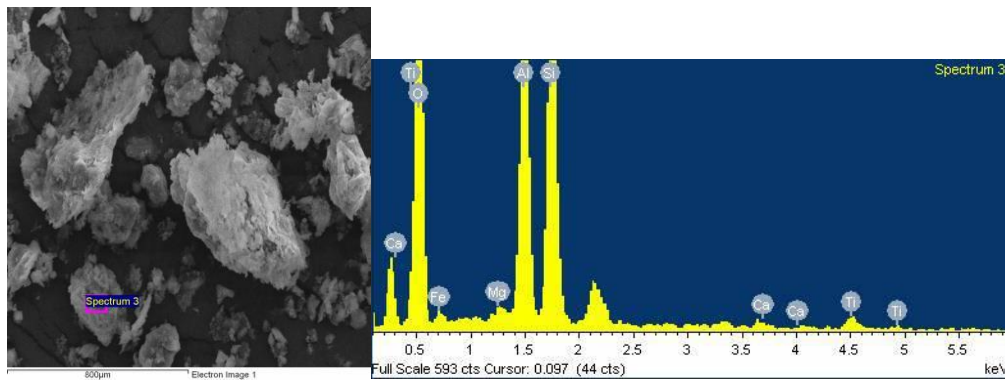
The insoluble compounds like Na_2SiF_6 gets dissolved which may form during HF leach. The SEM represents the ash for both the coals for untreated coals are of irregular structure. The homogeneously mixed minerals are seen in the cluster that's gets formed in the ash for both the coals for treated coals.



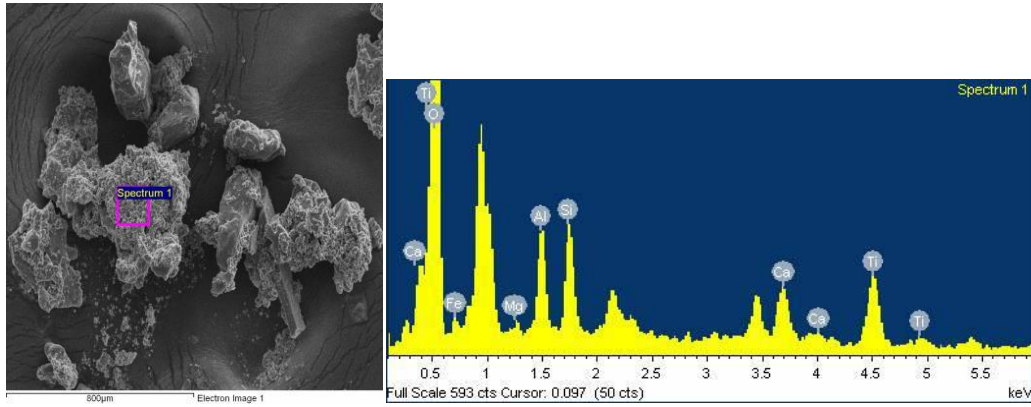
(a)



(b)

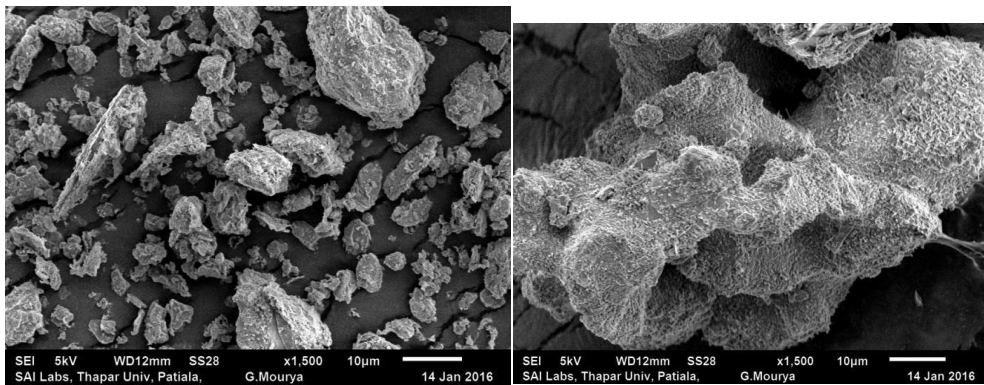


(c)

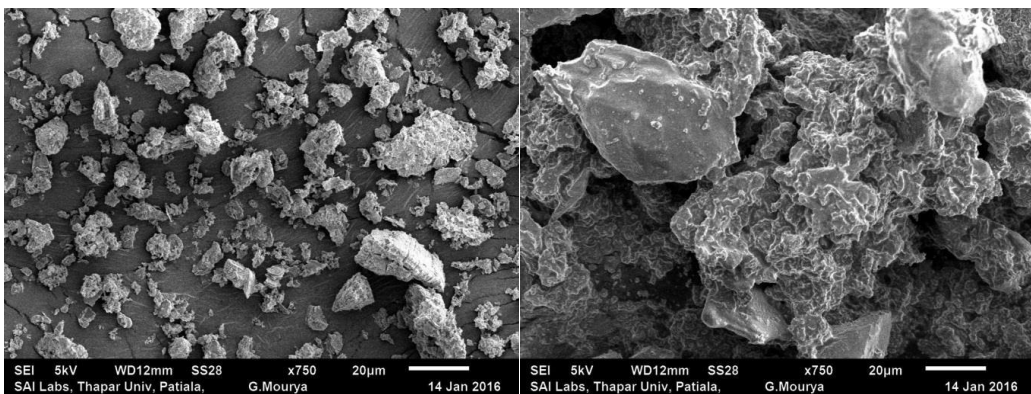


(d)

Figure 3.6 (a) represents the EDS image of untreated Coal A whereas (b) with 40% treated with HF and HNO₃ and Figure 3.6(c) represent the EDS image of untreated Coal B whereas (d) with 40% treated with HF and HNO₃



(a) (b)



(c)

(d)

Figure 3.7 (a) shows the SEM image of ash for untreated Coal A (b) shows the SEM image after washing (c) represents the SEM image of ash for untreated Coal B (d).

3.10.3 Determination of calorific value: The calorific value (CV) of coal samples were determined with the help of bomb calorimeter (IS 1350-2). The calorific value of coal with and without treated with chemical is given in Table 3.4. The calorific value of untreated coal (Coal B) was 4866 kcal/kg.

Table 3.4: Calorific value of coal samples with varying concentration of leaching

| Parameters | Coal A (kcal/kg) | Coal B (kcal/kg) |
|------------------|------------------|------------------|
| Untreated coal | 5362.5 | 4866 |
| 10% treated coal | 5337.25 | 4847.31 |
| 20% treated coal | 5302.87 | 4803.79 |
| 30% treated coal | 5287.64 | 4789.04 |
| 40% treated coal | 5271.95 | 4765 |

After washing of coal sample with 10, 20, 30 and 40% concentrations of HF and HNO₃, the calorific value of coal drop to 4847.31, 4803.49, 4789.04 and 4765 kcal/kg respectively. Similarly the CV of coal (Coal A) decreases from 5362.5 to 5337.25, 5302.87, 5287.64 and 5271.95 respectively. The result shows the loss in caloric value of coal indicated as the concentration of chemicals increased. CV reduces due to the attack on carbonaceous matrix which leads to the loss in Carbon but gain in Oxygen content. Also there was dramatic effect on the sulphur which gets reduced when Fe in pyrite gets oxidized during reaction with HNO₃ to form sulphate SO₄²⁻.

Chapter 4

Rheology of chemical leached coal oil slurry

4.1 Introduction

During the transportation of solid material through slurry pipelines, the approximation of energy, required for pumping, depends upon viscosity of slurry. The presence of solid particles in the carrier fluid varies the viscosity of fluid depending upon solid concentration, their shape and particle size distribution (PSD), etc. The rheological studies are very useful for determining the viscous characteristics of slurry with respect to the slurry concentration and material properties. In the present work, the rheological experimentation was carried out on coal oil slurries with and without chemical leached coal varying in their respective ash content. The rheological data was created with help of an Anton Paar RheolabQC rheometer.

4.2 Description of the equipment

The Anton Paar rheometer (Model: RheolabQC) used for the rheological experimentation was supplied by Anton Paar, Germany. A pictorial view of the Anton Paar (RheolabQC) rheometer installed in the Mechanical Engineering Department, Thapar University, Patiala, as shown in Fig. 4.1. It is a rotational type rheometer, that's works on Searle principles, consists of a high precision encoder with highly dynamic EC motor. The measurements can be obtained by selecting either controlled shear stress or controlled shear rates test settings. It has wide torque range and speed with very short motor response time. The measuring system is sensed automatically by inbuilt Tool mastersystem that certifies the exact measuring statistics to be used with high precision. DG42/SS/QC-LTD measuring system can be used as per the need of work.

The rheometer component consists of concentric cup and bob having a small annular gap in between them. The coal oil slurry was prepared for all measurement and was filled up to required mark in the measuring stationary cup. The measuring stationary cup was then implanted into the measuring cylinder and the system was devoted to the rotating spindle by pushing down the flanged coupling. The coal oil mixture was exposed to shearing action in between the annular space provided between measuring stationary cup

and rotating bob. Hence shear stress was measured as a function of shear rate. The output graphs were attained on Rheoplus software installed on laptop which is connected by LAN connection to rheometer.



Fig 4.1: Rheometer (anton parr)



Fig. 4.2: Cylindrical cup and bob

4.3 Materials and methods

The coal sample used for the study was collected from the L and T power plant in briquette form. Coal was crushed with the help of jaw crusher and roll mill to obtain the particle size of coal less than 5 cm. The crushed coal was again processed for pulverization in stainless steel ball milling at 120 rpm, with the ball to coal sample ratio of 7:1. The pulverized coal sample was dried in electric oven for 3 hours at $115\pm 2^{\circ}\text{C}$ to remove moisture from the coal.

The detailed procedure of the investigation is represented by Figure 4.3. The sample was further processed for dry sieving method using mechanical sieve shaker to obtain particle size $<106\mu\text{m}$ having sieves of BS-410 (British Standard). The sieve analysis was used to study the particle size distribution of pulverized coal. For the leaching of coal, 15 gram of pulverized coal was treated with 100ml aqueous solution of HF (hydrofluoric). The concentration of HF in aqueous solution varies from 10 to 40% for 8 hours duration at atmospheric pressure condition. After filtering the coal sample using filter paper, the demineralized coal was again treated with HNO_3 (nitric acid) for 3 hours duration. After filtration of treated coal, percentage of ash in the coal sample was determined using muffle furnace. The calorific value of coal was calculated with the help of bomb calorimeter. Energy dispersion x-ray spectrograph (EDS-JEOL, 6510LV) was

used to measure the morphology and elementary composition of untreated and ultra clean coal sample. The standard Rheometer (Rheolab Q-C Manufactured by Anton Paar Company Ltd, Germany) was used to measure the rheology of coal-oil suspension. The rheometer works on the Searle principle.

The rheological parameter of the COSL was valued by determining the shear stress at definite shear rate. For rheological experimentations, 50 ml of the coal-oil slurry was prepared by mixing the required quantity of oil with coal. The slurry suspension was stirred gently by using a glass rod. Before conducting the laboratory tests, the rotating bob and cup assembly was fixed using a locking device. The COSL was transferred into cup (cylinder) up to the indicated mark. The rheological tests were conducted by changing the shear rate from 0 to 500 sec^{-1} for all the solid concentration in coal-oil suspension at $293\pm 0.1\text{K}$. The solid concentration of slurry suspension was varies from 20 to 40% (by weight).

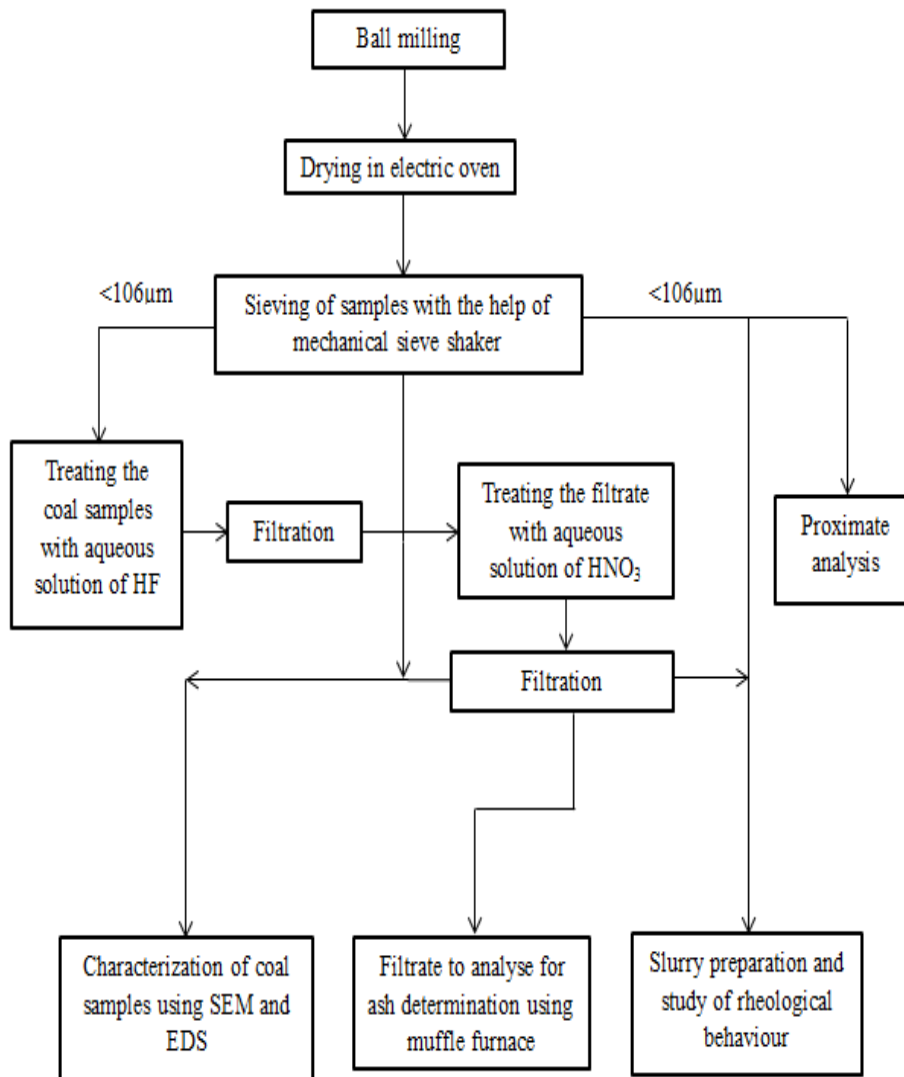


Fig 4.3: Detailed procedure of methodology adopted

4.4 Results and discussion

4.4.1 Rheological behaviour of coal: The COSL suspension was organized by involvement of coal and oil. The weight of the coal was measured with the help of electronic weighing machine having least count of 0.0001 gram. The slurry was continuously stirred by glass rod for 5 to 10 minutes to certify the homogenization of the coal-oil slurry. Appropriate care was taken to avoid spillage and attrition. The rheology experiments were conducted with solid loading of 20, 30 and 40% (by weight). The shear rate was functional from 0 to 500 sec^{-1} for a period of 3 minutes to measure the corresponding viscosity and shear stress under the monitoring shear rate. The rheological data were obtained in Rheoplus software. Steady shear measurements were performed at particular temperature of 20°C. The distinction in temperature was $\pm 0.1^\circ\text{C}$ using constant

temperature water based bath sensor connected to rheometer. The experiments were repeated to ascertain the reproducibility of results.

The experimental results were subjected to Power-law, Bingham, Herschel-Bulkley and Casson rheological models. Present experimental results found to be best fitted with Herschel-Bulkley model for non-Newtonian fluid. The Herschel-Bulkley model for fitting the shear stress/rate data is given by equation 4.1

$$\tau = \tau_H + K_H \dot{\gamma}^n \quad (4.1)$$

Where τ is shear stress (Pa), $\dot{\gamma}$ is shear rate (sec^{-1}), τ_H is the parameter for yield stress (Pa) and n and K_H are flow index and consistency respectively. The model parameters were calculated after fitting the values into rheological model (Table 4.1). The parameters for nonlinear regression equation for Herschel-Bulkley model at 293K with variation in solid concentration of coal were calculated. The shear stress-shear rate curve of the coal oil slurry at solid concentration of 20, 30, and 40% (by weight) are shown in Figure 4.4-4.6. It is observed that shear stress of slurry suspension is the function of shear rate and solid concentration. The value of yield stress also increases with solid concentration of the slurry. The yield stress value of untreated coal oil slurry was calculated as 0.071319, 0.075624 and 0.1352 (Pa) at the solid concentration of 20, 30 and 40% (by weight) respectively. Similar observations were also drawn by (Cui et al. 2008) with coal and oil slurry. The K_H value varies in the range of 0.35279-0.90393 and found inconsistent. The value for n lies in the range of 0.518 - 0.7001. Present rheological data shows that the value of n is less than 1 which exhibits the shear thinning behaviour of coal oil slurry.

Table 4.1: Herschel-Bulkley model parameters for nonlinear equation for treated and untreated coal and oil slurry

| Parameters | | τ_H (Pa) | K_H | n |
|--------------------------|-------------|---------------|----------|---------|
| 20 % solid concentration | Untreated | 0.071319 | 0.67673 | 0.7001 |
| | 10% treated | 0.17842 | 0.067105 | 0.73629 |
| | 20% treated | 0.77332 | 0.111143 | 0.697 |
| | 30% treated | 0.7925 | 0.41586 | 0.61693 |
| | Ultra-clean | 0.859 | 0.58483 | 0.63821 |
| 30% solid concentration | Untreated | 0.075624 | 0.35279 | 0.52256 |
| | 10% treated | 0.34429 | 0.28025 | 0.56962 |

| | | | | |
|-------------------------|-------------|----------|---------|---------|
| | 20% treated | 0.522395 | 0.20066 | 0.68957 |
| | 30% treated | 0.7005 | 0.15107 | 0.80952 |
| | Ultra-clean | 0.85739 | 0.15564 | 0.92884 |
| 40% solid concentration | Untreated | 0.1352 | 0.90393 | 0.518 |
| | 10% treated | 0.1662 | 0.7327 | 0.5581 |
| | 20% treated | 0.5658 | 0.46435 | 0.66255 |
| | 30% treated | 0.8654 | 0.196 | 0.767 |
| | Ultra-clean | 0.9414 | 0.31234 | 0.87291 |

Form Figures 4.4-4.6, it was noted that the shear stress increase with increase in chemical composition and solid concentration of coal in slurry. From Table 4.1, it was observed that the yield stress is affected for the treated coal oil slurry. The value of yield stress found to be in increasing order with increase in percentage of chemicals. The ultra-clean coal oil slurry was having maximum value of yield stress at all concentration. The maximum value of yield stress was found to be 0.859, 0.85739 and 0.9414 at 20, 30 and 40% respectively for solid concentration of coal. The value of K_H varies follows; $0.067105 \leq K_H \leq 0.7327$ for treated coal oil slurry at all solid concentration. It implies that the value of K_H was found to be inconsistent for treated coal oil slurry. The value for n lies in range of 0.5581-0.92884 which reveals that the treated coal oil slurry also exhibit shear thinning behaviour.

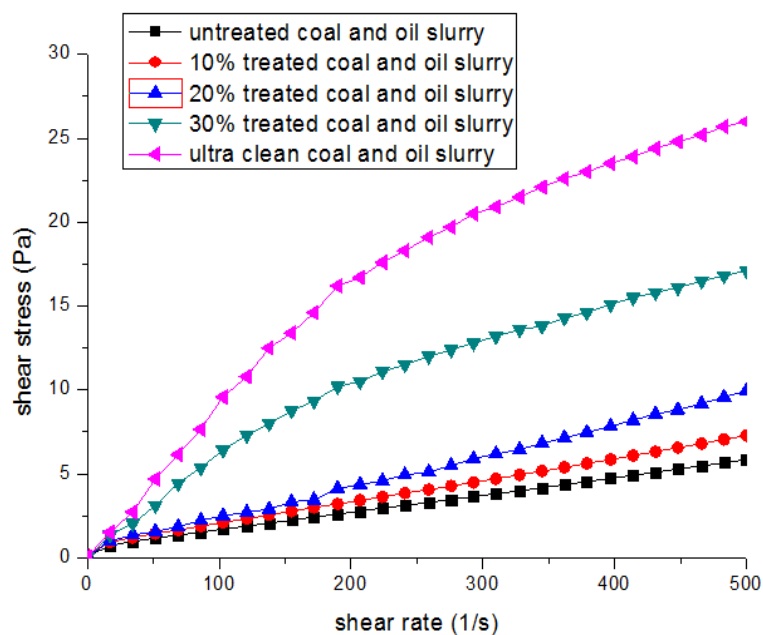


Fig. 4.4: Shear stress variation with increased shear rate for untreated and chemically treated coal oil slurry for 20% solid concentration at 293K.

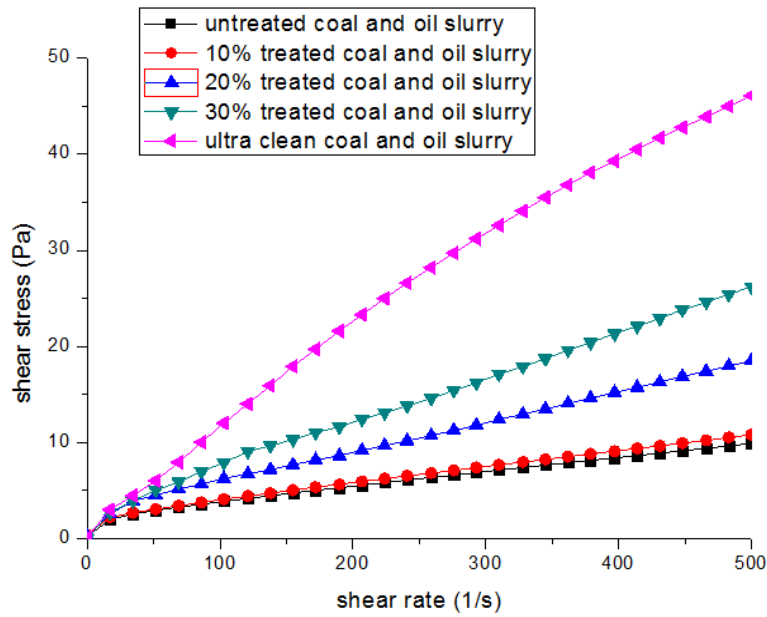


Fig. 4.5: Shear stress variation with increased shear rate for untreated and chemically treated coal oil slurry for 30% solid concentration at 293K.

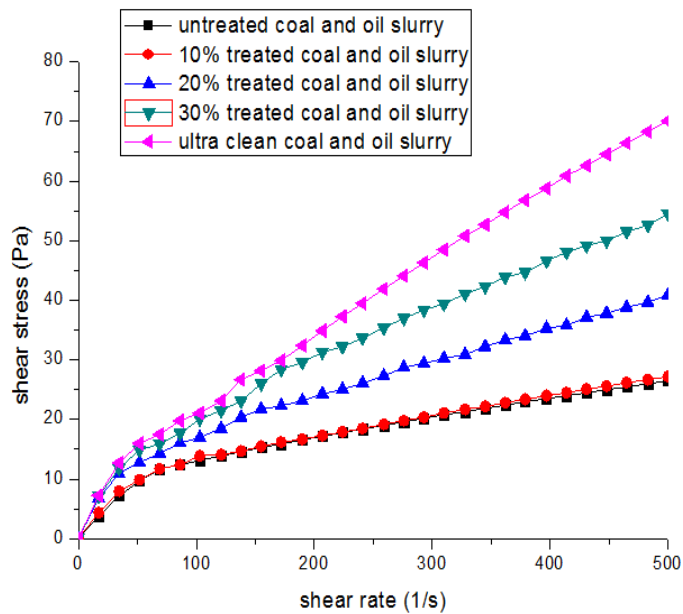


Fig. 4.6: Shear stress variation with increased shear rate for untreated and chemically treated coal oil slurry for 40% solid concentration at 293K.

4.4.2 Influence of leaching on viscosity of coal oil slurry: Rheological experiments were performed to measure the apparent viscosity with variation of shear rate from 0-500 sec^{-1} . The apparent viscosity of coal oil slurry was evaluated at different solid concentration of 20, 30 and 40% (by weight), as shown in Figure 4.7-4.9. It is observed that apparent viscosity decreases with increase in shear rate at given solid concentration. Rheological data (Figure 4.7-4.9) shows that apparent viscosity decreases more rapidly with shear rate up to 150 s^{-1} afterward marginal decrease in rate is observed. It is also seems that apparent viscosity of slurry suspension increases with increase in solid concentration. With the increase in solid concentration of coal in suspension, particle-to-particle shear interaction also increases. However, higher resistance force is required to flow the slurry particles which tends to enhance the apparent viscosity [12, 29].

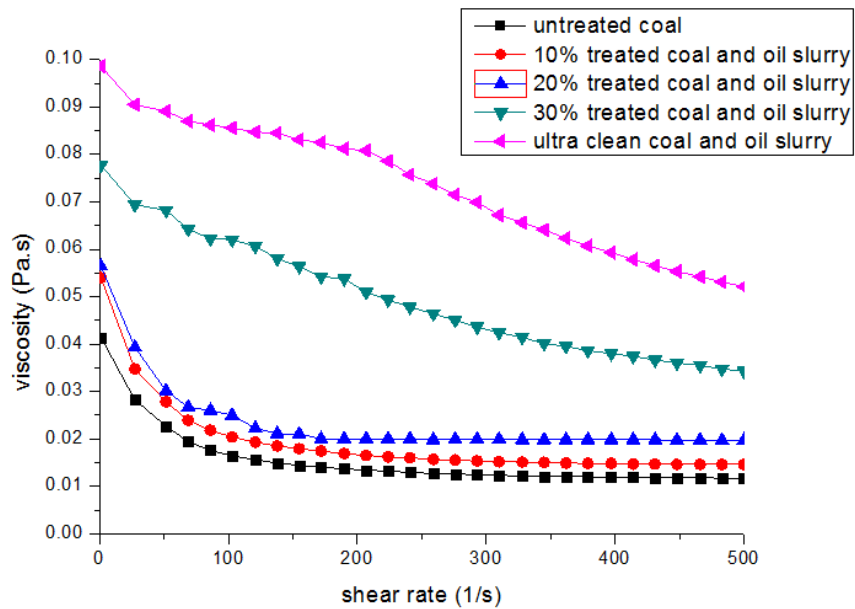


Fig. 4.7: Influence of shear rate on apparent viscosity of untreated and chemically treated coal oil slurry for 20% solid concentration at 293K.

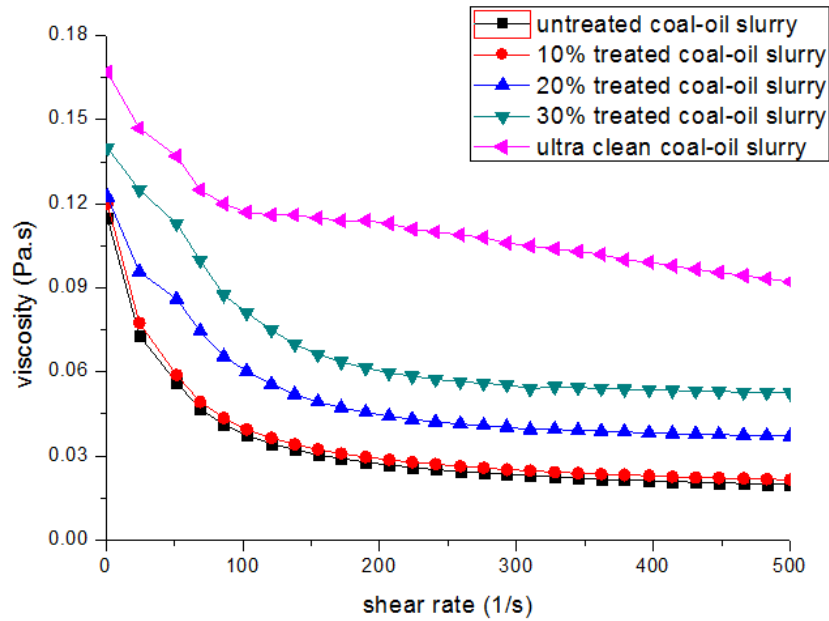


Fig. 4.8: Influence of shear rate on apparent viscosity of untreated and chemically treated coal oil slurry for 30% solid concentration at 293K.

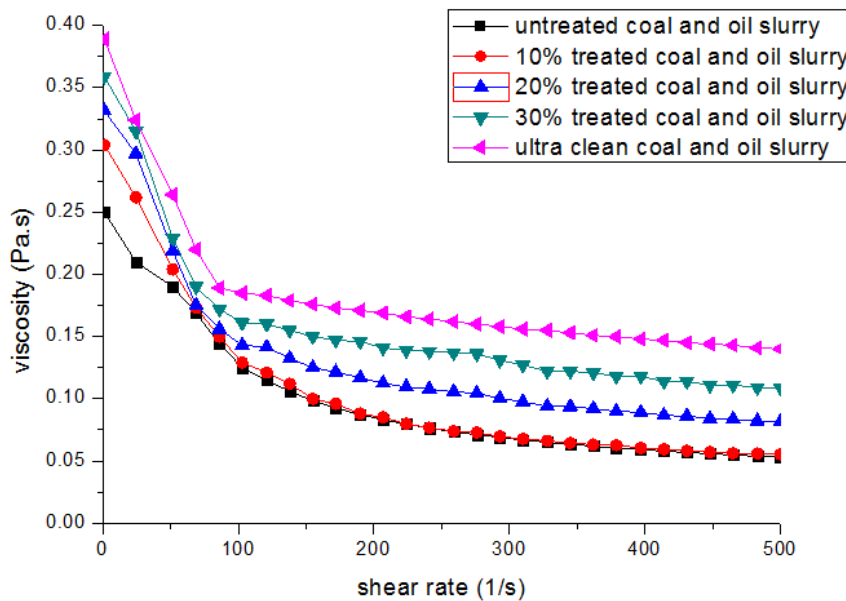


Fig. 4.9: Influence of shear rate on apparent viscosity of untreated and chemically treated coal oil slurry for 40% solid concentration at 293K.

The rheological experimentation extended to investigate the apparent viscosity of coal oil slurry at the different solid concentration 20, 30 and 40% (by weight). Experimental data shows that the apparent viscosity of the coal oil slurry increases with chemical leaching of HF and HNO₃. At 20% solid concentration of coal oil slurry, apparent

viscosity increases from 42 to 53, 57, 78 and 99 mPa-sec with chemical leaching concentration of 10, 20, 30 and 40% (by volume) respectively. Similar apparent viscosity increases from 115 to 116, 122, 140 and 166 mPa-s at 30% solid concentration of coal in slurry. At 40% solid concentration of coal oil slurry, apparent viscosity increases from 250 to 308, 330, 357 and 390 mPa-s with chemical leaching concentration of 10, 20, 30 and 40% (by volume) respectively. From the data, it is also observed that apparent viscosity of coal oil slurry increases with reduction in ash content and maximum viscosity is noticed for ultra-clean coal oil slurry. Similar observation is made by researcher [22]. SEM micrograph of untreated and ultra clean coal is shown in Figure 5-6. From the micrograph, it can be visualized that there are some non-porous materials present in the form of ash which gets removed on leaching. Due to large quantity of ash, the penetration of oil in non-porous material was not frequent. In case of ultra clean coal, the ash has been reduced from 38.5 to 0.9% (by weight) after chemical leaching. Hence the penetration of oil in remaining coal was extreme in case of ultra-clean coal as compared to the untreated coal. From the Rheological data, it can be concluded that the viscosity of coal oil slurry increases with reduction in ash content. The apparent viscosity value found maximum with ultra clean coal oil slurry at all solid concentration.

Chapter 5

Rheology of blended coal and oil slurry

5.1 Materials and methods

The three coal samples used for study were collected from the three different power plants of Indian origin in briquette form. All samples were categorized into different ranked on the basis of ash and moisture content. The three samples were labelled as Cn (high ranked coal), Cy (medium ranked coal) and Cr (low ranked coal). Coal samples were crushed using jaw crusher and roll mill to obtain the particle size of coal less than 5 cm. The crushed coal samples were again processed for pulverization in stainless steel ball milling at 120 rpm, with the ball to coal sample ratio of 7:1.

The calorific values (CV) of all samples were calculated with the help of bomb calorimeter. Energy dispersion x-ray spectrograph (EDS-JEOL, 6510LV) was used to measure the morphology and elementary composition of coal sample, which is shown by Table 5.1. A rotary type standard rheometer (Rheolab Q-C Manufactured by Anton Paar Company Ltd, Germany) working on Searle's principle, was used to measure the rheology of coal-oil slurry (COSL).

The rheological parameter of COSL suspension was estimated by calculating the shear stress at definite shear rate. For rheological analysis, 50 ml solution was organized by stirring the required quantity of oil with coal. The slurry suspension was mixed gently by continuous agitation device for 10 minutes. Before conducting the rheological tests, the rotating bob and stationary cup assembly was stable using locking device. The COSL suspension was transferred into stationary cup (cylinder) up to the indicated mark. The rheological experiments were conducted by changing the shear rate from $17.2\text{-}500\text{ s}^{-1}$ for all the solid concentration in COSL with different particle size and at different temperatures. The solid concentration of COSL suspension was varies from 30 to 50% (by weight). The fine particles (75-106 μm) and very fine particles (less than 75 μm) of coal samples were taken for the study. The temperatures used for the study were 293, 318 and 343 K. The present study considers three different cases to analyse rheological behaviour of COSL. The first circumstance is the variation in particle size that consider the size of the particle between 75–106 μm and less than 75 μm . The second circumstance is to study the

effect of temperature on rheology at all concentration. The third case is to study the effect of different ranked coal blending on rheology of COSL.

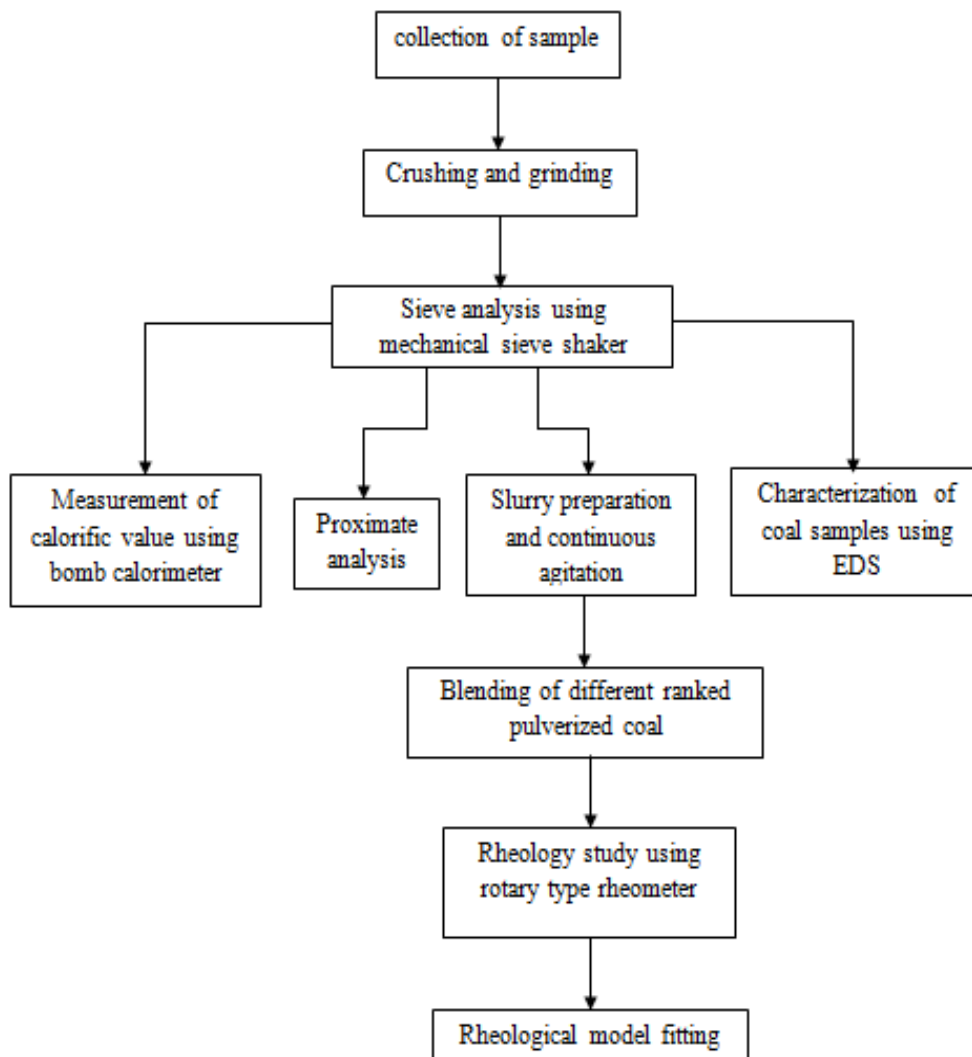


Fig. 5.1: Methodology adopted for rheology

5.2 Proximate analysis and EDS

The proximate analysis of coal was achieved to determine the percentages of ash, inherent moisture, fixed carbon and volatile matter present in a particular sample. The proximate analysis based upon moisture free basis, for three coals, was directed according to testing method of IS: 1350 and the result of the proximate analysis on moisture free basis is shown in Table 3.2. Energy dispersion x-ray spectrograph (EDS-JEOL, 6510LV) was used to measure the morphology and elementary composition of different ranked coal samples.

Table 5.1: Proximate and EDS analysis on moisture free basis

| | Element | Cn | | Cr | | Cy | |
|--------------------|---------|----------|----------|----------|----------|----------|----------|
| Proximate analysis | | Weight % | | Weight % | | Weight % | |
| | VM | 30 | | 27.42 | | 28.27 | |
| | FC | 58.28 | | 32.46 | | 47.73 | |
| | Ash | 11.72 | | 40.3 | | 24 | |
| | Total | 100 | | 100 | | 100 | |
| EDS | | Weight % | Atomic % | Weight % | Atomic % | Weight % | Atomic % |
| | C | 67.94 | 74.57 | 59.34 | 67.62 | 63.07 | 69.54 |
| | O | 29.17 | 24.04 | 34.75 | 29.73 | 36.73 | 30.41 |
| | F | 0.39 | 0.27 | 0.04 | 0.03 | - | - |
| | Al | 0.77 | 0.38 | 1.97 | 1.00 | - | - |
| | Si | 1.27 | 0.60 | 2.52 | 1.23 | 0.04 | 0.02 |
| | S | 0.26 | 0.11 | 0.35 | 0.15 | - | - |
| | Ti | - | - | 0.46 | 0.13 | 0.04 | 0.01 |
| | Zn | 0.19 | 0.04 | 0.57 | 0.12 | 0.11 | 0.02 |
| | Total | 100 | 100 | 100 | 100 | 100 | 100 |
| CV (kcal/kg) | | 55362.5 | | 4865.61 | | 5102.3 | |

5.3 Particle size distribution (PSD)

Subsequently rheological assets of COSL depend upon the particle size and solid concentration therefore PSD becomes crucial to define the estimated size range of particles existing in COSL. Standard weight of pulverized coal was reserved and sieved (using dry sieving method) through mechanical sieve shaker. The amount of pulverized coal sample retained on each sieve was measured using electric weighing machine having least count of 0.0001g and the amount retained was calculated. Figure 5.2 represents the PSD curve of all coal samples. The curves indicate that all the coal sample particles are finer than 500 μm , Cr coal has most fine particle as compared to Cy and Cn coal sample.

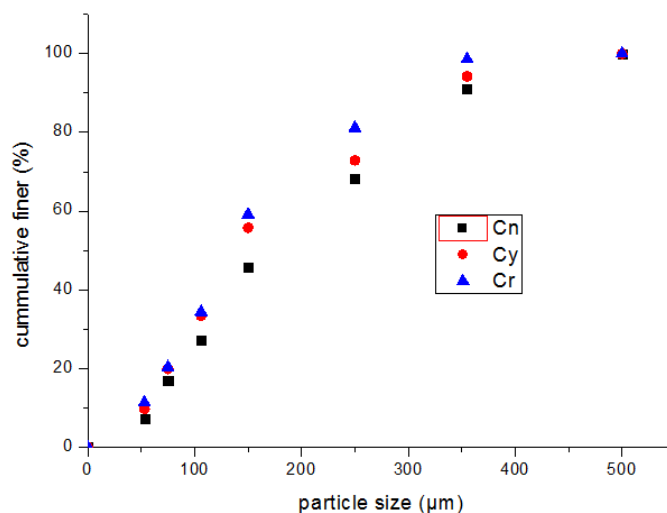


Fig. 5.2: Particle size distribution for all samples of coal

5.4 Results and discussions

5.4.1 Effect of solid loading on COSL: The rheological experiments were performed with a solid loading of 30%, 40% and 50% by weight and the shear rate is functional from 17.2–500 s^{-1} for a time intermission of 2.5 minutes to determine shear stress and apparent viscosity at particular given shear rate. The flow curves attained by the rheological experimentation exposed that the rheological behaviour of the COSL is greatly influenced by the distinction in the solid concentration in slurry. Figures 5.3, 5.6 and 5.8 shows the influence of shear stress with variation in shear rate for 30, 40 and 50% solid concentrations respectively of COSL and Figure 5.4, 5.5 and 5.7 shows the influence of the apparent viscosity with change in shear rate. From Figures 5.3-5.8, it was initiated that the solid loading had a substantial effect on the rheological behaviour of COSL. As the solids loading increased, the trend for apparent viscosity of the COSL also increased, which occurs due to more interaction of solid particles acquiring larger resistance force. The frictional force between the particles becomes significant and the accompanying resistance is reflected in the increase in viscosity [23].

Figures 5.3, 5.6 and 5.8 also reveals that the shear stress is independent of the shear rate for a 30% solid loading of COSL but the apparent viscosity decreased with an increase in the shear rate. It was found that the apparent viscosity of slurry is greatly affected upto shear rate of 150 sec^{-1} for 30 and 40% solid concentration and negligible changes was observed after 150 s^{-1} shear rate. But for 50% solid concentration, the

negligible effect was observed after 200 s^{-1} shear rate. This shows the pseudoplastic behaviour of fluid at a higher solid loading. It is also initiated that the decreasing trend of the apparent viscosity is up to the shear rate 150 s^{-1} for 30 and 40% solid loading and 200 s^{-1} for 50% concentrations and there is an almost negligible effect on the apparent viscosity for further increase in shear rate. The pseudoplastic behaviour of the COSL at higher solids concentration indicated by the Rheogram and viscosity curves may be due to the breakdown of the slurry structure that is similar to behaviour reported by Singh et al. [23].

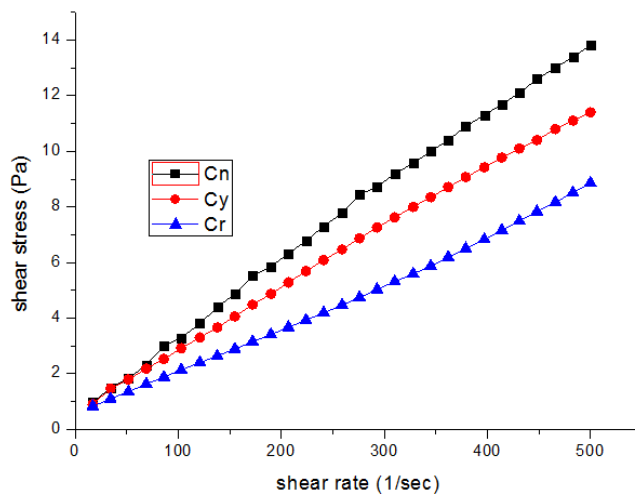


Fig. 5.3: Shear stress and shear strain at 30% solid loading of coal

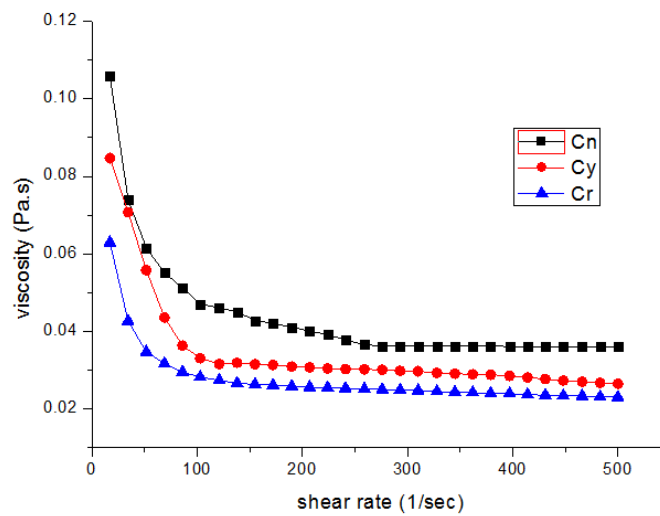


Fig. 5.4: Apparent viscosity with shear strain at 30% solid concentration

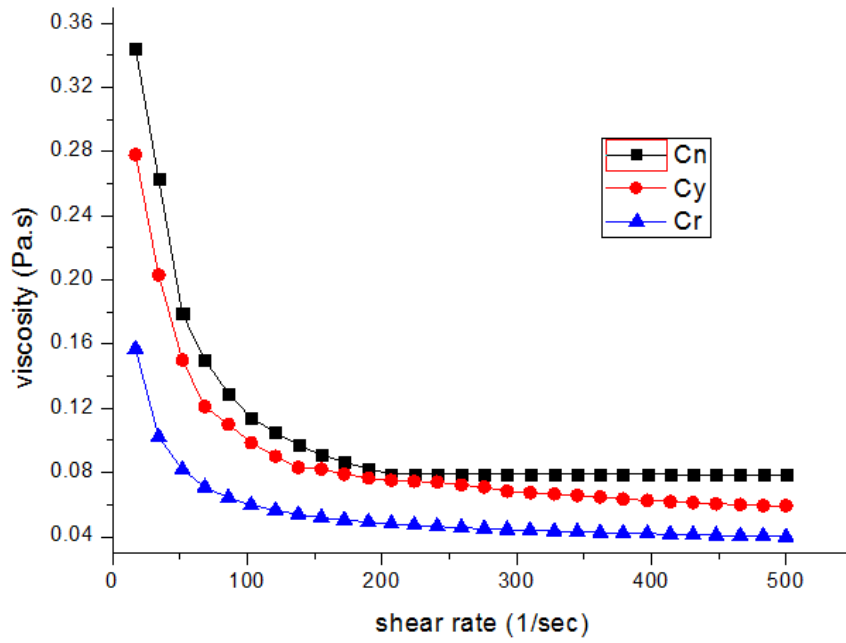


Fig. 5.5: Apparent viscosity with shear strain at 40 % solid concentration

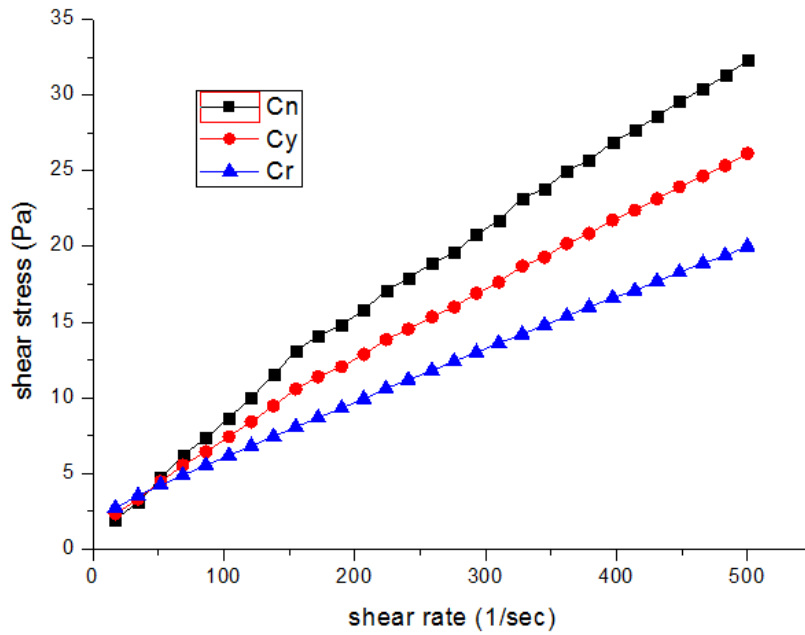


Fig. 5.6: Shear stress and shear strain at 40% solid loading of coal

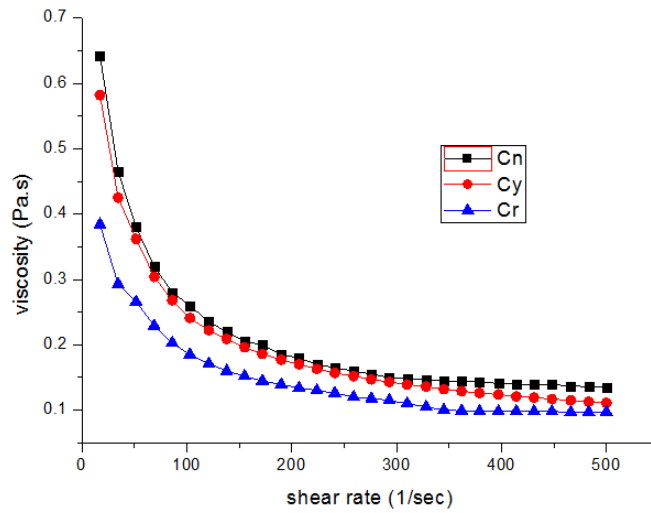


Fig. 5.7: Apparent viscosity with shear strain at 50 % solid concentration

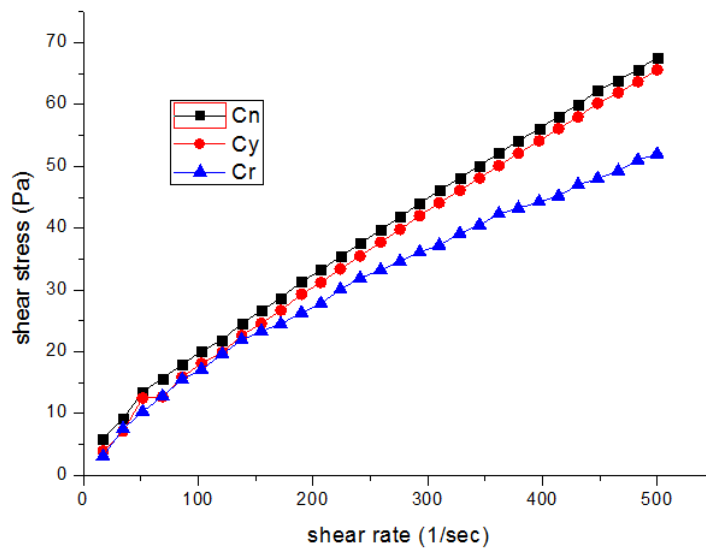


Fig. 5.8: Shear stress and shear strain at 50% solid loading of coal

5.4.2 Effect of temperature without blend for 50% solid concentration: The experiment was also performed to determine the effect of temperature on the apparent viscosity of the COSL. Figures 5.9-5.14 represent the influence on apparent viscosity and shear stress with increase in shear rate at 50% concentration COSL at different temperatures. It is established that increase in temperature causes decrease in COSL

apparent viscosity that happens due to K.E. of coal particles and drop in force (cohesive) between the oil molecules.

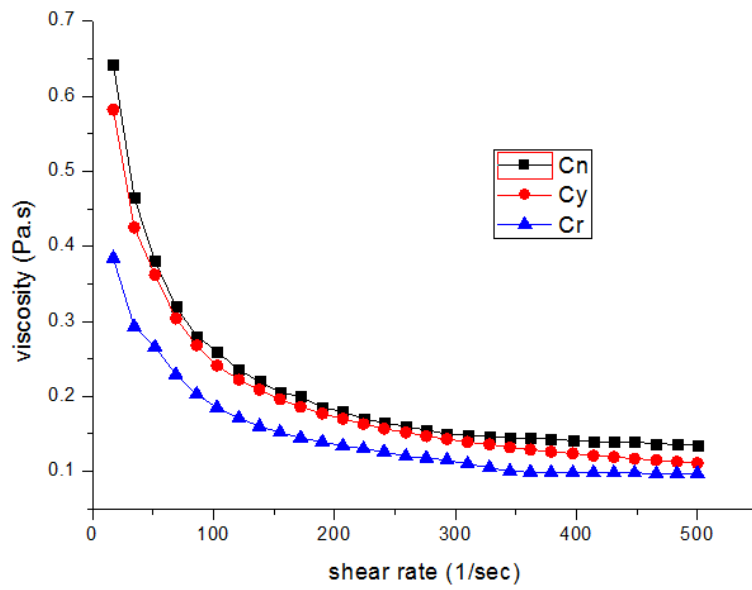


Fig. 5.9: Influence on apparent viscosity with increase in shear rate at 20°C for 50% solid concentration

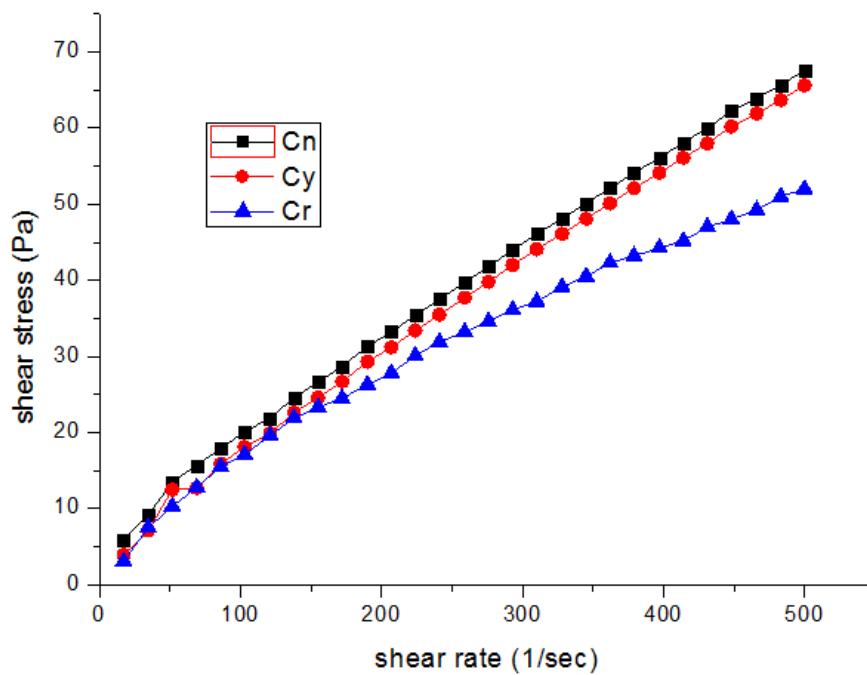


Fig. 5.10: Influence on shear stress with increase in shear rate at 20°C for 50% solid concentration

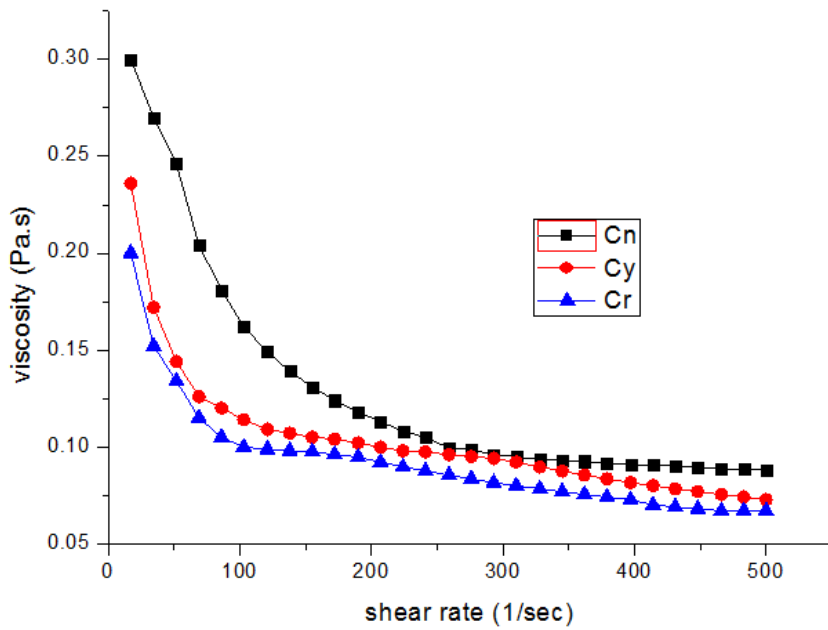


Fig. 5.11: Influence on apparent viscosity with increase in shear rate at 45°C for 50% solid concentration

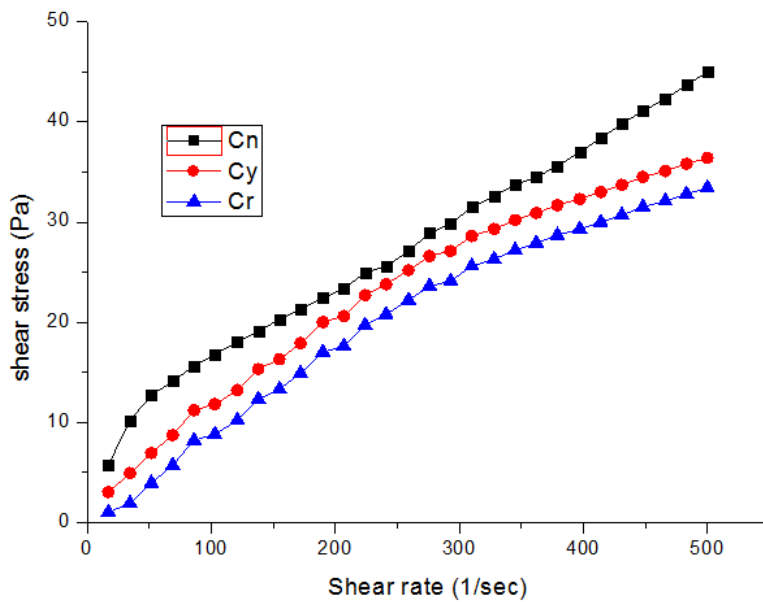


Fig. 5.12: Influence on shear stress with increase in shear rate at 20°C for 50% solid concentration

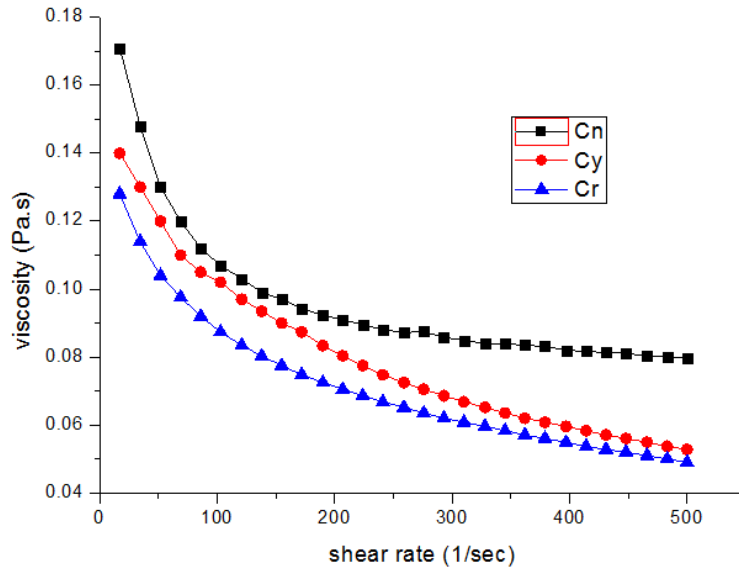


Fig. 5.13: Influence on apparent viscosity with increase in shear rate at 70°C for 50% solid concentration

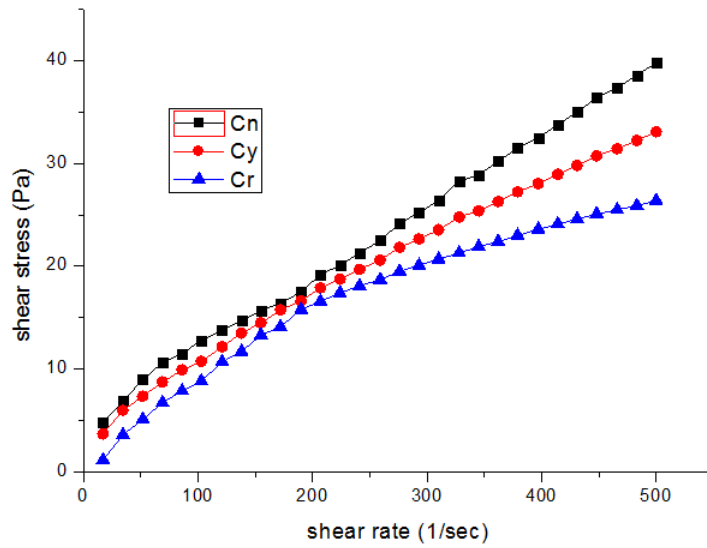


Fig. 5.14: Influence on shear stress with increase in shear rate at 70°C for 50% solid concentration

5.4.3 Effect of particle size on rheology: The rheology experiment was also performed to study the effect of particle size on the COSL. The apparent viscosity was analysed for COSL with particle size less than 75 μ m. similar flow curves were obtained but with reduced viscosity. It was found that the apparent viscosity of COSL decreases with decrease in particle size of coal.

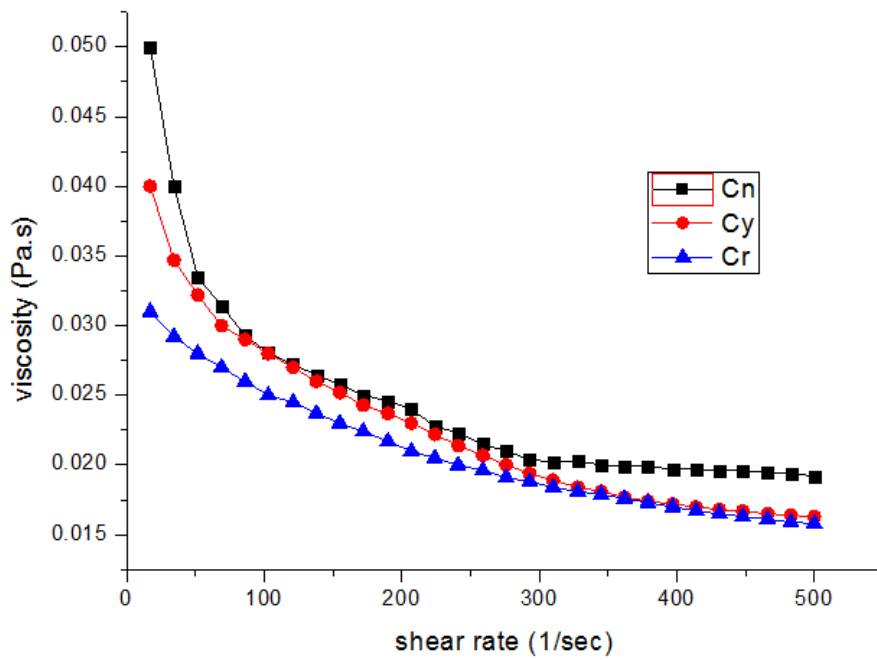


Fig. 5.15: Influence on apparent viscosity with increase in shear rate at 20°C for 30% solid concentration

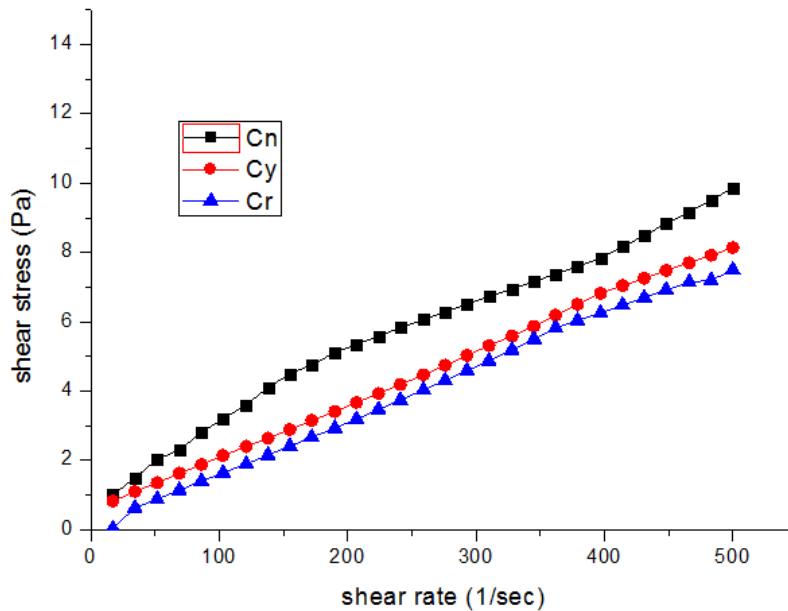


Fig. 5.16: Influence on shear stress with increase in shear rate at 20°C for 30 % solid concentration

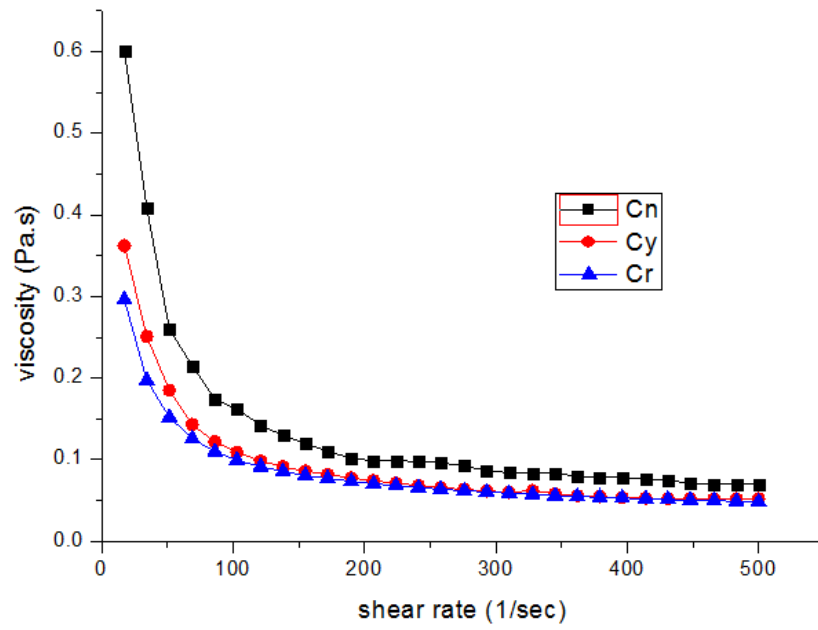


Fig. 5.17: Influence on apparent viscosity with increase in shear rate at 20°C for 40% solid concentration

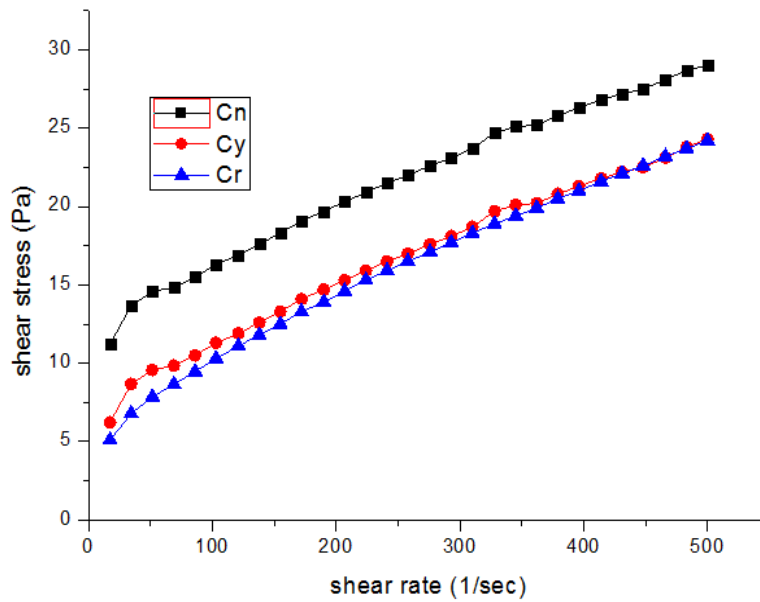


Fig. 5.18: Influence on shear stress with increase in shear rate at 20°C for 40% solid concentration

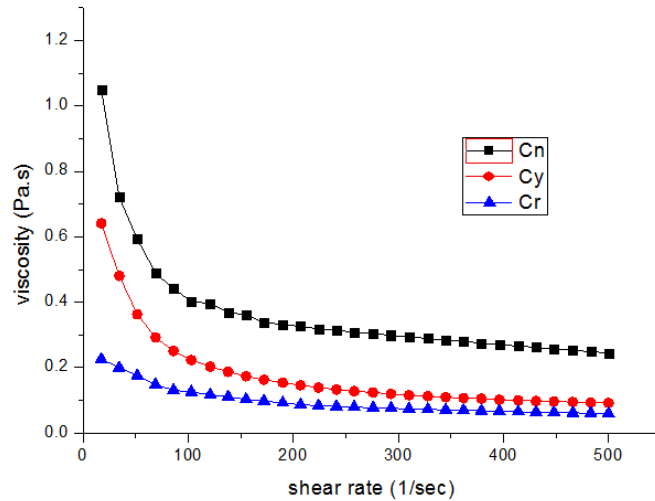


Fig. 5.19: Influence on apparent viscosity with increase in shear rate at 20°C for 50% solid concentration

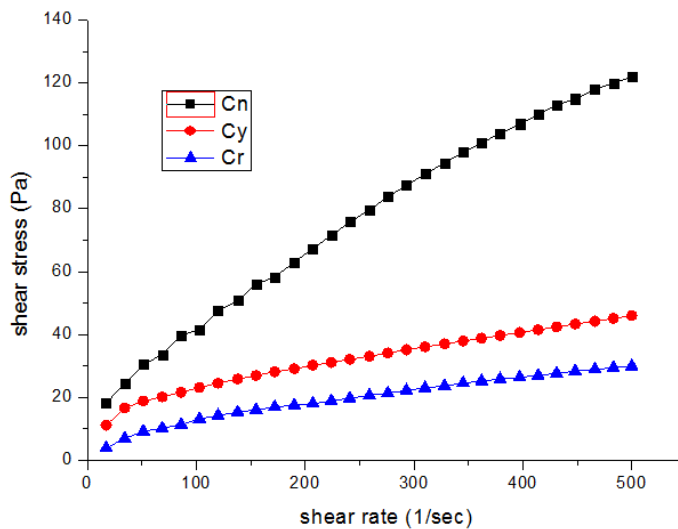


Fig. 5.20: Influence on shear stress with increase in shear rate at 20°C for 50% solid concentration

5.4.4 Effect of coal blending: Three different ranked coals were blended in different proportions as mention in figures. As the objective of transportation of slurry is to transport the maximum solid concentration of coal having low viscosity so it is required to find the optimum solution to transport the slurry at low cost. The experiment was performed for coal oil slurry for 30, 40 and 50% solid concentration of coal in solvent. By comparing the result for figure 5.21-5.26 for apparent viscosity and shear rate, it can be seen that the apparent viscosity of coal and oil slurry increases with increase in solid

concentration of coal in slurry. The initial apparent viscosity of COSL depends upon the moisture content of the coal. Also it was found that Cn:Cr:oil has the minimum viscosity as compared to other blending at the same concentration.

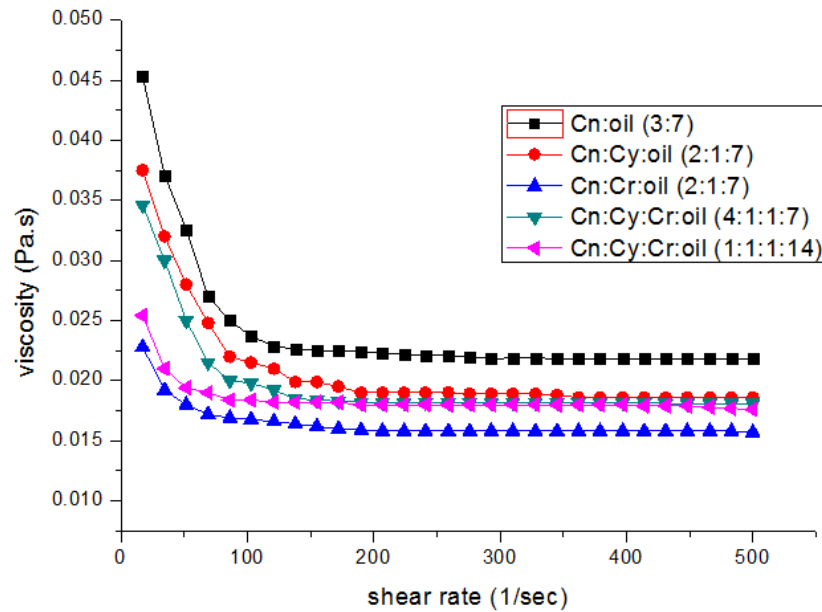


Fig. 5.21: Influence on apparent viscosity with increase in shear rate at 20°C for 30% solid concentration

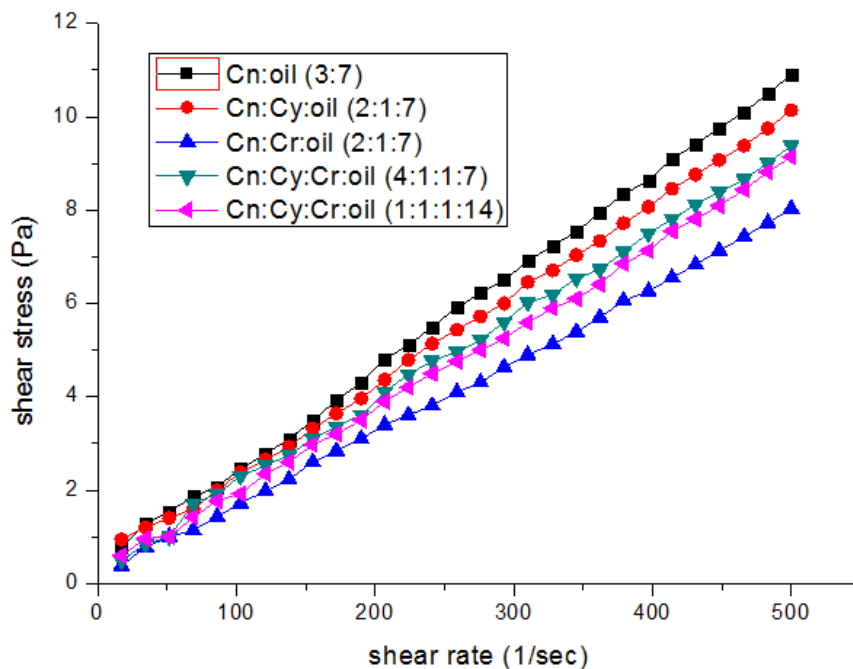


Fig. 5.22: Influence on shear stress with increase in shear rate at 20°C for 30% solid concentration

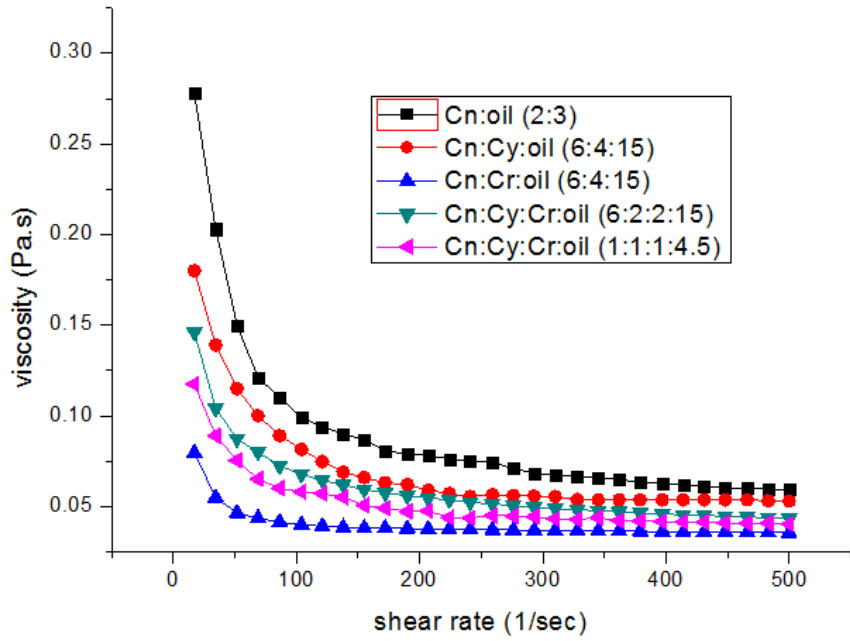


Fig. 5.23: Influence on apparent viscosity with increase in shear rate at 20°C for 40% solid concentration

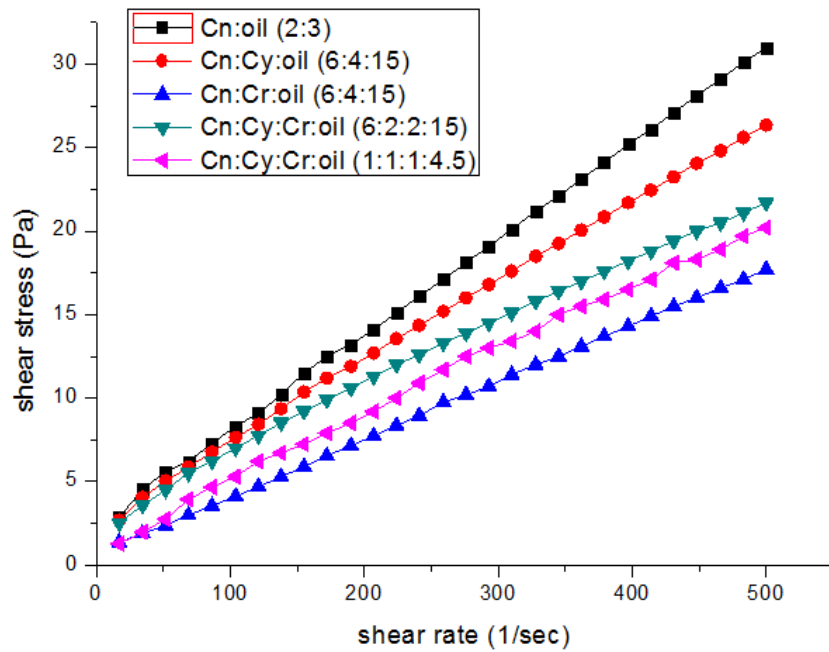


Fig. 5.24: Influence on shear stress with increase in shear rate at 20°C for 40% solid concentration

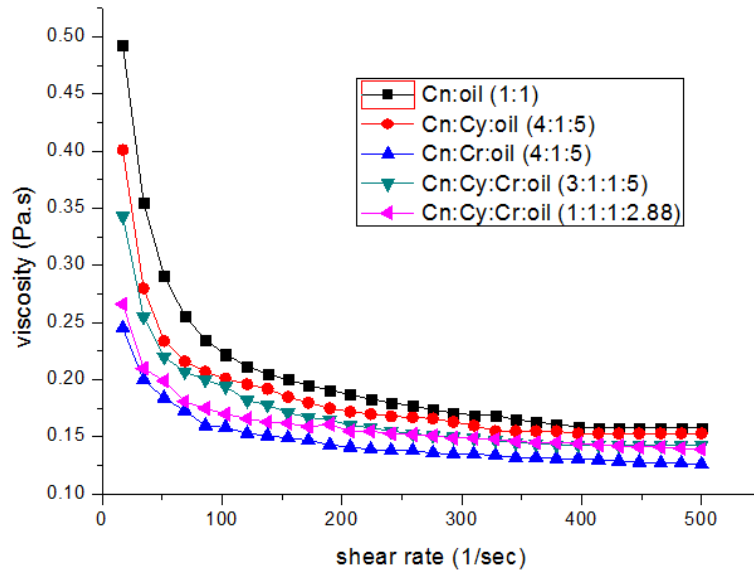


Fig. 5.25: Influence on apparent viscosity with increase in shear rate at 20°C for 50% solid concentration

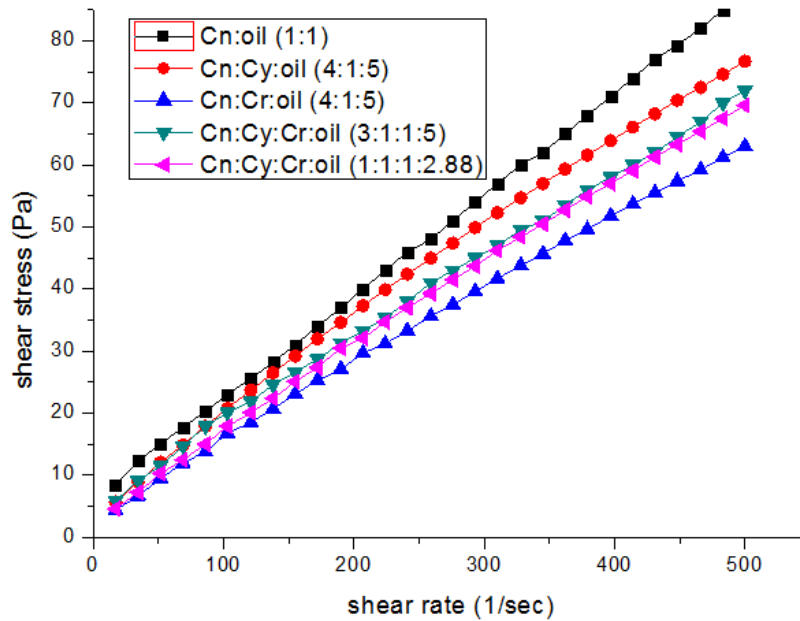


Fig. 5.26: Influence on shear stress with increase in shear rate at 20°C for 50% solid concentration

5.4.5 Effect of temperature on blended COSL at 40 % solid concentration: The experiment was also performed to determine the influence of temperature on the apparent viscosity of the blended COSL. Figures 5.27-5.32 reveal the variation of apparent viscosity

and shear stress with shear strain for a 40% concentration COSL at different temperatures. It is established that increase in temperature causes decrease in COSL apparent viscosity that happens due to K.E. of coal particles and drop in force (cohesive) between the oil molecules.

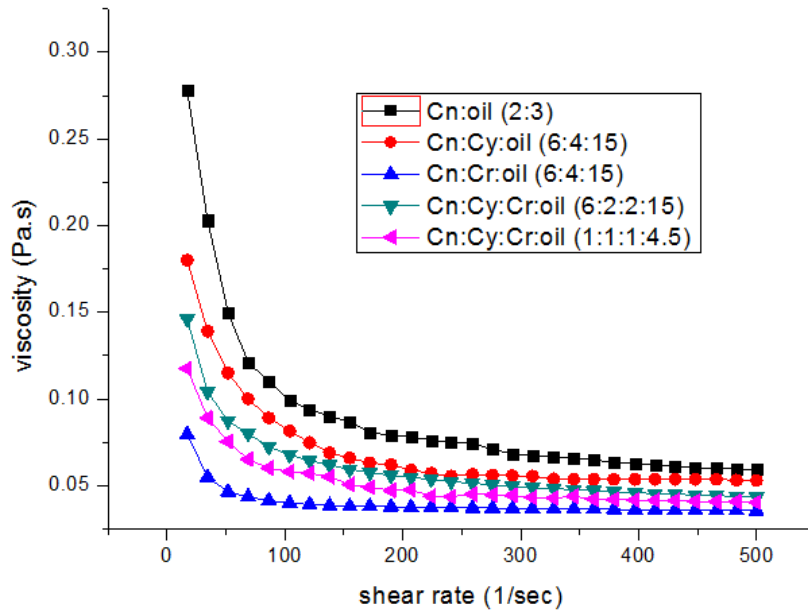


Fig. 5.27: Influence on apparent viscosity with increase in shear rate at 20°C for 40% solid concentration

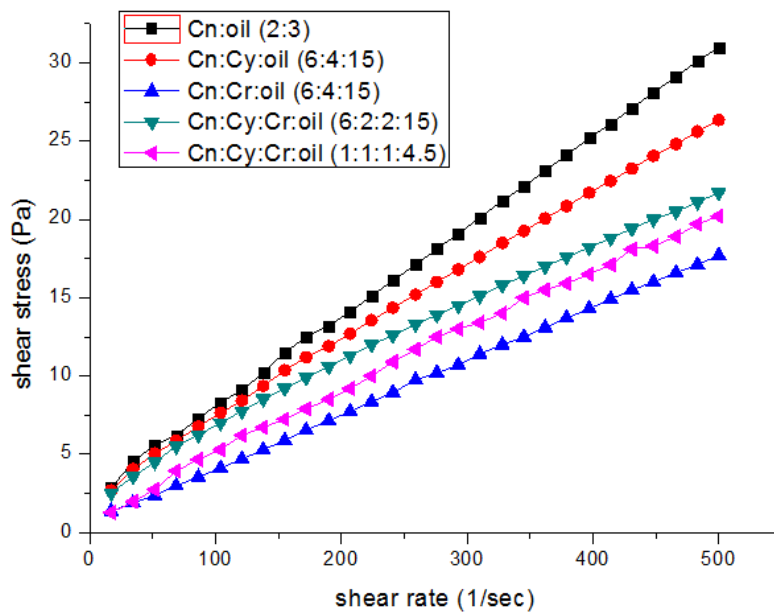


Fig. 5.28: Influence on shear stress with increase in shear rate at 20°C for 40% solid concentration

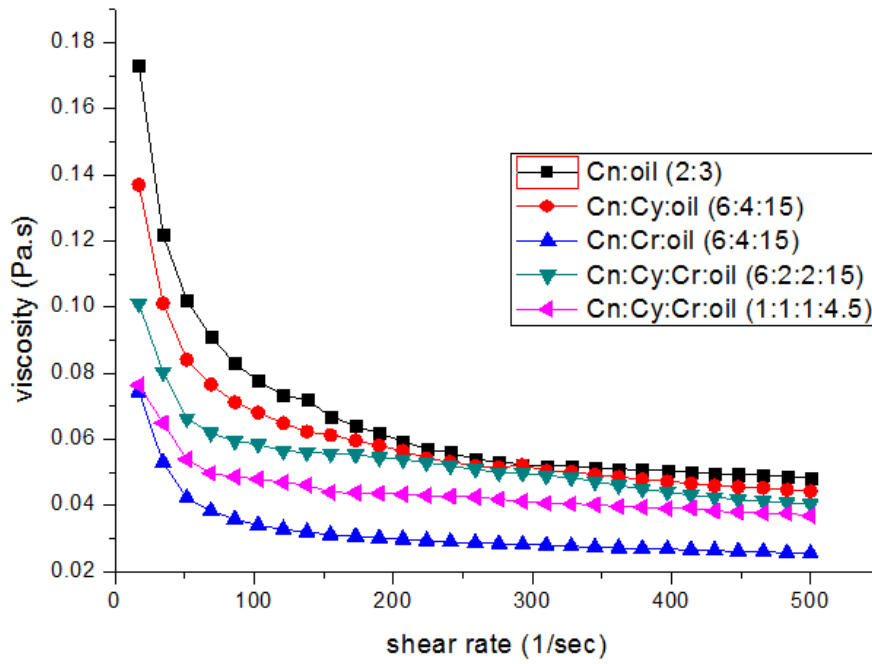


Fig. 5.29: Influence on apparent viscosity with increase in shear rate at 45°C for 40% solid concentration

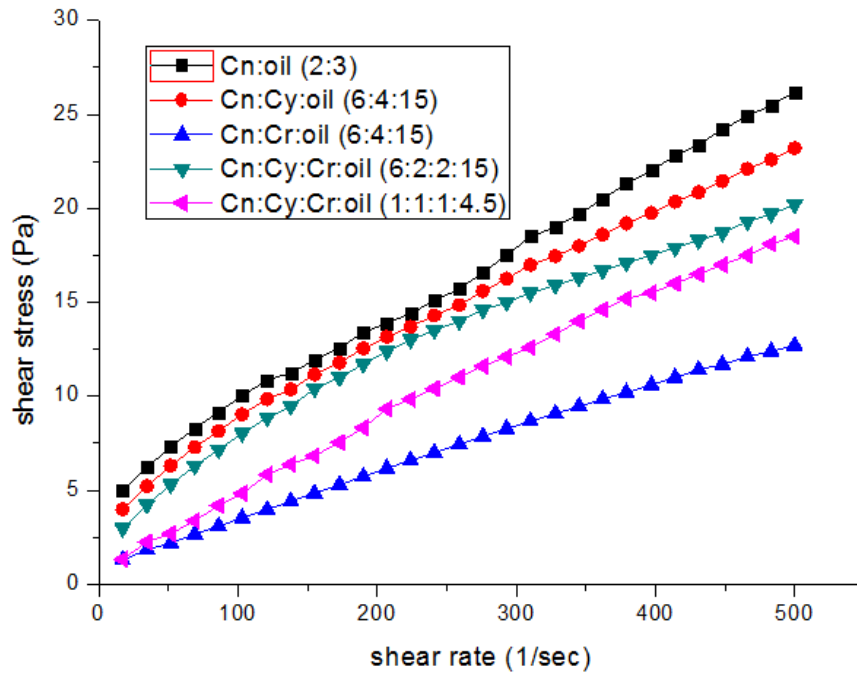


Fig. 5.30: Influence on shear stress with increase in shear rate at 45°C for 40% solid concentration

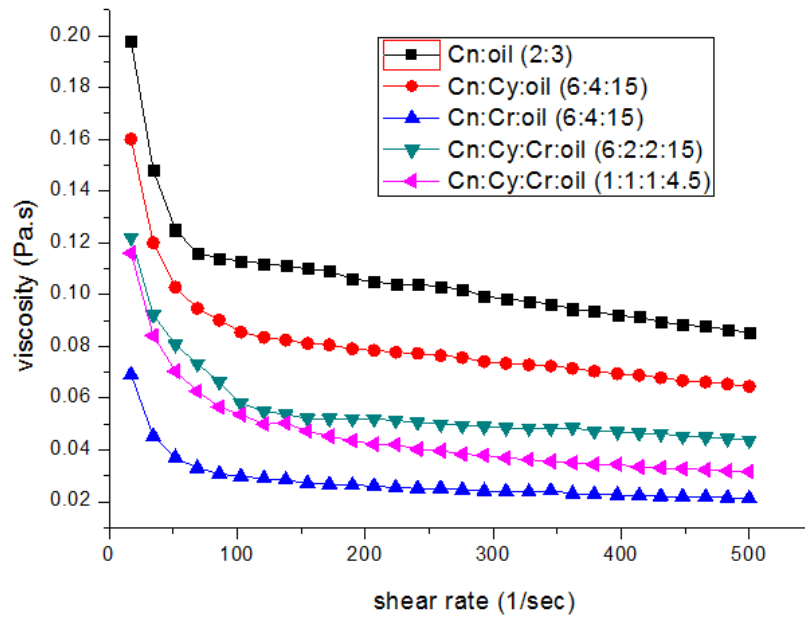


Fig. 5.31: Influence on apparent viscosity with increase in shear rate at 70°C for 40% solid concentration

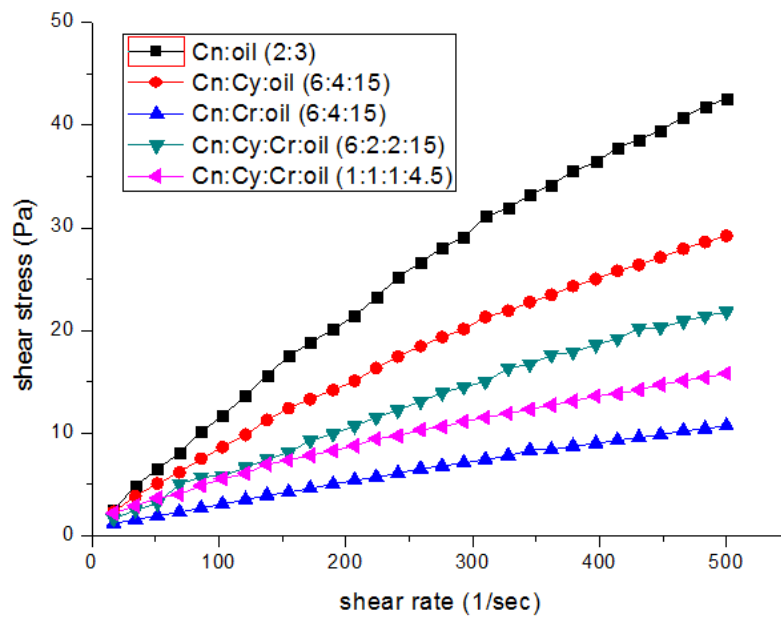


Fig. 5.32: Influence on shear stress with increase in shear rate at 70°C for 40% solid concentration

5.4.6 Effect of particle size on blending: The rheology experiment was also performed to study the effect of particle size on the blended coal oil slurry. The apparent viscosity and shear stress with specific shear rate was analysed for COSL with particle size less than $75\mu\text{m}$. Similar flow curves were obtained as for higher particles size but with reduced viscosity. It was found that the apparent viscosity of COSL decreases with decrease in particle size of coal.

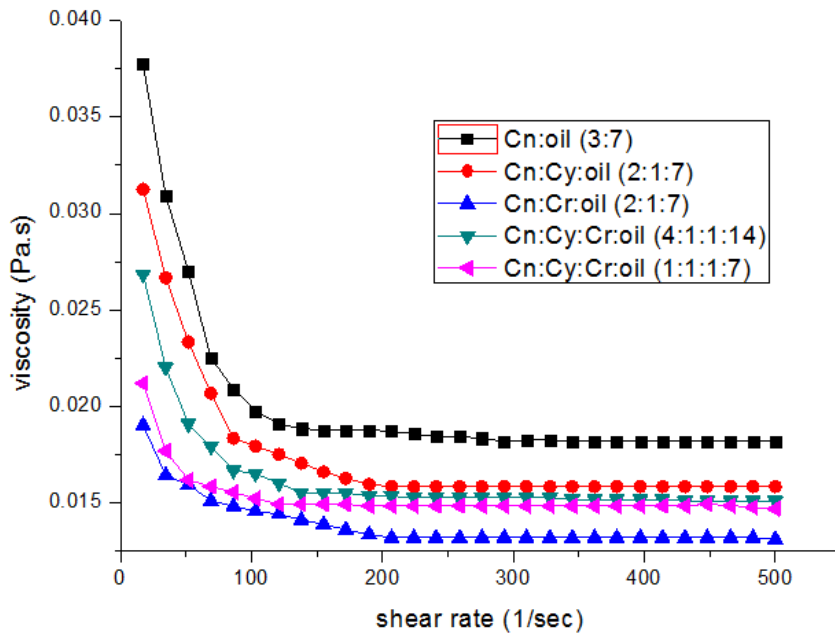


Fig. 5.33: Influence on apparent viscosity with increase in shear rate at 20°C for 30% solid concentration

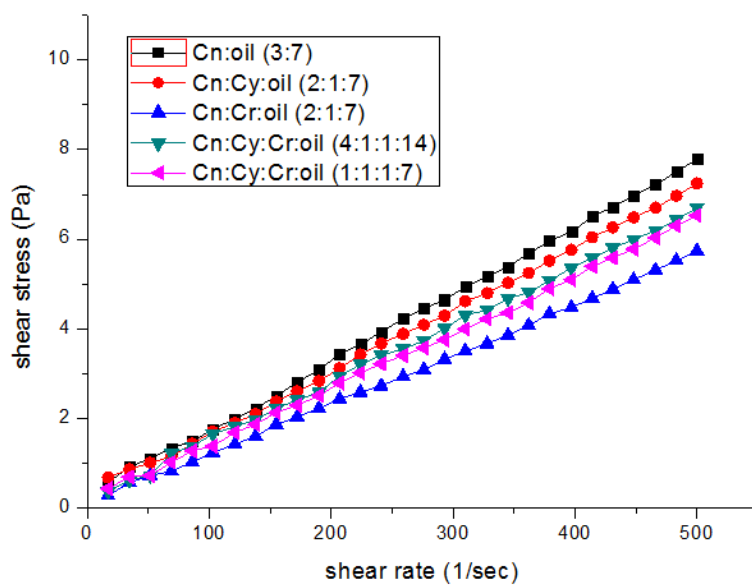


Fig. 5.34: Influence on shear stress with increase in shear rate at 20°C for 50% solid concentration

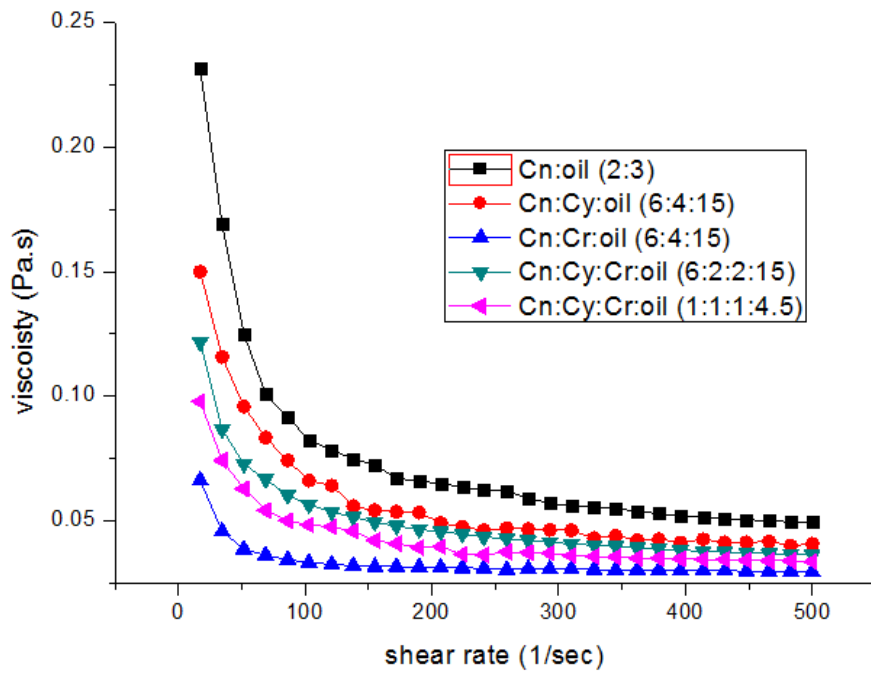


Fig. 5.35: Influence on apparent viscosity with increase in shear rate at 20°C for 40% solid concentration

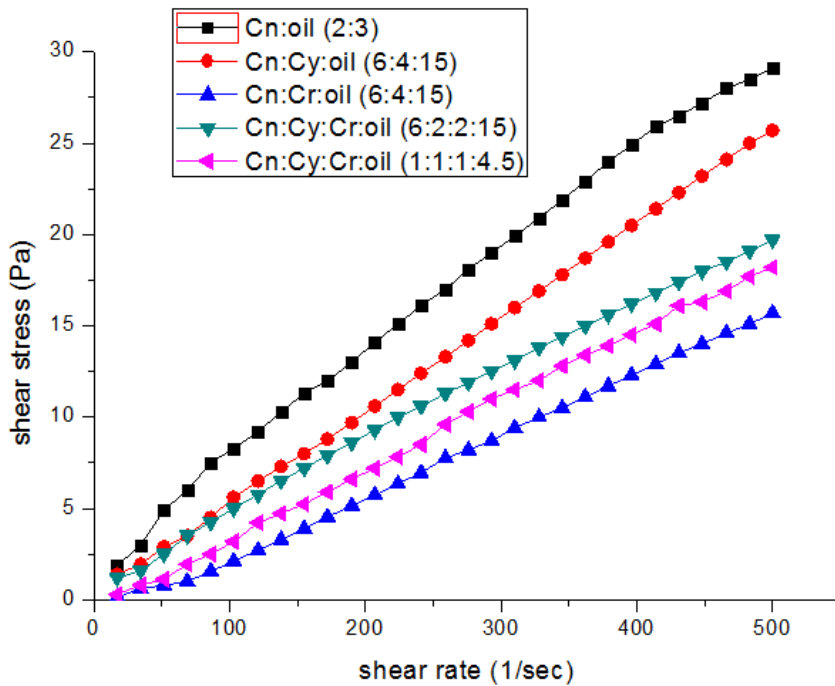


Fig. 5.36: Influence on shear stress with increase in shear rate at 20°C for 40% solid concentration

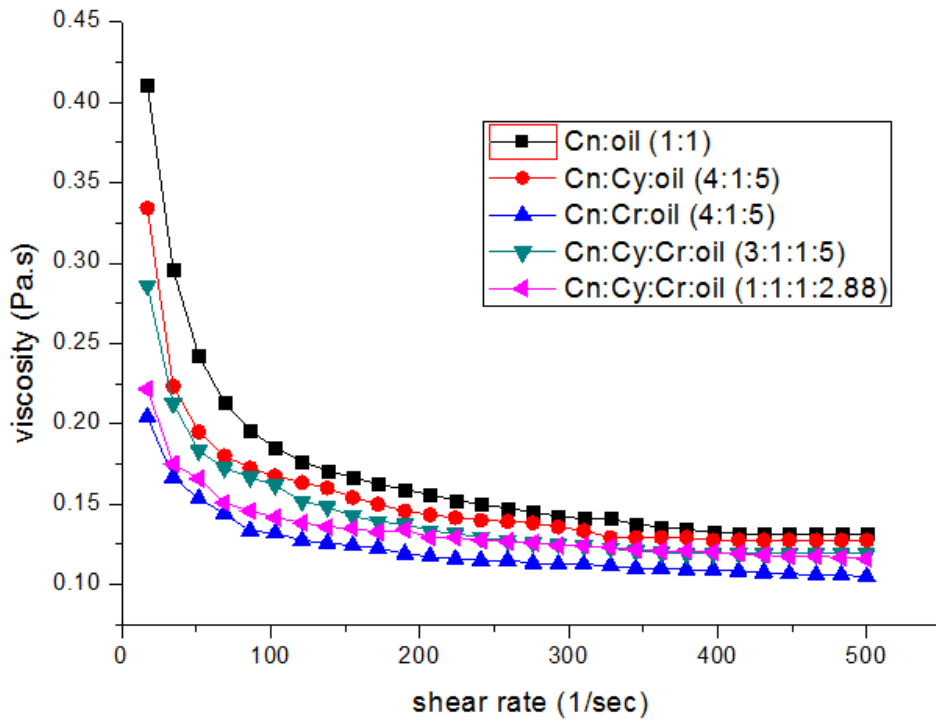


Fig. 5.37: Influence on apparent viscosity with increase in shear rate at 20°C for 50% solid concentration

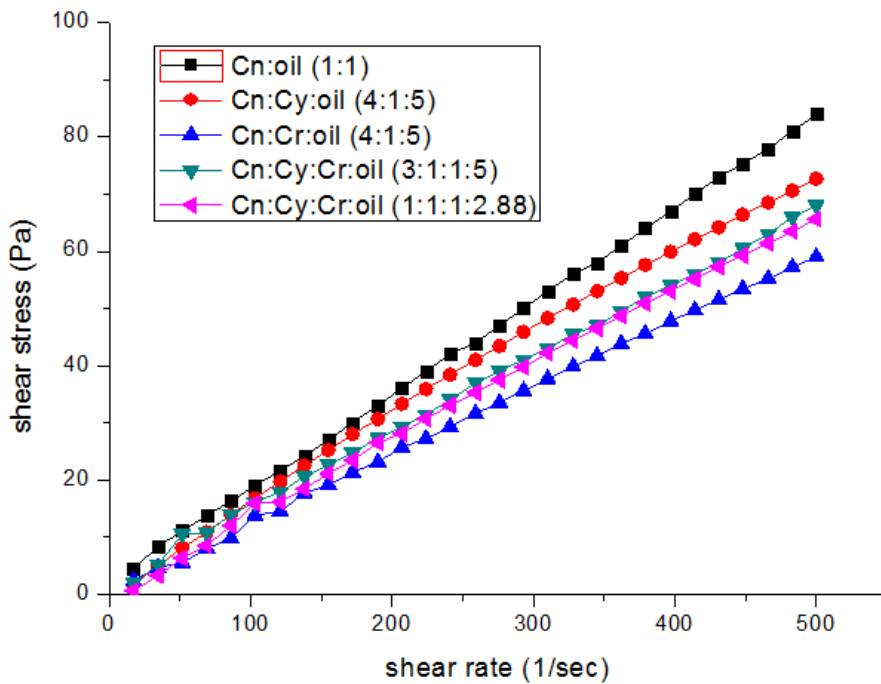


Fig. 5.38: Influence on shear stress with increase in shear rate at 20°C for 50% solid concentration

5.5 Rheological model fitting

The experimental data obtained from rheological study of COSL was fitted into rheological models to calculate various model parameters. A power law model having no yield stress model can be fitted but the Herschel-Bulkley model containing yield stress can be fitted in the flow behaviour. The model constraints were determined subsequently fitting after the experimentation results into the rheological model. It is found that the rheological data is best fitted for Herschel-Bulkley model for COSL for all concentrations and at all temperatures.

Chapter 6

Simulation of pipe flow characteristics

6.1 Introduction

The design of slurry pipeline is a complex process and requires that the design should be optimized that permits highly concentrated slurry transport with minimum pressure drop and wear. Viscosity data is taken from the experimental work that can be utilized to determine the pressure drop in coal oil slurry pipelines. In the present study, pressure drop characteristics of 12.7 mm diameter slurry pipeline were numerically evaluated using ANSYS FLUENT 14.0 code. The evaluation was done on a 90° bend of a 12.7 mm diameter pipe and 127 mm length. Also the pressure drop were determined for the three different curvature ratio (R_c/D) i.e. 1, 2 and 3 with three different concentrations of coal (includes 30%, 40% and 50% coal volume concentration) and with different velocities (2 to 4 m/sec with step size 0.5 m/sec).

6.2 Modelling of 90° pipe bend

The pipeline was modelled using design modeller available in ANSYS 14.0 workbench. The diameter and length 90° pipe bend was kept same i.e. 12.7 mm and 127mm respectively. The length was chosen to be 10 times the diameter for the fully developed flow condition. The radius of the bend was 12.7 mm, 25.4 mm and 38.1 mm. Figure 6.1-6.3 presents the pictorial view of 90° pipe bend modelled in Design Modeller of ANSYS 14.0 code.

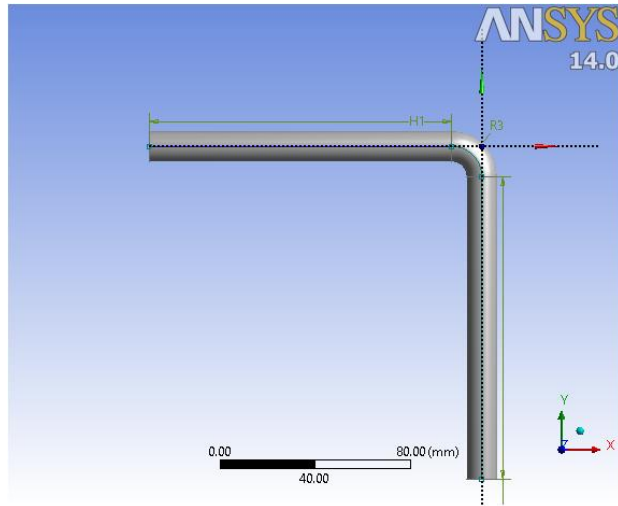


Figure 6.1 : Modelling of pipe bend having curvature ratio 1

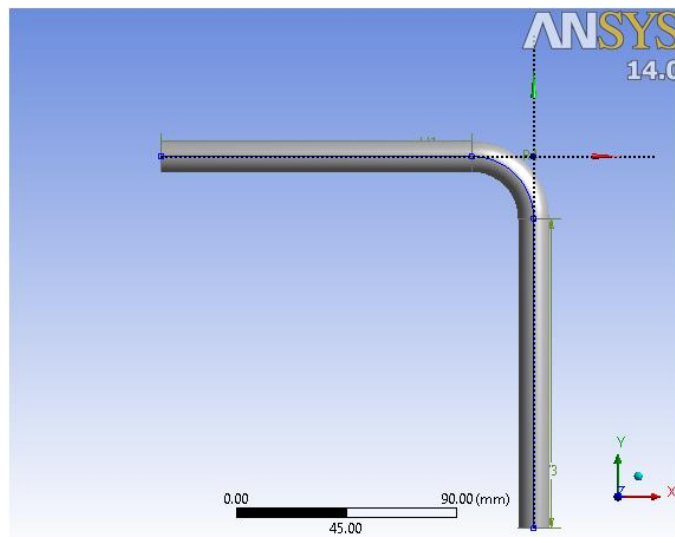


Figure 6.2: Modelling and meshing of pipe bend having curvature ratio 2

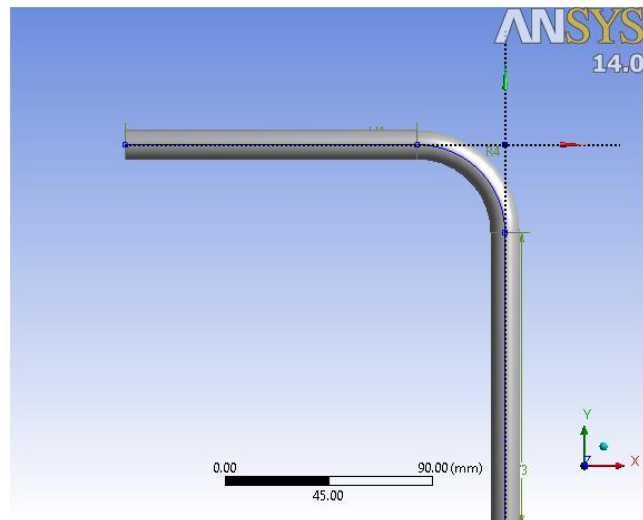


Figure 6.3: Modelling and meshing of pipe bend having curvature ratio 3

6.3 Meshing of 90° pipe bend

The model generated for the 90° pipe bend was meshed using the meshing function available in ANSYS 14.0 workbench. Tetrahedron mesh was generated with inflation provided on the pipe walls to get more elements generated on the pipe wall. Figures 6.4-6.6 shows the mesh generation of pipe bend for different curvature ratios. The numbers of elements for grid size 1mm are 143945, 152372 and 161391 for curvature ratio 1, 2 and 3 respectively.

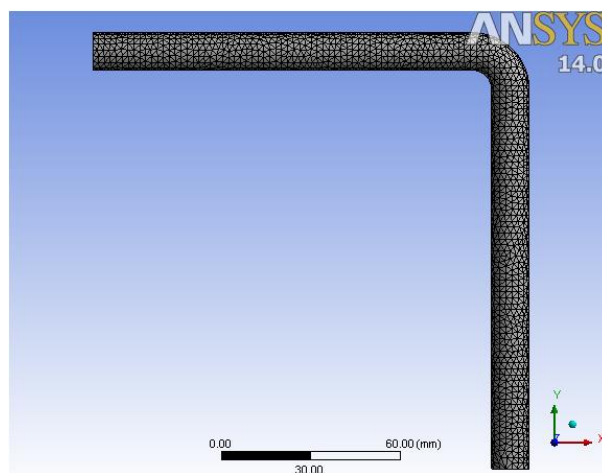


Fig. 6.4: Meshing of pipe bend having curvature ratio 1

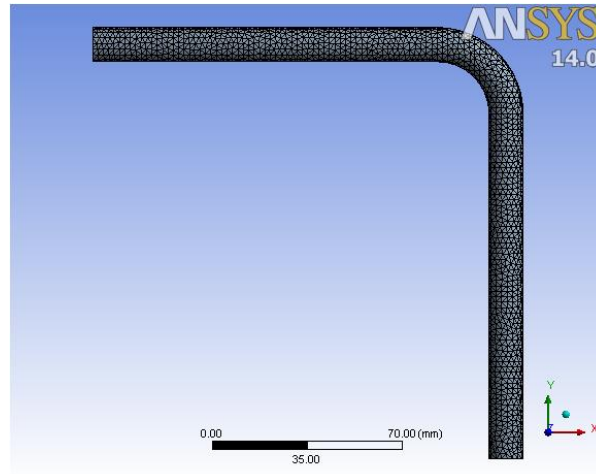


Fig. 6.5: Meshing of pipe bend having curvature ratio 2

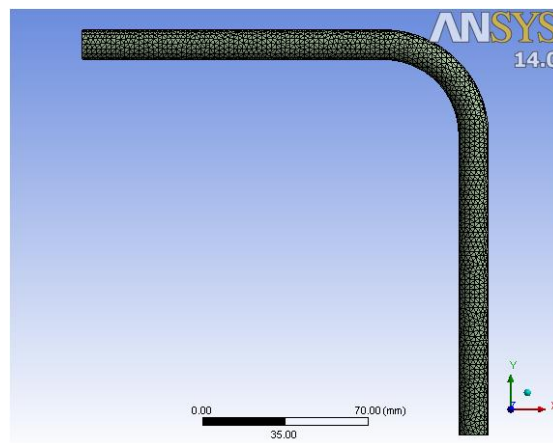


Fig. 6.6: Meshing of pipe bend having curvature ratio 3

6.4 Problem formulation

The problem that is considered here is the fluid flow characteristics of two phase flow through 90° pipes bend having inner diameter 12.7 mm for curvature ratio (R_c/D) 1, 2 and 3. The inlet and outlet length of straight pipe in calculations was set up to 10 D for fully developed flow. The pressure distributions were determined for Reynolds number 5×10^5 . The fluid medium was coal (specific heat 1500 J/kg-k, molecular weight 18.412 kg/kgmol, density 750 kg/m³ and viscosity .0172 kg/m-sec) and oil (specific heat 2090 J/kg-k, density 730 kg/m³, viscosity .0024 kg/m-sec, molecular weight 142.284 Kg/kgmol and latent heat 277000J/kg). For present study three dimensional unstructured meshes was used containing tetrahedron elements.

6.3 Boundary conditions

| Category | Description | Input |
|----------------------------------|----------------------------|--|
| Model | Multiphase model | <ul style="list-style-type: none"> Eulerian model No of phases:2 |
| | Viscous model | <ul style="list-style-type: none"> k-ϵ turbulence, standard Standard wall function Dispersed properties |
| Phase properties and interaction | Phase 1 (primary) | Oil |
| | Phase 2(secondary) | Coal |
| | Particle diameter | 53 μm |
| | Granular viscosity | Syamlal-Obrien |
| | Granular Bulk Viscosity | Lun-et-al |
| | Phase Interaction | Syamlal-Obrien |
| Operating conditions | Operating pressure | 101325 pa |
| | Gravitational acceleration | 0 |
| Boundary conditions | Inlet | Inlet velocity (U_{in}), the turbulent kinetic energy, the Specific Dissipation Rate is given. |
| | Outlet | Pressure outlet with 0 gauge pressure with constant backflow volume fraction |
| | Wall | No slip at wall. |

6.6 Results and discussion

The given figures show the contour of volume fraction of coal at different velocities and at different concentrations. As the particle size used in present simulation for the coal is below $53\mu\text{m}$ the flow is homogenous flow in which solid particle are fully mixed with carrier fluid as shown in below figures only small proportion of the solid particle are settled at low velocities which are again lifting up with increase in the velocity of the flow due to increase in turbulent energy which make particles suspended.

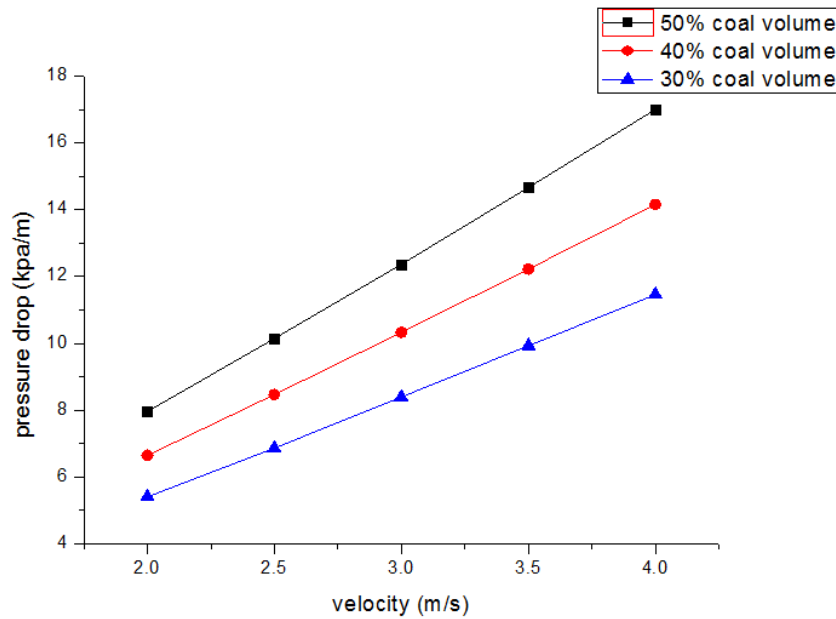


Fig. 6.7: Pressure drop variation with velocity for pipe bend having curvature ratio 1

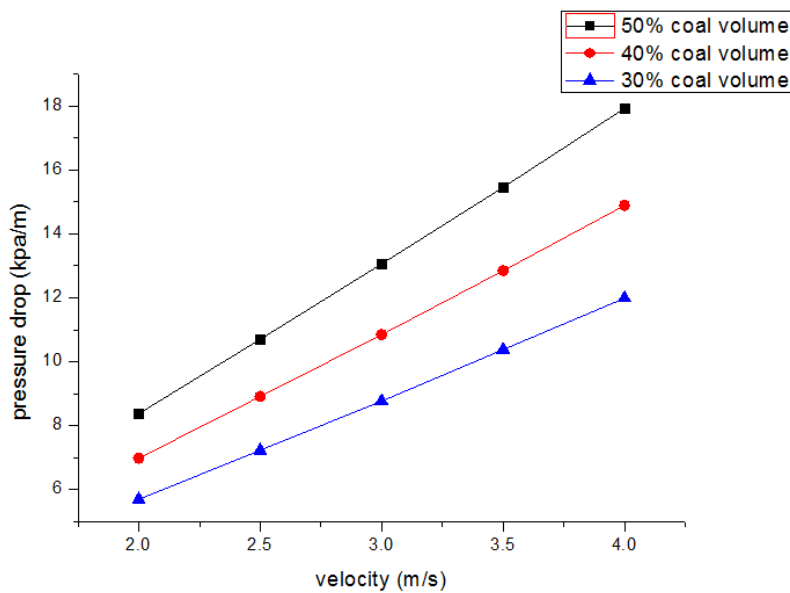


Fig. 6.8: Pressure drop variation with velocity for pipe bend having curvature ratio 2

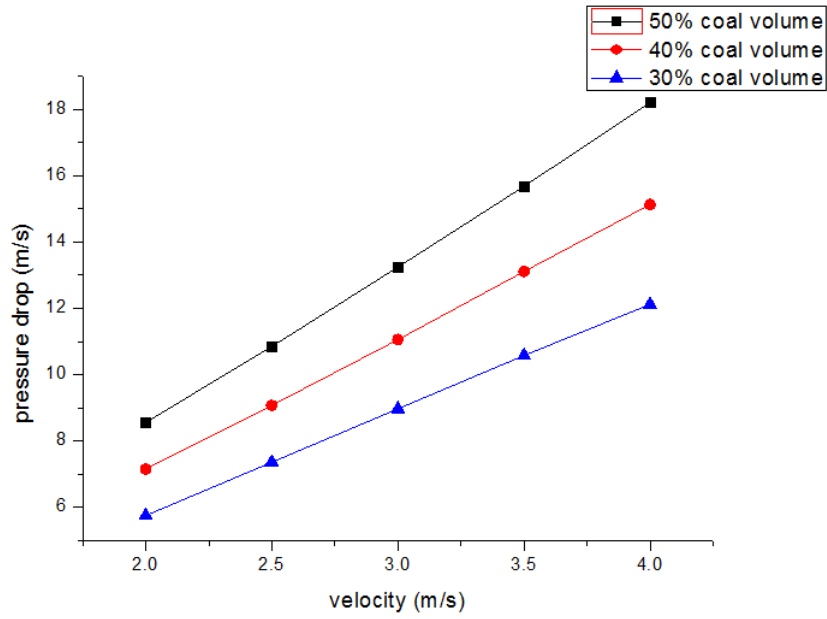


Fig. 6.9: Pressure drop variation with velocity for pipe bend having curvature ratio 3

It was observed that the pressure drop in 90° pipe bend increased as the mean flow velocity increased. The pressure drop also increased with an increase in solids concentration of coal water slurry which was due to the increase in apparent viscosity of coal water slurry at increasing solids concentration by weight.

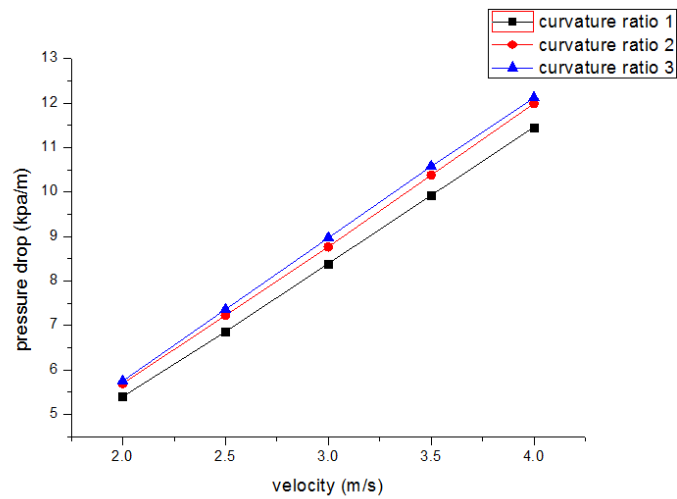


Fig. 6.10: Pressure drop for 30% volume fraction of coal

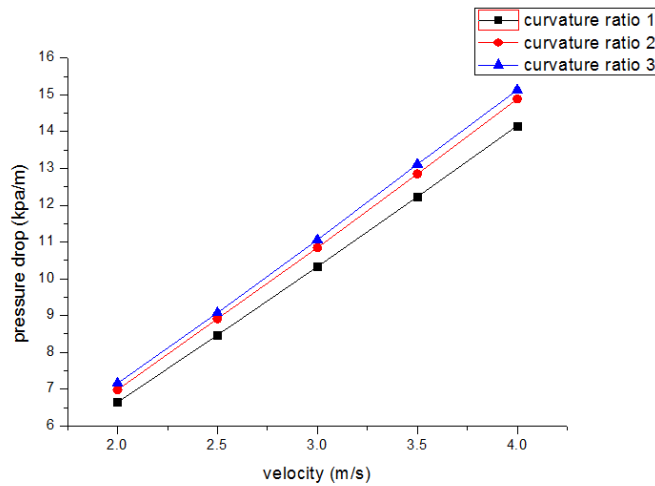


Fig. 6.11: Pressure drop for 40% volume fraction of coal

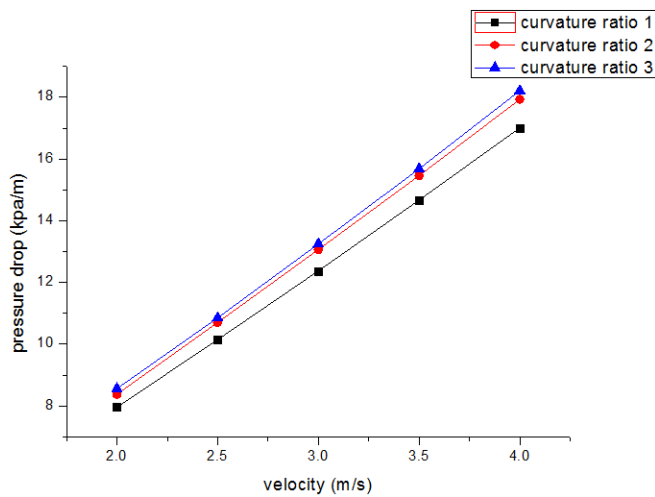


Fig. 6.12: Pressure drop for 50% volume fraction of coal

It was observed that the pressure drop increases when the curvature ratio increases from 1 to 2 but it almost overlaps when the curvature ratio increased from 2 to 3. Also it can be seen that the maximum pressure drop occurs at the bend with curvature ratio 1 but when moved to the higher value for curvature ratio there is less formation of eddies and there is lesser value of pressure drop at bend as compared to the pressure drop for the lower value of curvature ratio. Similar result has been obtained for all the concentration of coal values i.e. for 40% and 50%.

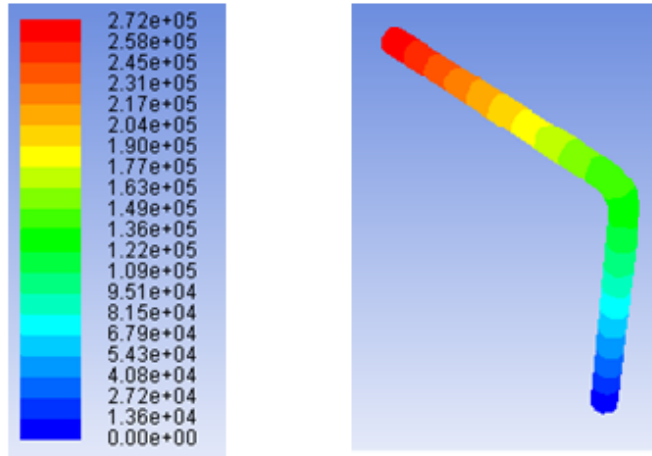


Fig. 6.13: Contour of static pressure of COSL at $C_s=30\%$ for 3.5 m/sec curvature ratio 1

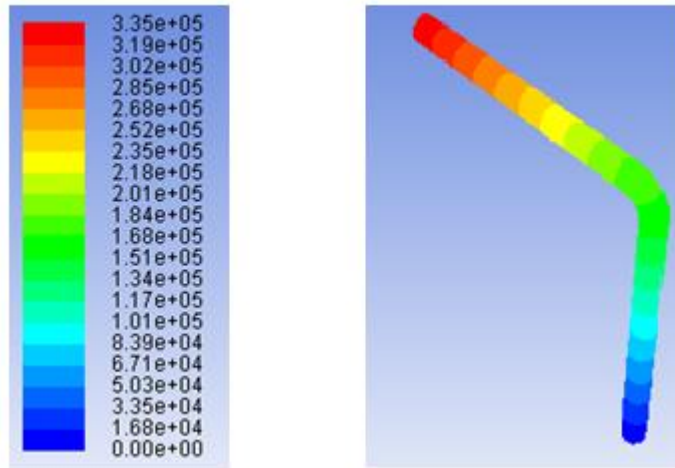


Fig. 6.14 Contour of static pressure of COSL at $C_s=40\%$ for 3.5 m/sec curvature ratio 1

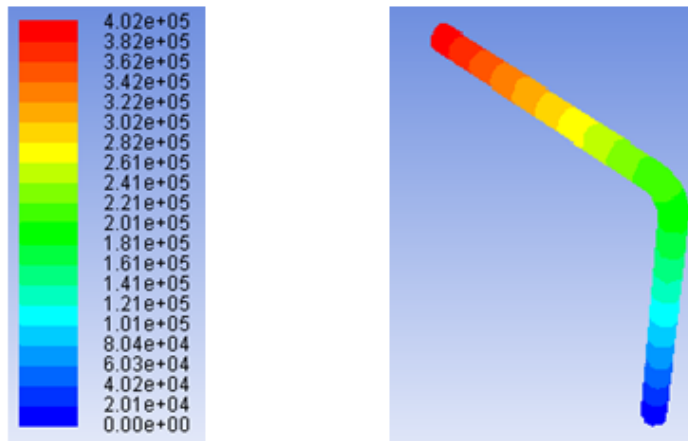


Fig. 6.15: Contour of static pressure of COSLat $C_s=50\%$ for 3.5 m/sec curvature ratio 1

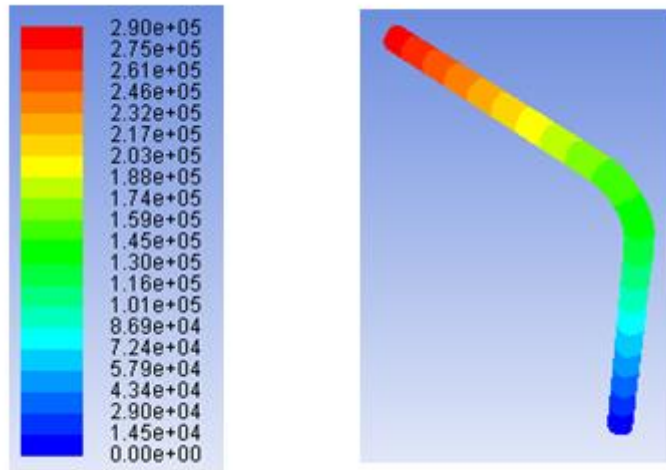


Fig. 6.16: Contour of static pressure of COSLat $C_s=30\%$ for 3.5 m/sec curvature ratio 2

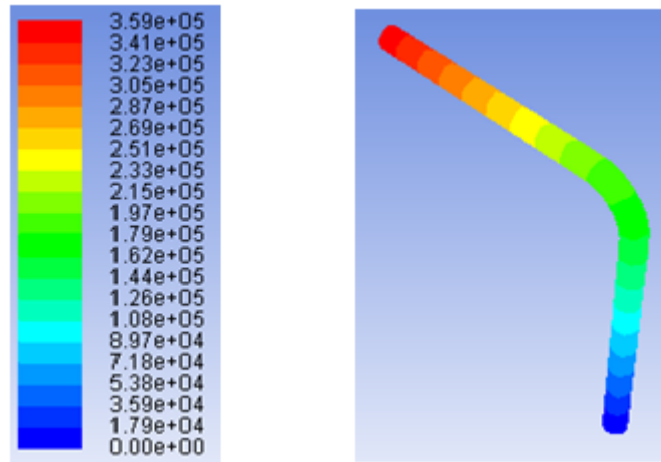


Fig. 6.17: Contour of static pressure of COSLat $C_s=40\%$ for 3.5 m/sec curvature ratio 2

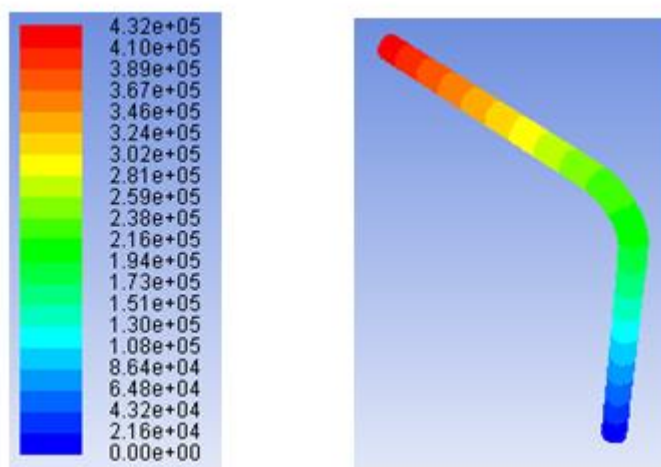


Fig. 6.18: Contour of static pressure of COSLat Cs=50% for 3.5 m/sec curvature ratio 2

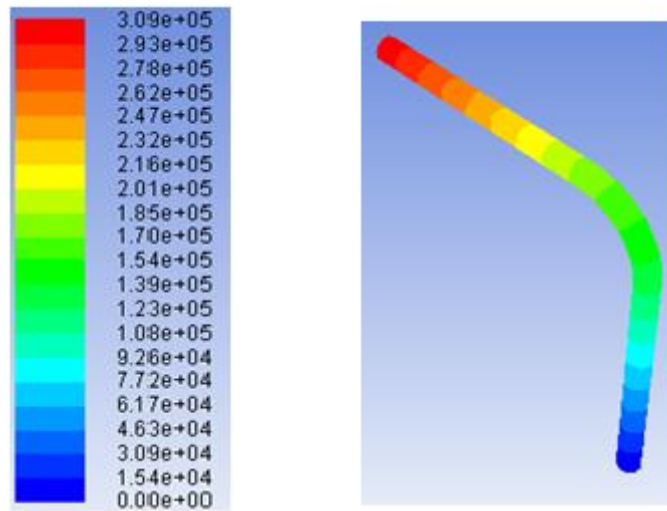


Fig. 6.19: Contour of static pressure of COSLat Cs=30% for 3.5 m/sec curvature ratio 3

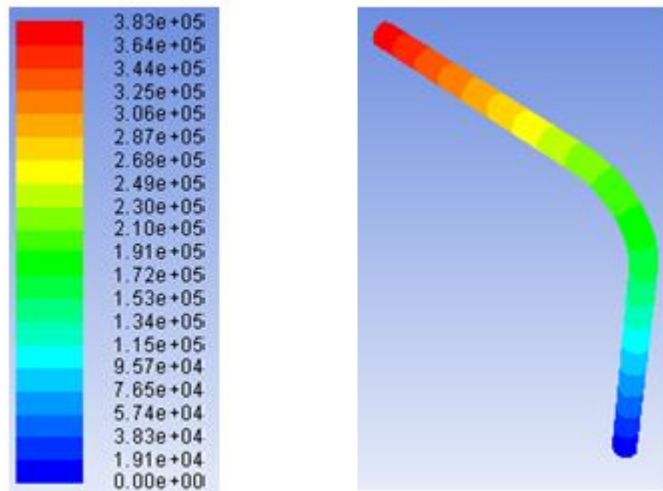


Fig. 6.20: Contour of static pressure of COSLat Cs=40% for 3.5 m/sec curvature ratio 3

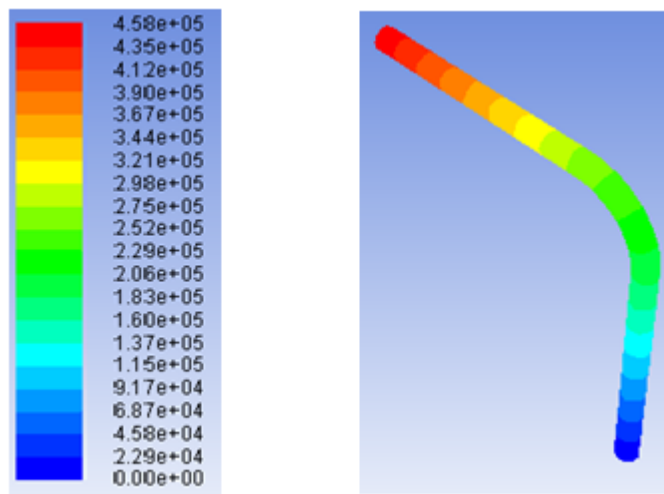


Fig. 6.21: Contour of static pressure of COSLat Cs=50% for 3.5 m/sec curvature ratio 3

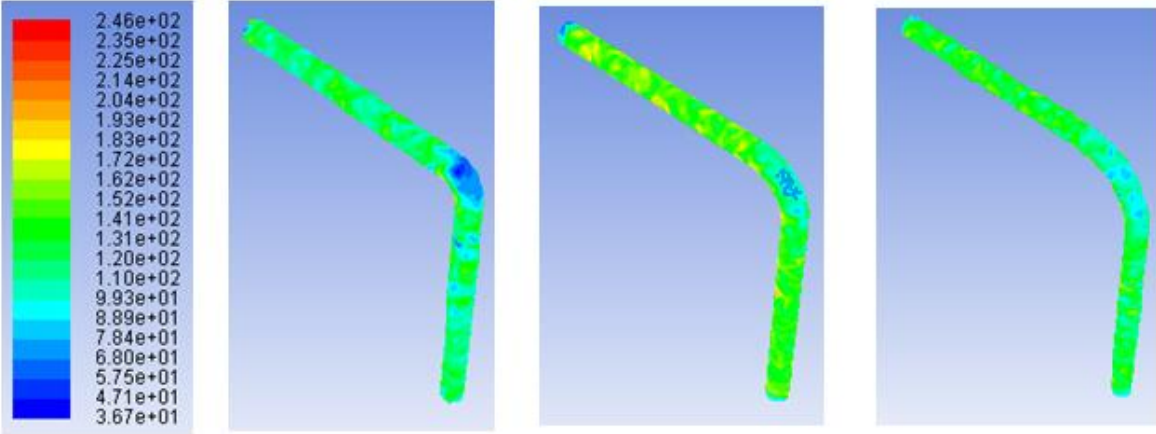


Fig. 6.22: Contour of dynamic pressure of 3.5 m/s for curvature ratio 1, 2 and 3

Chapter 7

Conclusion and future scope

7.1 Summary and conclusion

The present study entitled “Investigation of flow characteristics for coal-oil slurry” was carried out using three different ranked coal collected from different power plant from Indian origin. The coals were ranked on the basis of moisture and ash content. The characterization analysis were done before conducting the rheology study to determine PSD, moisture and ash content, effect of chemical concentration on ash reduction, CV, morphology and morphology of chemical leached ash. The three coals showed different moisture and ash content. Different ranked coal was labelled as Cn (higher rank), Cy (middle rank) and Cr (lower rank). The PSD curve revealed that the maximum amount of fine coal particles was found in Cr.

In the first objective, the two coal samples were taken for chemical leaching with HF and HNO₃. The two coals were labelled as Coal A (higher rank) and Coal B (lower rank). The ash content in two Indian coal containing ash level of 11.2 and 40.3 wt.% was reduced to 0.87 and 0.96 wt.% respectively by the physical washing of coal with HF and HNO₃. Although with the removal of mineral matter on washing the CV for Coal A drops from 5362.5 to 5271.95 kcal/kg and for Coal B the CV drops from 4865.61 to 4765.11 kcal/kg. The attack on carbonaceous matrix during the leaching process reduces the carbon content for both the samples while the oxygen and nitrogen contents increases. It was investigated by EDS that the sulphur content was removed but with high concentration of HNO₃ the F compounds increases for both the samples. The SEM shows the cluster formation for both ash samples of coals washed with acid. The EDS characterization of ash shows that the major compounds of ash for untreated coal has been dissolved for treated coal ash. This may be due to H⁺ combined with F⁻ ions. As from the results, it can be seen that the initial ash content is reduced from 38.5 to 2.33% and 9.75 to 1.01% for lignite and sub-bituminous coal respectively by using dual acid washing of 40% aqueous solution of HF followed by HNO₃.

In the second objective, the flow curves were obtained for chemically leached coal with different concentration of chemical. The study was done to as to study the effect of ash

content on rheology of COSL. The slurry was prepared with diesel oil with 20, 30 and 40% solid concentration of treated and untreated coal at 293K. The rheology result shows that ash has more impact on the viscosity of coal as the viscosity of coal decreases with increase in ash content. The viscosity curves and rheological model show the slurry has shear thinning behaviour.

In third objective, the different ranked coal was blended with different proportion so as to find the feasible and efficient proportion for slurry transportation. Different ranked coal was labelled as Cn (higher rank), Cy (middle rank) and Cr (lower rank). The rheology experiments were conducted for different particle size at 30, 40 and 50% solid loading with temperature 20, 45 and 70°C. The slurries exhibit non-Newtonian behaviour with shear thinning phase for all concentrations. The rheological data was best fitted for Herschel-Bulkley model and value of flow behaviour index found to be less than 1, which shows the shear thinning behaviour for all flow curves. The decrease in particle size reduces the apparent viscosity for all COSL. This could be due to the fact that with reduction in particle size the surface area per unit mass of coal increases providing greater frictional effects. The apparent viscosity of Cn was always greater than Cy and Cr at all coal concentrations and temperatures at given particle size range. It can be because of different moisture and ash content. The blended coal and oil slurry indicated that Cn:Cr:oil for all concentration is best suited for transportation having lower viscosity than other blending.

The rheological data produced was consumed in calculating flow features of coal oil slurry with the help of numerical techniques. The 90° pipe bend was modelled with the help of design modeller (ANSYS) package. Using ANSYS FLUENT 14.0, the mesh of the geometry was created using meshing tool. It was observed that the pressure drop for coal oil slurry increases with increase in velocity of slurry as well as solid loading of coal. Also the dynamic pressure of different curvature ratio revealed that with increase in curvature ratio, the pressure drop at bend decreases. The complete study was commenced to advance perception into COSL technology with perspective regarding its rheology study as well as transportation requirement.

7.2 Future scope in COSL technology

The experimental work in present study was aimed to generate rheological flow curves and pressure drop values for characterizing the COSL rheological behaviour and consuming

that data to appraise transportation performance by forecasting pressure drop in slurry pipeline using CFD code. Various features can supplement present work

- I. Validation of simulated pressure drop with experimentation using pipeline setup.
- II. Erosion wears rate analysis for COSL pipeline for variation in solid loading of coal.
- III. Influence on surrounding temperature of COSL rheological behaviour.

Still there is large scope for COSL utilization and transportation for its efficient use.

References

1. Wang Yong-Gang, Yan Yan, Guo Xiang-Kun, Xu De-Ping, (2009). Rheological behavior of Shengli coal-solvent slurry at low-temperatures and atmospheric pressure. *Mining Science and Technology*.v.19, pp. 0779–0783.
2. Wilson, K.C., Addie, G.R., Sellgren, A., Clift, R., (2005). *Slurry transport using centrifugal pumps*. Springer.
3. Kaushal, D.R., Sato, K., Toyota, T., Funatsu, K., Tomita, Y., (2005). Effect of particle size distribution on pressure drop and concentration profile in pipeline flow of highly concentrated slurry. *International Journal of Multiphase Flow*, v.31, pp. 809-823.
4. Abulnaga, B., 2002, *Slurry System Handbook*, McGraw-Hill
5. Adiga, K.C., Pithapurwala, Y.K., Shah, D.O. and Moudgil, B.M., (1983). Rheology of coal slurries in no.2 oil and ethanol blends: effect of water. *RheologicaActa*. v.22, pp. 402-409.
6. Adiga, K.C., Pithapurwala, Y.K., Shah, D.O. and Moudgil, B.M., (1988). Coal slurries in mixed liquid fuels: rheology and ignition characteristics. *Fuel ProcessingTechnology*. v.18, pp. 59-69.
7. Steel, K. and Patrick, J.,(2001). The production of ultra clean coal by chemical demineralization. *Fuel and Energy Centre, Nottingham University, Nottingham, UK. Fuel*.v.80, pp. 2019-2023.
8. K.M. Steel, J.W. Patrick, (2003). The production of ultra clean coal by sequential leaching with HF followed by HNO₃. *Fuel*. v.82, pp. 1917–1920.
9. Wan Nik, W.B., Ani, F.N., Masjuki, H.H. and EngGiap, S.G., (2005). Rheology of bioedible oils according to several rheological models and its potential as hydraulic fluid. *Industrial Crops and Products*. v.22, pp. 249–255.
10. Cui L, An. L and Jiang H, (2007). A novel process for preparation of ultra-clean superfine coal-oil slurry. *Fuels*. v.87, pp. 2296-2303.
11. Wu Zhiheng, Steel Karen M., (2007). Demineralization of a UK bituminous coal using HF and ferric ions. *Nottingham Fuel and Energy Centre, School of Chemical, Environmental and Mining Engineering, Nottingham University, UK. Fuel*. v.86, pp. 2194–2200.

12. Yong-gang, W., Yan, Y., Xiang-kun, G. and De-ping, X., (2009). Rheological behaviour of Shengli coal-solvent slurry at low-temperatures and atmospheric pressure. *Mining Science and Technology*. v.19, pp. 0779–0783.
13. He, Q., Wang, R., Wang, W., Xu, R. and Hu, B., (2011). Effect of particle sizedistribution of petroleum coke on the properties of petroleum coke–oil slurry. *Fuel*. v.90,pp. 2896–2901.
14. Chen, R., Wilson, M., Leong, Y.K., Bryant, P., Yang, H. and Zhang, D.K., (2011). Preparation and rheology of biochar, lignite char and coal slurry fuels. *Fuel*. v.90, pp. 1689–1695.
15. Ren, Y., Zhang, D. and Gao, J., (2011). Viscosity variations of coal-oil slurry under high temperature and high pressure during heating process. *Fuel Processing Technology*. v.92, pp. 2272–2277.
16. Chen, R., Wilson M., Leong Y.K., Bryant P., H. Yang and Zhang D.K., (2011). Preparation and rheology of biochar, lignite char and coal slurry fuels. *Fuels*. v.90, pp.1689-1695.
17. Wang, R., Liu, J., Gao, F., Zhou, J. and Cen, K., (2012). The slurring properties of slurry fuels made of petroleum coke and petrochemical sludge. *Fuel Processing Technology*. v.104, pp. 57–66.
18. QuamrulH.Mazumder, (2012). CFD analysis of the effect of elbow radius on pressure drops in multiphase flow. *Mechanical Engineering, University of Michigan-Flint, Flint, MI 48502, USA*.
19. Quamrul H. Mazumder., (2012).CFD analysis of single and multiphase flow characteristics in elbow. *Asian Transactions on Engineering*.v.22, pp. 249–255.
20. Xu, M., Zhang, J., Liu, H., Zhao, H. and Li, W., (2014). The resource utilization of oily sludge by co-gasification with coal. *Fuel*. v.126, pp. 55–61.
21. P. Dutta and N. Nandi, (2009). Study on pressure drop characteristics of single phase turbulent flow in pipe bend for high Reynolds number. *ARPN Journal of Engineering and Applied Sciences*.v.10, ISSN 1819-6608.
22. Sui H., Wang H. and Chen H., (2015). Rheological behavior and steam gasification of bio-slurry. *The 7th International Conference on Applied Energy – ICAE2015*. v.75, pp. 220-225.

23. Singh M.K., Ratha D., Kumar S. and Kumar D., (2016). Influence of particle-size distribution and temperature on rheological behaviour of coal slurry. *International Journal of Coal Preparation and Utilization*. v.36, pp. 44-54.
24. Ganeshan G. and Panda D., (2016). Effect of oil viscosity on rheology of coal-oil mixtures. *International Journal of Coal Preparation and Utilization*.
25. U.C. Mishra, (2004). Environmental impact of coal industry and thermal power plants in India. *Journal of Environment Radioactivity*. v.72, pp.35–40,
26. A.P. Chikkatur, A.D. Sagar, T.L. Sankar, (2009). Sustainable development of the Indian coal sector. *Energy*. v.34, pp. 942–953,
27. S. Balakrishnan, R. Nagarajan, (2013). Fouling intensity of three Indian coals. *Coal Combustion and Gasification Production*. v.5, pp. 31–38,
28. S. Balakrishnan, R. Nagarajan, Role of bouncing potential in molten ash impaction, *Chem. Eng. Commun.* (in press).
29. S. Balakrishnan, R. Nagarajan, (2014). Effect of surface roughness and surface energy on molten fly ash deposition. *International Journal of Advancement in Engineering Sciences and Applied Mathematics*. v.6, pp.41–48.
30. W. Bryers, (1996). Fireside slagging, fouling and high-temperature corrosion of heat-transfer surface due to impurities in steam-raising fuels. *Progress in Energy and Combustion Science*. v.72, pp. 29–120.
31. S. Balakrishnan, R. Nagarajan, K. Karthick, (2015). Mechanistic modeling, numerical simulation and validation of slag layer growth in a coal-fired boiler. *Energy*. v.81, pp. 462–470.
32. K.M. Steel, J. Besida, T.A. O'Donnell, D.G. Wood, (2001). Production of ultra clean coal Part II—Ionic equilibria in solution when mineral matter from black coal is treated with aqueous hydrofluoric acid. *Fuel Processing Technology*.v.70, pp. 193–219.
33. C.M. Urban, H.E. Mecredy, T.W. Ryan, M.N. Ingalls, B.T. Jett, (1988). Coal–water slurry in an EMD diesel engine. *Journal of Engineering for Gas Turbines and Power*. v.110, pp. 437–443.
34. P.L. Flynn, B.D. Hsu, G.L. Leonard, (1990). Coal fuelled diesel engine progress at GE transportation systems, *Internal Combustion Engine Division*. v.12, pp. 1–9.
35. World coal institute, (2009). *The coal resource: A comprehensive overview of coal*, pp. 1–42.

36. CSIRO research project, (2001). Direct Firing of Coal into Turbines - Ultraclean Coal.
37. Yaman, R. Yavuz, S. Küçükbayrak, Y. Taptýk, (2001). Stepwise demineralization and chemical isolation of the mineral matter of göynük lignite. *Energy Conversion and Management*. v.42, pp. 2119-2127.
38. J. Hycnar, K. Rondio, M. Sciazko, (1994). Tests on demineralization of high sulfur steam coal fines in TRW Gravimelt process, International Coal Preparation Congress on 12th International Coal Preparation. pp. 425–431.
39. N.P. Vasilakos, S.C. Clinton, (1994), Chemical beneficiation of coal with aqueous hydrogen peroxide/sulphuric acid solutions. *Fuel*. v.63, pp.1561-1563.
40. D.J. Boron, R.S. Taylor, *Fuel* 64 (1985) 209.
41. J.K. Kinding, J.E. Reynolds, (1987). Integrated coal cleaning process with mixed acid regeneration. US Patent 4,695,290.
42. A. Nabeel, T.A. Khan, D.K. Sharma, (2009). Studies on the production of ultra-clean coal by alkali-acid leaching of low-grade coals. *Energy Source*. v.31, pp. 594–601.
43. K.M. Steel, J.W. Patrick, (2003). The production of ultra clean coal by sequential leaching with HF followed by HNO₃. *Fuel*.v.82, pp.1917–1920.